Deliverable D1 (D1.3)

Report on source apportionment studies and recommendations for source apportionment procedures

RI-URBANS

Research Infrastructures Services Reinforcing Air Quality Monitoring Capacities in European Urban & Industrial AreaS (GA n. 101036245)

By

CSIC, IMT, PSI, AMU, UoB, UGA, INERIS & ARPA Lombardia

29th September 2023

RI-URBANS (www.RIURBANS.eu) is supported by the European Commission under the Horizon 2020 – Research and Innovation Framework Programme, H2020-GD-2020, Grant Agreement number: 101036245

Deliverable D3 (D1.3): Report on source apportionment studies and recommendations for source apportionment procedures

Authors: Fulvio Amato (CSIC), Marta Via (CSIC), Marjan Savadkoohi (CSIC), Marco Pandolfi (CSIC), Meritxell Garcia (CSIC), Rosa Lara (CSIC), Marten in't Veld (CSIC), Angeliki Karanasiou (CSIC), Cristina Reche (CSIC), Noemí Perez (CSIC), Therese Salameh (IMT), Marvin Dufresne (IMT) Mannos Manousakas (PSI), Benjamin Chazeau (AMU), Roy M. Harrison (UoB), Barend L. van Drooge (CSIC), Jean-Luc Jaffrezo (University of Grenoble, UGA), André S.H. Prevot (PSI), Olivier Favez (INERIS), Cristina Colombi (ARPA Lombardia), Eleonora Cuccia (ARPA Lombardia), Guido Lanzani (ARPA Lombardia), Andrés Alastuey (CSIC) and Xavier Querol (CSIC)

Work package (WP)	WP1 Novel AQ metrics and advanced source apportionment STs for PM, and nanoparticles
Deliverable	D3 (D1.3)
Lead beneficiary	CSIC
Deliverable type	■ R (document, report) ☐ DEC (websites, patent filings, videos,….) ☐ Other: ORDP (open research data pilot)
Dissemination level	■ PU (public) ☐ CO (confidential, only members of consortium and European Commission))
Estimated delivery deadline	M24 (30/09/2023)
Actual delivery deadline	29/09/2023
Version	Final
Reviewed by	WP1 leaders and coordinators
Accepted by	Project Coordination Team
Comments	This report offers several state-of-the-art source apportionment studies at several EU urban background sites for PM and emerging air quality metrics such as off-line PM chemistry, non-refractory PM, equivalent Black Carbon (eBC), Particle Number Size Distribution (PNSD), on-line elements and off-line Volatile Organic Compounds (VOCs). Based on such centralized analysis, reccomendations on best procedures are provided for each metric.

RI-URBANS (www.RIURBANS.eu) is supported by the European Commission under the Horizon 2020 – Research and Innovation Framework Programme, H2020-GD-2020, Grant Agreement number: 101036245

Table of Contents

1. ABOUT THIS DOCUMENT 1

2. OFF-LINE PM CHEMISTRY 1

2.1 RECOMMENDATIONS 15

3. NON-REFRACTORY PM1 (NR-PM1) 16

3.1 RECOMMENDATIONS 21

4. ONLINE AND OFFLINE DATASETS COMBINATION IN A SINGLE PMF: MULTI-TIME-RESOLUTION PMF 22

4.1 RECOMMENDATIONS 23

5. EQUIVALENT BLACK CARBON (EBC) 23

5.1 RECOMMENDATIONS 27

5.1.1 eBC concentrations as provided by Aethalometers 27

5.1.2 Harmonization of absorption measurements 28

5.1.3 Selection of AAE_T and AAE_{RC} for eBC source apportionment 28

6. PARTICLE NUMBER SIZE DISTRIBUTION (PNSD) 38

6.1 RECOMMENDATIONS 42

7. RECOMMENDATIONS ON ON-LINE ELEMENTS 44

8. VOLATILE ORGANIC COMPOUNDS 45

8.1 RECOMMENDATIONS 49

9. REFERENCES 50

RI-URBANS (www.RIURBANS.eu) is supported by the European Commission under the Horizon 2020 – Research and Innovation Framework Programme, H2020-GD-2020, Grant Agreement number: 101036245

1. About this document

This report offers several state-of-the-art source apportionment studies at several EU urban background sites for PM and emerging air quality metrics such as off-line PM chemistry, non-refractory PM, equivalent Black Carbon (eBC), Particle Number Size Distribution (PNSD), on-line elements and off-line Volatile Organic Compounds (VOCs). Based on such centralized analysis, reccomendations on best procedures are provided for each metric.

This is a public document that will be distributed to all RI-URBANS partners for their use and submitted to European Commission as a RI-URBANS deliverable D3 (D1.3). This document can be downloaded at https://riurbans.eu/work-package-1/#deliverables-wp1

This replied the requests from T1.2 on developing and implementing advanced source apportionment STs This task aims at providing STs, based on best procedures and methodologies, to apportion novel health-related AQ metrics. We will evaluate and apply the most suited source apportionment receptor models for operational applications, considering previous work in FAIRMODE, EMEP and COLOSSAL (COST Action: Chemical On-Line cOmpoSition and Source Apportionment of fine aerosoL). State-of-the-art source apportionment methodologies are being applied in RI-URBANS on nanoparticle PNSD, online and offline PM chemical speciation, BC and VOCs datasets from T1.1 to provide the source contributions to each of these in a harmonized way. This report offers a pan-European centralized source apportionment database required for compiling new exposure indicators for health effect studies (WP2) and datasets for inter-comparison with chemical transport models (WP3).

2. Off-line PM chemistry

Source apportionment (SA) is a common modelling exercise aimed at identifying sources of pollutants, mostly of particulate matter (PM), and estimate source contributions to PM levels. Among the diverse SA modelling techniques, Positive Matrix Factorization (PMF) is the most widely used model that uses the time-series concentrations (and their uncertainties) of multiple PM components to identify the main factors/sources responsible for their variations.

Given that the different factors/sources are identified by means of their chemical profiles, it is of crucial importance the choice of chemical analyses to be performed prior to the PMF analysis. A large body of literature aimed, during the last decades, to identify the most appropriate tracers for specific sources. For example, for the inorganic elements Cu, Sb, Sn, Ba, Fe among others have been linked to brake wear emissions, Zn to tyre wear emissions, Pb, Mn, Zn and Cd to metallurgy, V and Ni to shipping emissions. For the organic fraction, PAHs are associated mostly to primary combustion products, polyols to plant debris, levoglucosan, mannosan and galactosan to biomass combustion and several other molecular markers for biogenic and anthropogenic secondary aerosols. However, the choice of chemical analyses of PM samples depends on many different factors beside their suitability as tracers, such as available laboratory instrumentation and standards, budget limitation and sample mass limitation. In addition, there is no standard procedure to select the most appropriate components neither specific recommendation on this direction. This generates uncertainty in SA outputs not only in terms of number of sources identified but also, and consequently, in the source contributions estimates. In fact, PMF tends to reproduce most of PM mass, regardless of the percentage of PM mass which has been chemically characterized, so that the lack of one specific source tracers (e.g. levoglucosan) can potentially affect the whole source apportionment study. Sensitivity tests are limited in literature and aimed to investigate the influence of heavy-pollution days (e.g. desert dust outbreaks) time resolution, meteorological period, peak episode, interpolation method showing an impact on

RI-URBANS (www.RIURBANS.eu) is supported by the European Commission under the Horizon 2020 – Research and Innovation Framework Programme, H2020-GD-2020, Grant Agreement number: 101036245

source contributions up to 16 % of change. Additional sensitivity analyses showed that excluding some dates or reducing the associated temporal resolution (from 12-h to 24-h) retrieved fewer source factors and increased the errors of source contribution estimates. Concerning instead the input variables, Cesari et al. (2016), performed a few tests on complete datasets (using the full range of available chemical species) and incomplete datasets (with reduced number of chemical species) showing thatthe profiles and the contributions of the different sources calculated with PMF were comparable within the estimated uncertainties indicating a good stability and robustness of PMF results. However, the study from Cesari et al., was performed only on inorganic PM speciation datasets and the choice of excluded components was aleatory.

This study evaluates quantitatively the impact of lacking specific sources' tracers on the whole source apportionment, both in terms of identified sources and source contributions, with the aim of providing first recommendations on the most suitable and critical components to be included in the PMF analyses in order to reduce PMF output uncertainty as much as possible. To this aim we performed three sensitivity analyses on three different datasets across EU in order to cover different types of climatic (Mediterranean, Continental and Alpine), urban conditions, source types and PM fractions.

In the framework of the RI-URBANS (Research Infrastructures Services Reinforcing Air Quality Monitoring Capacities in European Urban & Industrial AreaS) project (H2020-GD, 101036245) we compiled existing European PM speciation datasets at urban background locations and selected 3 of them for the purpose of this study. The main selection criteria were: i) at least 1 year of measurements; ii) at least 120 samples; iii) presence of both organic and inorganic components. The three data sets were from:

- Barcelona (Spain), including an urban background air quality station (Palau Reial, 41°23'14.5"N 2°06'55.6"E; 68 m a.s.l.) and a traffic site (Eixample). The city of Barcelona lies along the western coast of the Mediterranean Basin, and it is delimited by two river basins (Besòs in the North and Llobregat in the South) and a forest mountain range in the West. The city is densely populated (15.880 inhabitants/km^2) counting 1.6 million inhabitants which doubles when the whole metropolitan area is considered (36 municipalities). The city suffers poor air quality in terms of particulate matter and NO_2, mostly due to road traffic emissions, although other significant contributions to PM levels are originated from industries, harbour and urban works (Amato et al., 2016). No significant impact of residential heating has been historically observed. The urban background sampling site is located in the University Campus area, 250 m away from one of the main roads in the city, while the traffic site is located on a busy road uphill with an average traffic volume of 80,000 vehicles/day. PM10 and PM1 samples were collected on quartz filters during 3 different campaigns in 2010, 2019 and 2021, collecting a total of 440 samples. Merging samples obtained in distant periods in the PMF analysis may produce bias due to the possible variation in chemical profile of PM sources. However, given that the 2010 campaign consisted of >100 samples separated between day and night we decided to include them in the analysis as it is known that samples with high contrast of source contributions improve significantly the PMF results (Norris et al., 2014). A fraction of each filter was acid digested (5 mL HF, 2.5 mL HNO_3, 2.5 mL $HClO_4$) for the determination of major and trace elements (Querol et al., 2001) (Table 1); another fraction was leached for the determination of water-soluble ions by ionic chromatography (IC), using 20 mL of MilliQ water (with an ultrasonic bath for 30 min); another fraction was used for determination of organic carbon (OC) and elemental carbon (EC) by thermal–optical analysis with the EUSAAR2 temperature program (Cavalli et al., 2010) by means of Sunset analysers. Organic components, namely, polycyclic aromatic hydrocarbons (PAHs), sugars, anhydro-sugars, hopanes, acids, and polyols were analysed by means of GC-MS (Alier et al., 2013; Fontal et al., 2015).
- Grenoble (France), urban background air quality station (Les Frênes, 45°09'41" N, 5°44'07" E). The city, surrounded by three mountain ranges, is considered the most densely populated area (160,000 inhabitants) of the French Alps. In addition to the urbanized area, forests, including both deciduous and coniferous

RI-URBANS (www.RIURBANS.eu) is supported by the European Commission under the Horizon 2020 – Research and Innovation Framework Programme, H2020-GD-2020, Grant Agreement number: 101036245

species, and agriculture areas (pastures) dominate the land cover around Grenoble. This region experiences frequent severe PM pollution events in the winter due to the formation of thermal inversion layers that may promote pollutant accumulation (Bessagnet et al., 2020). Previous PMF studies have shown that residential heating, mainly biomass burning, accounts for a major fraction of PM in the winter, but that many other sources are also important for the composition of PM (Favez et al., 2010; Srivastava et al., 2018; Weber et al., 2019; Borlaza et al., 2021). Traffic and industrial activities contribute significantly to the observed PM concentration levels in Grenoble (Polo-Rehn et al., 2014), and primary and secondary biogenic organic aerosol are also largely present in the PM10 (Samake et al., 2019). The current study focuses on the PM10 samples (Tissu-quartz, Pallflex, Ø = 150 mm) collected every third day for one year (2013) using high volume samplers (DA-80, Digitel; sampling duration of 24 h at 30 m^3h^{-1}). Overall, approximately 194 species were quantified in each sample. EC/OC was measured using a Sunset lab analyzer using the EUSAAR-2 thermal protocol (Cavalli et al., 2010). HuLiS were analysed following the protocol described by Baduel et al. (2010). Anions (Cl^-, NO_3^-, SO_4^{2-}), cations (NH_4^+, Ca^{2+}, Na^+, Mg^{2+}, K^+), methanesulfonic acid (MSA) and oxalate ($C_2O_4^{2-}$) were analysed by ionic chromatography (Jaffrezo et al., 2005). Thirty-four metals and trace elements were quantified by ICP-MS (Alleman et al., 2010). Cellulose combustion markers (biomass burning) (levoglucosan, mannosan and galactosan), 3 polyols (arabitol, sorbitol and mannitol) and glucose were quantified using HPLC-PAD (Piot et al., 2012). Twenty-one PAHs, 27 oxy-PAHs, and 32 nitro-PAHs were quantified using UPLC/UV-Fluorescence and GC/NICID (Srivastava et al. 2018) (Albinet et al., 2006; Albinet et al., 2014; Albinet et al., 2013; Tomaz et al., 2016). Twenty-seven higher alkanes (C13–C39), 10 hopanes, pristane, phytane, 5 sulfur containing PAHs, 5 lignin combustion markers (vanillin, coniferaldehyde …) (Golly et al., 2015) and 11 compounds usually recognized as SOA markers (α-methylglyceric acid, pinic acid, methyl-nitrocatechols…) (Nozière et al., 2015) were analysed by GC/ EI-MS. Note that the quantification of all SOA markers was performed using authentic standards.

- Milan (Italy), urban background air quality station (Pascal, 45◦28044 N, 9◦14007 E). Milan, and the Po Valley in general, experiences one of the worst air quality across Europe, due to high anthropogenic emission of primary PM but also of gaseous precursors (mostly NH_3) from the agricultural sector, provoking high formation of secondary aerosols. The station is part of the ARPA Lombardia Air Quality Network, and it is one of the Italian supersites. It is located on the eastern side of Milan, the University area called Città Studi, in a playground about 130 m from the road traffic. PM10 and PM2.5 samples were collected during 2017-2019 on Teflon (Pall), mixed cellulose ester (MCE, Advantec) and quartz microfibre (Pall) filters (47 mm diameter), with low-volume US-EPA reference method samplers (TECORA). Metals, EC/OC, ions and anhydro-sugars were analysed by X-ray fluorescence (XRF), thermo-optical analysis and ionic chromatography respectively (Amato et al., 2016).

Table 1. *Description of the input data used for three PMF base solutions, and classification into strong and weak variables based on S/N ratio.*

			Stations	Strong components	Weak components	Seed	Number of runs	Additional uncertainty
Barcelona (Spain)	PM10, PM1	2010, 2019, 2021	Urban background Traffic	PM, Al, Ca, Fe, K, Mg, Na, S, Li, Mn, Ti, V, Cr Co, Ni, Cu, Zn, As, Rb, Sr, Zr, Cd, Sn, Sb, La, Pb, Ba, OC, EC, NO_3^-, Cl, NH_4^+, succinic acid, glutaric acid, phthalic acid, cis-pinonic acid, malic acid, 3-hydroxyglutaric acid, methylbutanetricarboxylic acid (MBTCA), 2-	azealic acid, 2-methylthreitol, 2-methylerythritol, 17a(H)21β(H)-29-norhopane, 17a(H)21β(H)-hopane	23	10	10

RI-URBANS (www.RIURBANS.eu) is supported by the European Commission under the Horizon 2020 – Research and Innovation Framework Programme, H2020-GD-2020, Grant Agreement number: 101036245

				methylglyceric acid, galactosan, mannosan, levoglucosan, benzanthracene, chrysene, benz(b+j+k)fluoranthene, benzo(e)pyrene, benzo(a)pyrene, benzo[ghi]perylene,				
Milan (Italy)	PM10	2017-2019	Urban background	Al, Si, Cl, K, Ca, Ti, Fe, Cu, Zn, Pb, OC, EC, NO_3^-, SO_4^{2-}, NH_4^+, Levoglucosan	Mn, Ni, Br, PM10	38	20	10
Grenoble (France)	PM10	2013	Urban background	OC, EC, HULIS, Na^+, NH_4^+, Mg^{2+}, Cl^-, NO_3^-, SO_4^{2-}, Levoglucosan, Arabitol, Sorbitol, Benzo[a]pyrene, Benzo[g,h,i]perylene, In.[1,2,3-cd]pyrene, Coronene, Acenaphthenequinone , 6H-Dibenzo [b,d] Pyran-6-one 1,8-Naphthalic anhydride, 1-Nitropyrene, Ba, Cu, Pb, Sb, Ti, Zn, Cr, V, Al, Ca, Fe, C27, C29, C31, C33, HP6, HP7, Coniferylaldehyde, Vanillic acid, Alpha-methyl glyceric acid, DHOPA, 3-Hydroxyglutaric Acid, Phthalic Acid, 2-Methyl erythritol	PM10, HP5, HP8	55	20	5

Positive Matrix Factorization (PMF) is the most common receptor model used for SA and it is based on the mass conservation principle:

$$x_{ij} = \sum_{k=1}^{p} g_{ik} f_{jk} + e_{ij} \quad i=1,2,\ldots,m \quad j=1, 2\ldots. n \qquad (1)$$

where x_{ij} is the concentration of the species j in the i^{th} sample, g_{ik} is the contribution of the k^{th} source in the i^{th} sample, f_{jk} is the concentration of the species j in source k and e_{ij} is the residual concentration. PMF can be solved with the Multilinear Engine (ME-2) developed by Paatero (1999) and implemented in the version 5 of the US EPA PMF. In this study, the US EPA PMF v5 was applied to the three datasets independently. For each dataset, a different method was used for calculating measurement uncertainties given that the laboratories were different. For Barcelona, we used the method published by Amato et al. (2009), for Milan the method published by (…) and for Grenoble the method published by Srivastava et al. (2018). In the case of Barcelona, all the samples were merged into a unique input matrix, combining PM10 and PM1, urban background and traffic sites. The selection of PM components to be used as input for PMF was based on several criteria:

i) The S/N ratio (Paatero and Hopke, 2003)
ii) The percentage of data above detection limit (Amato et al., 2009)
iii) Additionally, we discarded several components in order to meet a maximum number of chemical species equal of 1/3 of that of samples, as suggested by the US EPA PMF manual.

The list of strong and weak variables (determined with the S/N ratio) used for each dataset is shown in Table 1, together with the additional input parameters (seed number, number of runs and the additional uncertainty used in order to meet the criterion of $Q_{robust}/Q_{expected} < 2$).

RI-URBANS (www.RIURBANS.eu) is supported by the European Commission under the Horizon 2020 – Research and Innovation Framework Programme, H2020-GD-2020, Grant Agreement number: 101036245

Once the base solution was definitively selected, (without any further addition of constraints on these base cases), the sensitivity analysis was based on a "brute force" approach, by excluding families of analytes, one at a time. A family of analytes is defined as the group of analytes which are determined by the same laboratory technique (e.g. X-Ray Fluorescence or Ionic Chromatography), in order to mimic choices of input data that would be resulting from availability of the chemical technique. Therefore, for each dataset, we obtained a number of N solutions where N is the number of families of analytes. N is equal to 8, 7, 5 for Grenoble, Barcelona, and Milan, respectively (Tables 2, 3, 4). Each solution was compared with the base solution to identify the impact of excluding that specific family of analytes on the number/type of factors (f) and on the source contribution (g).

In Figures 1 to 6, the uncertainty intervals due to the choice of input chemical components are plotted, for each source, versus the reference solution (base case). Such intervals do not include those cases in which that specific source is not identified, which would deliver a null contribution. For Barcelona, the plots are made separately for the urban and the traffic sites, and for the PM10 and PM1. The following discussion is organized according to the type of sources of PM.

Primary traffic: This factor was always found in Grenoble, regardless of which family of analytes was excluded, due to the fact that is traced by two family of analytes: EC (with OC/EC ratio lower than 1) and elements such as Ba, Cu, Sb (among others). However, when elements' family was excluded, this factor was merged with the one of fungal spores, thus hampering the separation of the two sources contributions. The sensitivity analysis reveals for Primary traffic source contributions a symmetric interval error in Grenoble (±28% compared to the base case solution) when a family of analytes is excluded.

RI-URBANS (www.RIURBANS.eu) is supported by the European Commission under the Horizon 2020 – Research and Innovation Framework Programme, H2020-GD-2020, Grant Agreement number: 101036245

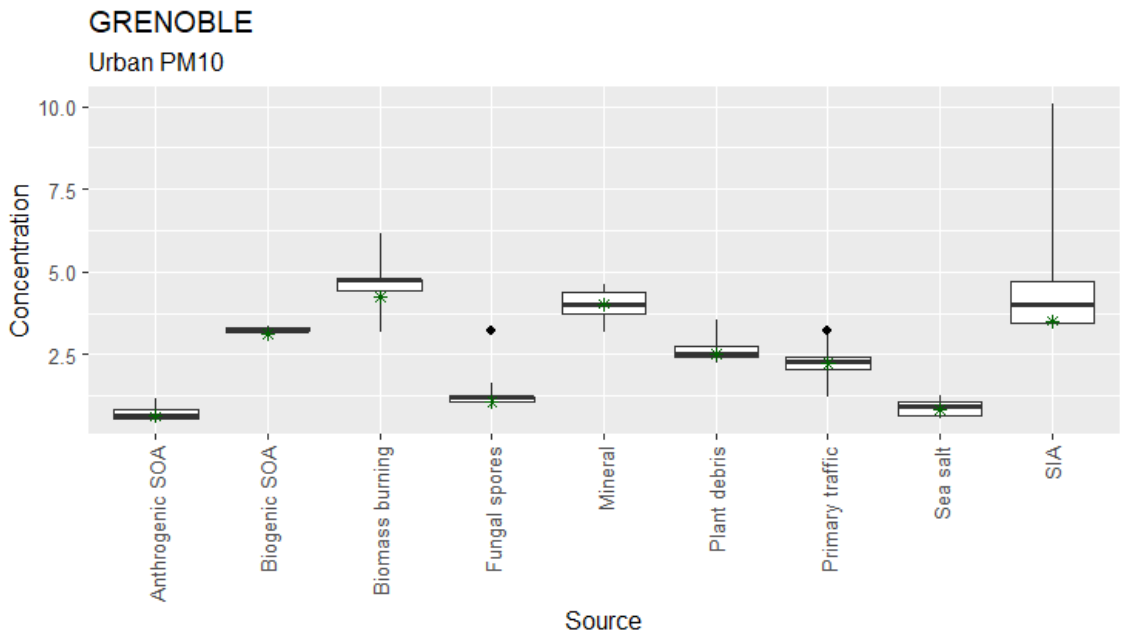

***Figure 1**. Uncertainty intervals of PMF source contributions (µg/m³) in Grenoble urban PM10 due to the exclusion of different families of analytes. The case(s) in which a factor is not identified is not presented (i.e. null contribution). Stars indicate the base reference solution. Dots indicate fusions of factors.*

Vehicle exhaust: in Barcelona and Milan the total traffic contribution was separated in 2 main factors: the vehicle exhaust and the vehicle non-exhaust factors. In Milan, the exhaust factor was mostly of primary origin as it was traced by Zn and an OC/EC ratio of 1 and it was always found, regardless of the input components chosen. The interval error of Vehicle exhaust source contributions was also symmetric in Milan (±15%) when a family of analytes is excluded, except in the case that elements are excluded provoking a merging of exhaust and non-exhaust contributions in one factor with also an overestimation of this exhaust + non-exhaust contributions (13.6 µg/m³ vs 7.3 µg/m³) compared to the reference solution. In Barcelona it was traced by several PAHs and hopanes (17a(H)21β(H)-29-norhopane, 17a(H)21β(H)-hopane, benzanthracene, chrysene, benz(b+j+k)fluoranthene, benzo(e)pyrene, benzo(a)pyrene and benzo[ghi]perylene) and EC and an OC/EC ratio of 1.93 indicating the inclusion of some SOA. This factor was always found except when non-polar organics were excluded.

In Barcelona urban PM10, we observed an asymmetric interval with a more likely underestimation (-44%) of exhaust source contributions when families of analytes are excluded. When non-polar organics are excluded, we observed a merging of exhaust and non-exhaust contributions in one factor but with an underestimation of total contribution (5.8 µg/m³ vs 8.8 µg/m³). For urban PM1, the figure is similar but the underestimation of exhaust + non-exhaust contributions, when non-polar organics are excluded, is even more important (0.4 µg/m³ vs 3.9 µg/m³). In the Barcelona traffic site, we observe a systematic overestimation (up to 3.5 and 2 .5 times for PM10 and PM1 respectively) when some analytes are excluded.

RI-URBANS (www.RIURBANS.eu) is supported by the European Commission under the Horizon 2020 – Research and Innovation Framework Programme, H2020-GD-2020, Grant Agreement number: 101036245

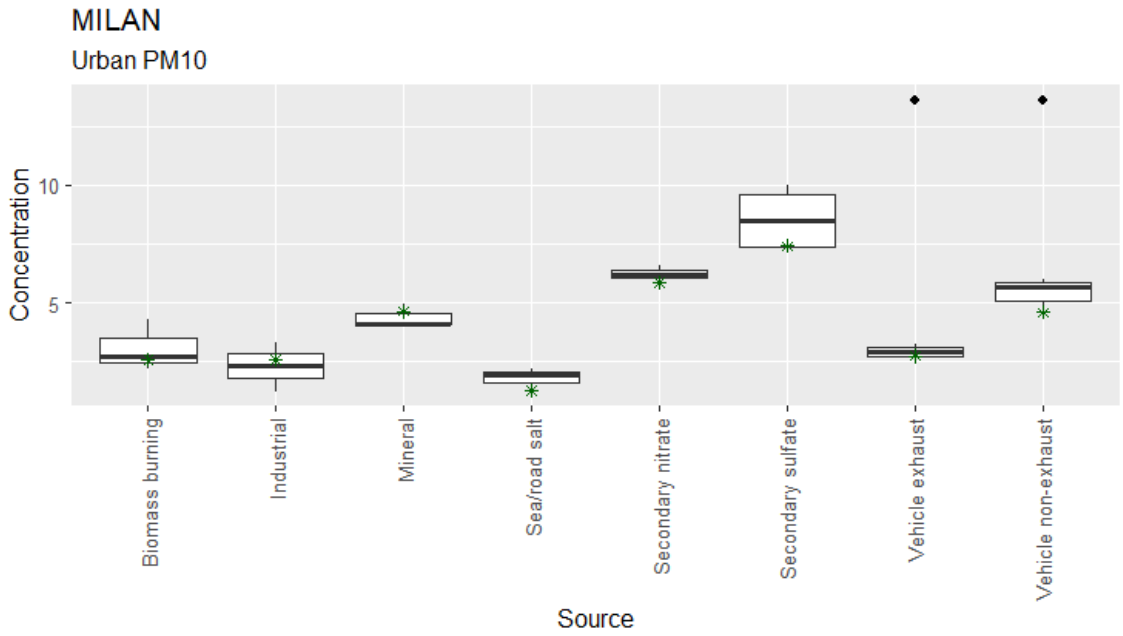

***Figure 2**. Uncertainty intervals of PMF source contributions (µg/m³) in Milan urban PM10 due to the exclusion of different families of analytes. The case(s) in which a factor is not identified is not presented (i.e. null contribution). Stars indicate the base reference solution. Dots indicate fusions of factors.*

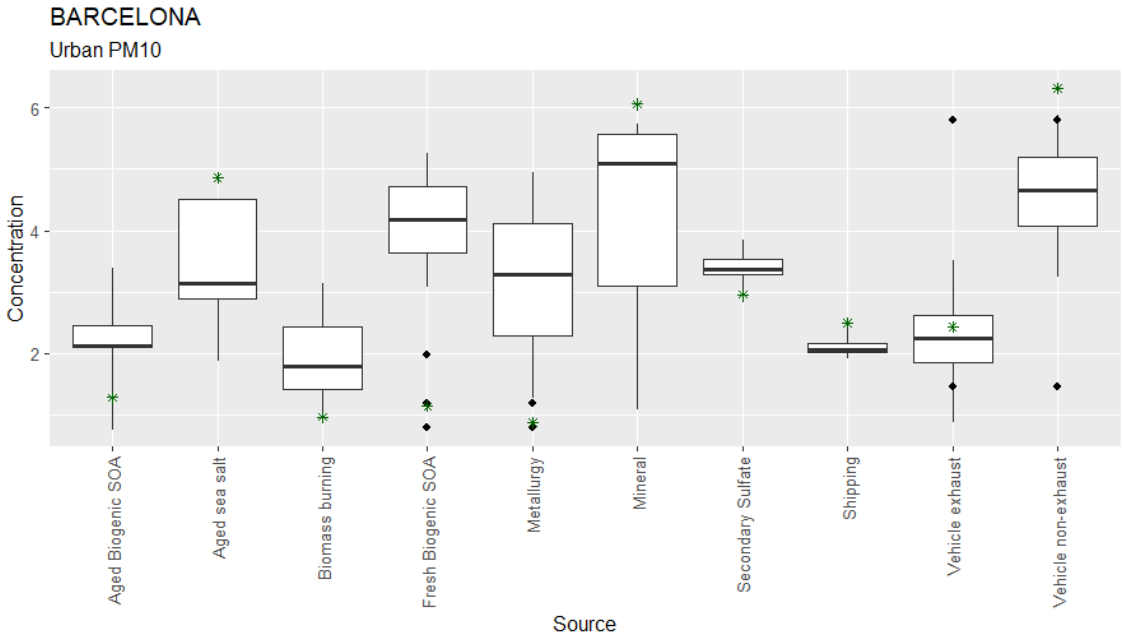

***Figure 3**. Uncertainty intervals of PMF source contributions (µg/m³) in Barcelona urban PM10 due to the exclusion of different families of analytes. The case(s) in which a factor is not identified is not presented (i.e. null contribution). Stars indicate the base reference solution. Dots indicate fusions of factors.*

RI-URBANS (www.RIURBANS.eu) is supported by the European Commission under the Horizon 2020 – Research and Innovation Framework Programme, H2020-GD-2020, Grant Agreement number: 101036245

Vehicle non-exhaust: The non-exhaust fraction of vehicle emissions was traced in both Barcelona and Milan by heavy metals and metalloids such as Cu, Sb, Sn, Ba, Fe, Cr and EC with an OC/EC ratio of 2.2 in Barcelona and Cu, Fe, Pb and EC with an OC/EC ratio of 2.3 in Milan. In both cities, this factor was found except when elements were excluded from the PMF analysis, yielding to a unique traffic factor, as already mentioned earlier. For Barcelona, removing non-polar organics also provoked the loss of separation between exhaust and non-exhaust source contributions. The interval error of Vehicle non-exhaust source contributions reveals a systematic underestimation in Barcelona for PM10 at the traffic and background sites (down to 50%) when a family of analytes is excluded except in the case that ion chromatography is excluded provoking an overestimation (45%) of non-exhaust contributions. In Milan, instead, we observed a generic overestimation (up to 30%) of the N solutions excluding families of components.

Biomass burning: We observed very different outcomes from the sensitivity analyses in the three cities. In Milan and Barcelona, levoglucosan was crucial to identify BB contributions in spite of the presence of PAHs in Barcelona, while for the case of Grenoble, even discarding levoglucosan, the presence of PAHs allowed identifying the BB factor, as confirmed by the high correlation between the two source profiles, mostly for the concentrations of tracers such as EC, OC and PAHs In Milan and Barcelona, the uncertainty due to the different input components selection was estimated in a generic underestimation (up to a factor 2) of biomass burning source contributions, both in PM10 and PM1 fractions, at both urban background and traffic sites.

Shipping. The shipping emissions were identified only in Barcelona due to the presence of the harbour, and traced by V and Ni. As expected, such contribution was missing when elements were excluded from the PMF analysis. Among the rest of solutions, the uncertainty due to the different input components selection was narrow, and estimated in 8% in PM10 and 12% in PM1 with a generic underestimation of 6-20% in source contributions.

Industrial sources. Industrial factors were identified only in Milan and Barcelona and traced by Pb, Ni, Br, Zn and Mn in Milan and Pb, Zn, Mn, Cd and As in Barcelona. This factor has been identified in Grenoble in some other PMF studies (Weber, 2019; Borlaza et al., 2021), but only represent a few % of the PM. While in Milan this industrial factor was sensitive only to the presence of elements, in Barcelona, it was also merged to the fresh biogenic SOA (cis-pinonic acid from a-pinene oxidation) in several cases, when excluding ions, non-polar organics, or ammonium. This merging is interpreted as transport related as both Industries and forests are located to the NW sector of the monitoring city site (Amato et al., 2016). In those cases, however, the total source contributions were much smaller than the sum of industrial and fresh biogenic SOA contribution of the base solution. The uncertainty due to the selections of input components was quite narrow in Milan (40%), but very large in Barcelona (overestimated up to a factor of 5). The reason of such difference is unclear.

Secondary Organic Aerosols: In Grenoble the base solution provided two factors related to SOA: Aged Biogenic SOA and Anthropogenic SOA. Both of them were sensitive to their tracers, namely the oxidation products of isoprene (α-methylglyceric acid (α-MGA) and 2-methylerythritol (2-MT)) and of α-pinene (hydroxyglutaric acid (3-HGA)) (Carlton et al., 2009; Jaoui et al., 2008) for biogenic SOA and acenaphthenequinone, 6H–dibenzo[b,d]pyran-6-one, 1,8- naphthalic anhydride and DHOPA for anthropogenic SOA. In Barcelona, the same is true for the Aged Biogenic SOA factor, traced by malic acid, 3-hydroxyglutaric acid, methylbutanetricarboxylic acid (3-MBTCA), 2-methylglyceric acid, 2-methylthreitol, 2-methylerythritol, and fresh Bio SOA traced by cis-pinonic acid. In Milan, no SOA factor was identified due to the lack of tracers. The uncertainty due to the different input components selections is very narrow for Aged Biogenic SOA (3%) but very large for Anthropogenic SOA (40% in Grenoble and 120% in Barcelona), resulting in a systematic overestimation (except at the Traffic site for PM10 in Barcelona) of Anthropogenic SOA due mostly to one large peak, where concentrations can vary up more than 100%.

Secondary Inorganic Aerosols. In Grenoble, a single SIA factor was identified in the base case solution. The reason is unclear, since other PMF works at this site generally indicate clear separation of sulfate-rich and nitrate-rich

RI-URBANS (www.RIURBANS.eu) is supported by the European Commission under the Horizon 2020 – Research and Innovation Framework Programme, H2020-GD-2020, Grant Agreement number: 101036245

factors (Weber et al., 2019; Borlaza et al., 2021). Such SIA factor was identified as long as ions were selected as input information. If GC / EI-MS analytes were excluded, the SIA factor was split in two the factors Nitrate-rich and Sulfate-rich, but source contributions were largely overestimated compared to the base case. In Barcelona also a single SIA factor was identified, more related to sulfate than nitrate, probably due to the dominance of warmer months in the sampling campaigns. Such Sulfate factor was always identified since it can be trace either by S and SO_4^{2-}. In Milan, secondary sulfate factor and secondary nitrate factor were separated in all solutions except when ions were not used as input species. In that case, Secondary Sulfate (traced by S) contributions were increased by approximately 50%, probably due to the higher ammonium content. Among the rest of solutions, the uncertainty due to the different input components selection was a general overestimation.

Dust sources. In all cities, the mineral factor is found in the base case and characterized with ….. Consequently, it was sensitive to the presence of these elements among the input species. Among the rest of solutions, the uncertainty due to the different input components selection was estimated at ±11% in Milan and ±13% in Grenoble, but large in Barcelona (39%) with a systematic underestimation.

Sea salt. The identification of sea salt factor is more site-dependent due to several reasons. In Barcelona, it was traced either by ions (Cl^-, NO_3^-, Mg^{2+},..) and elements (Na, Cl, Mg, S) so that it was always found, and even split in two factors (aged and fresh) when OC/EC or polar organics were not selected as input species. In Grenoble, no elemental Na nor Cl were available so that the identification of sea salt was sensitive to the ions analysis. In Milan the sea salt was merged to road salt contributions and sensitive to the elemental analysis. Among the rest of solutions, the uncertainty due to the different input components selection was estimated in 33-45% among the three cities, generally symmetric with respect to the reference value.

Primary biogenic particles. Two factors related to primary biogenic aerosols were identified in Grenoble thanks to the analysis of specific tracers of Fungal spores (arabitol and sorbitol, Bauer et al., 2008; Caseiro et al., 2009; Rogge et al., 2007; Yttri et al., 2011) and plant debris (odd number higher alkanes (C27 to C31) (Rogge et al., 1993). As expected both factors were sensitive to the presence of their specific tracers, but, in addition, we observed a merging of the one of Fungal spores with the Primary traffic factor, when elements were excluded from the analysis. The reason of that remains unclear. Among the rest of solutions, the symmetric uncertainty due to the different input components selection was estimated in 23% and 18% respectively.

RI-URBANS (www.RIURBANS.eu) is supported by the European Commission under the Horizon 2020 – Research and Innovation Framework Programme, H2020-GD-2020, Grant Agreement number: 101036245

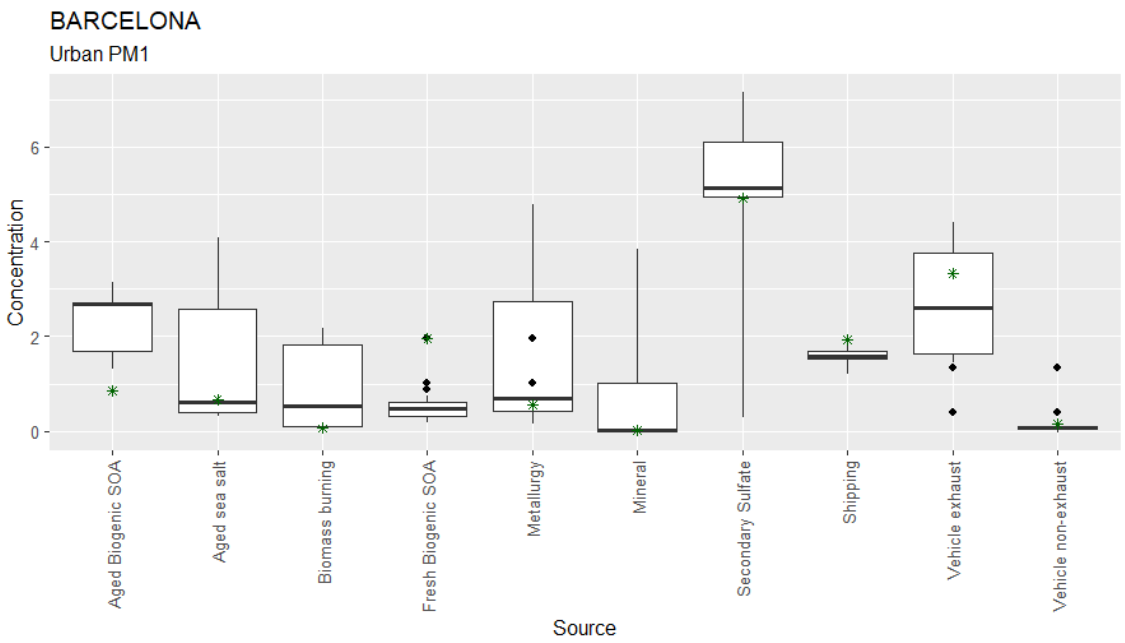

***Figure 4**. Uncertainty intervals of PMF source contributions (µg/m³) in Barcelona urban PM1 due to the exclusion of different families of analytes. The case(s) in which a factor is not identified is not presented (i.e. null contribution). Stars indicate the base reference solution. Dots indicate fusions of factors.*

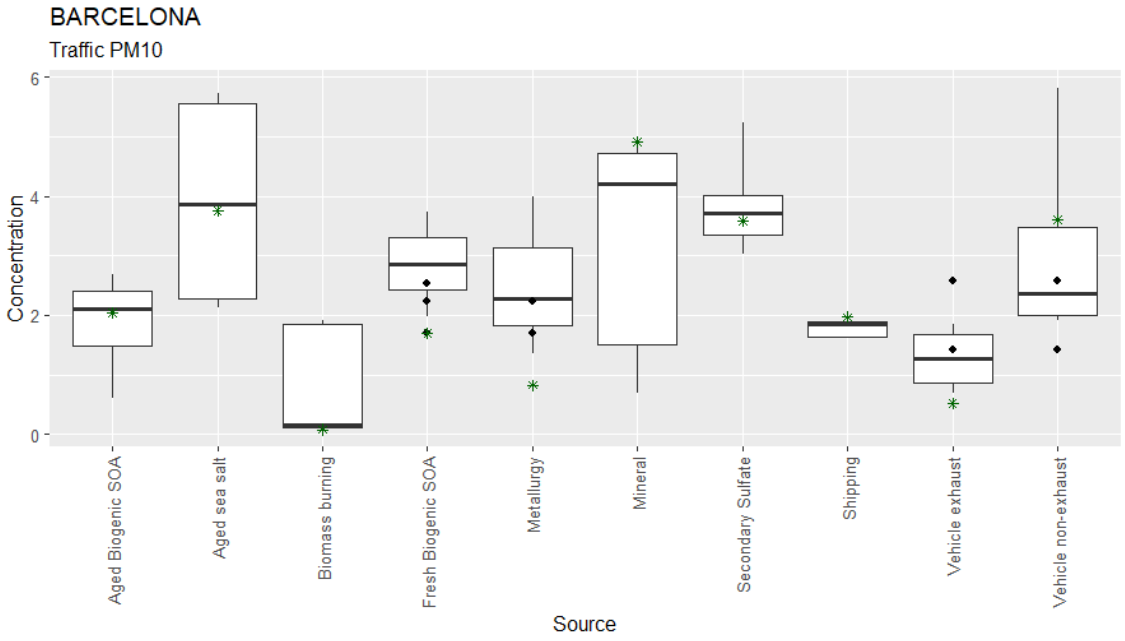

***Figure 5**. Uncertainty intervals of PMF source contributions (µg/m³) in Barcelona traffic PM10 due to the exclusion of different families of analytes. The case(s) in which a factor is not identified is not presented (i.e. null contribution). Stars indicate the base reference solution. Dots indicate fusions of factors.*

RI-URBANS (www.RIURBANS.eu) is supported by the European Commission under the Horizon 2020 – Research and Innovation Framework Programme, H2020-GD-2020, Grant Agreement number: 101036245

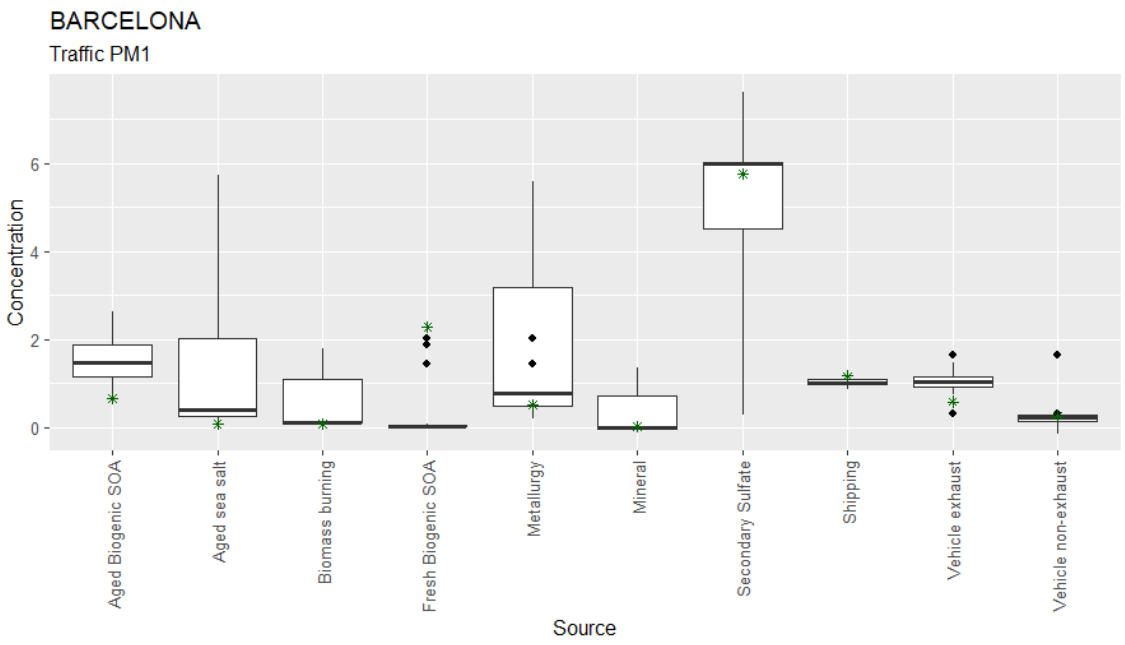

***Figure 6**. Uncertainty intervals of PMF source contributions (µg/m³) n Barcelona traffic PM1 due to the exclusion of different families of analytes. The case(s) in which a factor is not identified is not presented (i.e. null contribution). Stars indicate the base reference solution. Dots indicate fusions of factors.*

***Table 2**. The different PMF solutions in Grenoble varying the number of families of components.*

Grenoble	Characterized mass (%)	Reconstructed mass (%)	# of factors	Type of factors (average % of contribution)
Base solution	67	93	9	Mineral (17%) Sea salt (4%) Primary Traffic (9%) Anthropogenic SOA (3%) Biogenic SOA (13%) Plant debris (11%) Fungal spores (4%) SIA (17%) Biomass burning (18%)
Excluding EC/OC	37	93	9	Mineral (16%) Sea salt (4%) Primary Traffic (8%) Anthropogenic SOA (2%) Biogenic SOA (13%) Plant debris (10%) Fungal spores (5%) SIA (15%) Biomass burning (19%)
Excluding ions	41	90	7	Mineral (19%) Primary Traffic (10%) Anthropogenic SOA (5%) Biogenic SOA (14%) Plant Debris (12%) Fungal spores (4%) Biomass burning (26%)

RI-URBANS (www.RIURBANS.eu) is supported by the European Commission under the Horizon 2020 – Research and Innovation Framework Programme, H2020-GD-2020, Grant Agreement number: 101036245

Excluding elements	62	91	7	Sea salt (5%) Primary Traffic + Fungal spores (13%) Anthropogenic SOA (4%) Biogenic SOA (14%) Plant Debris (15%) SIA (20%) Biomass burning (20%)
Excluding GC/ EI-MS analytes	67	92	8	Mineral (13%) Sea salt (2%) Primary Traffic (5%) Nitrate (16%) Anthropogenic SOA (2%) Fungal spores (7%) Sulfate (26%) Biomass burning (20%)
Excluding PAHs	67	92	8	Mineral (15%) Sea salt (2%) Primary Traffic (13%) Biogenic SOA (14%) Plant Debris (11%) Fungal spores (5%) SIA (19%) Biomass burning (13%)
Excluding Levoglucosan, arabitol, sorbitol	65	93	8	Mineral (19%) Sea salt (5%) Primary Traffic (10%) Anthropogenic SOA (3%) Biogenic SOA (13%) Plant Debris (9%) SIA (14%) Biomass burning (20%)
Excluding HULIS	64	93	9	Mineral (17%) Sea salt (4%) Primary Traffic (9%) Anthropogenic SOA (3%) Biogenic SOA (13%) Plant Debris (10%) Fungal spores (4%) SIA (14%) Biomass burning (18%)

RI-URBANS (www.RIURBANS.eu) is supported by the European Commission under the Horizon 2020 – Research and Innovation Framework Programme, H2020-GD-2020, Grant Agreement number: 101036245

***Table 3**. The different PMF solutions in Barcelona varying the number of families of components.*

Barcelona	Characterized mass (%)	Reconstructed mass (%)	# of factors	Type of factors (average % of contribution)
Base solution	47	94	10	Aged biogenic SOA (6%) Vehicle exhaust (7%) Biomass burning (1%) Mineral (13%) Shipping (9%) Fresh biogenic SOA (9%) Aged sea salt (11%) Metallurgy (3%) Vehicle non-exhaust (12%) Regional Sulfate (21%)
Excluding EC/OC	31	94	10	Aged biogenic SOA (11%) Vehicle exhaust (3%) Biomass burning (6%) Vehicle non-exhaust (10%) Mineral (12%) Shipping (8%) Fresh biogenic SOA + Metallurgy (6%) Aged sea salt (10%) Fresh sea salt (7%) Regional Sulfate (22%)
Excluding ions	39	94	8	Aged biogenic SOA (9%) Vehicle exhaust (9%) Biomass burning (7%) Mineral (11%) Shipping (9%) Fresh biogenic SOA + Metallurgy (5%) Aged sea salt (14%) Vehicle non-exhaust (9%) Regional Sulfate (21%)
Excluding elements	36	91	6	Aged biogenic SOA (7%) Traffic (8%) Biomass burning (11%) Fresh biogenic SOA + Fresh sea salt (9%) Secondary nitrate (31%) Regional Sulfate (24%)
Excluding polar organics	47	94	9	Vehicle exhaust (11%) Vehicle non-exhaust (6%) Hopanes (1%) Mineral (13%) Shipping (7%) Metallurgy (5%) Aged sea salt (16%) Fresh sea salt (7%) Regional Sulfate (28%)
Excluding NH_4^+	45	94	10	Aged biogenic SOA (13%) Vehicle exhaust (8 %) Vehicle non-exhaust (8 %) Biomass burning (2%) Mineral (11%) Shipping (8%) Fresh biogenic SOA + Metallurgy (6%) Aged sea salt (14%) Fresh sea salt (5%) Regional Sulfate (19%)
Excluding non-polar organics	47	94	9	Aged biogenic SOA (11%) Traffic (10%)

RI-URBANS (www.RIURBANS.eu) is supported by the European Commission under the Horizon 2020 – Research and Innovation Framework Programme, H2020-GD-2020, Grant Agreement number: 101036245

				Biomass burning (1%) Mineral (13%) Shipping (7%) Fresh biogenic SOA + Metallurgy (9%) Aged sea salt (14%) Fresh sea salt (5%) Regional Sulfate (23%)

***Table 4**. The different PMF solutions in Milan varying the number of families of components.*

Milan	Characterized mass (%)	Reconstructed mass (%)	# of factors	Type of factors (average % of contribution)
Base solution	69	99	8	Vehicle exhaust (9%) Vehicle non-exhaust (14%) Secondary sulfate (23%) Secondary nitrate (18%) Mineral (15%) Biomass burning (8%) Industrial (8%) Sea/road salt (4%)
Excluding EC/OC	42	99	8	Vehicle exhaust (9%) Vehicle non-exhaust (14%) Secondary sulfate (22%) Secondary nitrate (18%) Mineral (16%) Biomass burning (9%) Industrial (7%) Sea/road salt (4%)
Excluding ions	39	96	7	Vehicle exhaust (10%) Vehicle non-exhaust (19%) Secondary sulfate (31%) Mineral (13%) Biomass burning (13%) Industrial (4%) Sea/road salt (6%)
Excluding elements	57	98	4	Traffic (43%) Secondary sulfate (30%) Secondary nitrate (19%) Biomass burning (7%)
Excluding sugars	68	99	7	Vehicle exhaust (8%) Vehicle non-exhaust (18%) Secondary sulfate (23%) Secondary nitrate (20%) Mineral (13%) Industrial (10%) Sea/road salt (7%)

RI-URBANS (www.RIURBANS.eu) is supported by the European Commission under the Horizon 2020 – Research and Innovation Framework Programme, H2020-GD-2020, Grant Agreement number: 101036245

2.1 Recommendations

In conclusion, road traffic sources are generally identified by analysing at least 2 groups of analytes, namely OC/EC and PAHs and/or elements. The exhaust source resulted to be less sensitive to the choice of analytes, although source contributions estimates can deviate significantly up to 44% (positively or negatively). On the other hand, for the detection of the non-exhaust one is clearly necessary to analyze specific inorganic elements. Still, the exclusion of another group of analytes can provoke a bias of non-exhaust contributions up to 50%. The choice of not analysing non-polar organics likely cause the loss of separation of exhaust and non-exhaust factors, thus obtaining a unique road traffic source, which provoke a significant bias of total contribution.

Levoglucosan was in most cases crucial to identify biomass burning contributions in Milan and in Barcelona, in spite of the presence of PAHs in Barcelona, while for the case of Grenoble, even discarding Levoglucosan, the presence of PAHs allowed identifying the BB factor. Modifying the rest of analytes provoke a systematic underestimation of biomass burning source contributions.

SIA factors resulted to be generally overestimated with respect to the base case analysis, also in the case that ions were not included in the PMF analysis.

Trace elements were crucial to identify shipping emissions (V and Ni) and industrial sources (Pb, Ni, Br, Zn, Mn, Cd and As). When changing the rest of input variables, the uncertainty was narrow for shipping but large for industrial processes. Major and trace elements were also crucial to identify the mineral/soil factor at all cities. The modelling error when others analytes were excluded was estimated to be very narrow in Milan and Grenoble (11-13%) but large in Barcelona (39%) with a systematic underestimation.

Biogenic SOA and Anthropogenic SOA factors were sensitive to the presence of their molecular tracers, being OC only unable to separate a SOA factor alone. This contrarily to what found by Veld et al., (2022) where a SOA-like factor was found when combining urban and rural sites in a single PMF matrix. In addition, while Biogenic SOA contributions were very robust in the sensitivity analysis, the opposite was found for the Anthropogenic SOA.

Sea salt was traced either by ions (Cl^-, NO_3^-, Mg^{2+}..) and elements (Na, Cl, Mg, S) so that it is generally well identified, and even splitted in two factors (aged and fresh) depending on the input matrix. Error interval ranges within 33-45%.

Arabitol and sorbitol were crucial to detect fungal spores while odd number higher alkanes (C27 to C31) for plant debris. When other groups of analytes were excluded the error intervals in source contributions were symmetric and estimated in 23% and 18% respectively.

Based on the above results, the following general recommendations can be drawn for selecting the most appropriate species as input for PMF receptor modelling:

- In order to perform a decent source apportionment with the PMF technique, a data base including at least EC-OC, major ions (using ionic chromatography), trace element (by ICP-MS), and analysis of BB tracers (either by LC-PAD or by GC-MS) should be mandatory. This allows to identify most of the main contributors to PM in Europe, i.e dust, sea-salt (eventually separated into fresh and aged sea salt), traffic emissions (eventually separated between exhaust and non-exhaust), biomass burning aerosols, industrial emissions (possibly separated in different types depending on the knowledge of the emissions at the site), and possibly shipping emissions (characterized with V and Ni). It also leads to the determination of secondary inorganic aerosol factors (commonly separated into nitrate- and sulfate-rich components. However, such an approach does not allow to properly apportion primary biogenic emission, nor the various SOA fractions.

RI-URBANS (www.RIURBANS.eu) is supported by the European Commission under the Horizon 2020 – Research and Innovation Framework Programme, H2020-GD-2020, Grant Agreement number: 101036245

- If IC measurements include MSA and oxalate, it may lead to further determination of the main marine SOA fraction (traced with MSA) and to roughly apportion aged SOA factors originating from various origins (traced with oxalate),
- HPLC-PAD measurements for sugars alcohols (in particular arabitol and mannitol) may lead to the further determination of primary biogenic that can be a substantial PM fraction at some sampling sites, especially from Spring to late Autumn.

A refined PMF analysis, including the determination of further sources, requires additional measurements, such as secondary biogenic emission, including tracers like 3-MBTCA, 2-MT's, etc measured with techniques like GC-MS, LC-MS, and or IC-MS.

Inclusion of a range of PAH's measurements (or some HAP derivatives) may lead to some improvement in some combustion sources separations but results should be studied with caution in terms of chemical profile, since these species are coming from many various origins.

Inclusion of species like higher alkanes may also lead to some improvements in organic sources determination, especially plant debris, but results should also be considered with caution.

3. Non-refractory PM1 (NR-PM1)

The non-refractory PM_1 (NR-PM_1) is a group of pollutants, defined by their capacity to flash-vaporise at 600º, which are the main contributor to fine aerosol in Europe (Bressi et al., 2021). Near-real-time measurements of NR-PM_1 species are usually carried out throughfrom ACSM or AMS. These instruments use a mass spectrometer to measure the spectral composition of the incoming air after vaporisation and ionisation. Posteriorly, the ions are deconvolved to NR-PM_1 compounds by means of a fragmentation table and electronic signals to mass through calculations needing routine calibrations. After these steps, the software provides the non-refractory time series of OA, SO_4^{2-}, NO_3^-, NH_4^+, and Cl^-. The OA information can also be exported as a matrix of all the spectral species and time series. An error matrix is also provided, calculated as in Ulbrich et al. (2009).

According to Bressi et al. (2021), NR-PM_1 concentrations in Europe are higher in urban areas compared to regional and coastal sites. Latitudinally, there is also a clear pattern, being the highest concentrations in mid-latitude sites and followed by south-latitude and north-latitude sites, in this order. Although plenty of studies are carried out at regional sites, the focus of this document is set on the urban, peri-urban, urban background, and industrial sites, in which a broader aerosol chemical composition can be observed. For 17 European urban and industrial sites accounting 20 periods of measurement comprised between 2011 – 2019, the mean value of NR-PM_1 is 10.7 ± 7.0 $\mu g \cdot m^3$ (mean ± standard deviation, Table 5). Figure 7 shows the concentrations of NR-PM_1 across Europe, illustrating how the highest concentrations are located in the mid-latitudes.

Measurements from 2011 to 2021 from different studies using year-long datasets in European urban sites indicate that OA is the major contributor to PM_1 (46 ± 9%) (Bressi et al., 2021; Chen et al., 2022), as shown in Table 5. Also campaigns carried out in the 2008-2021 periods show similar proportion of OA with respect to the fine PM (Crippa et al., 2014; Petit et al., 2014; Srivastava et al., 2019). Mean proportions, in % of PM_1, of the other compounds are: (18 ± 7) for SO_4^{2-}, (16 ± 8) for NO_3^-, and (12 ± 4) for NH_4^+. During highly-polluted episodes, the concentrations of NO_3^- become more relevant, however, OA remains the main component of PM_1 (Bressi et al., 2021).

RI-URBANS (www.RIURBANS.eu) is supported by the European Commission under the Horizon 2020 – Research and Innovation Framework Programme, H2020-GD-2020, Grant Agreement number: 101036245

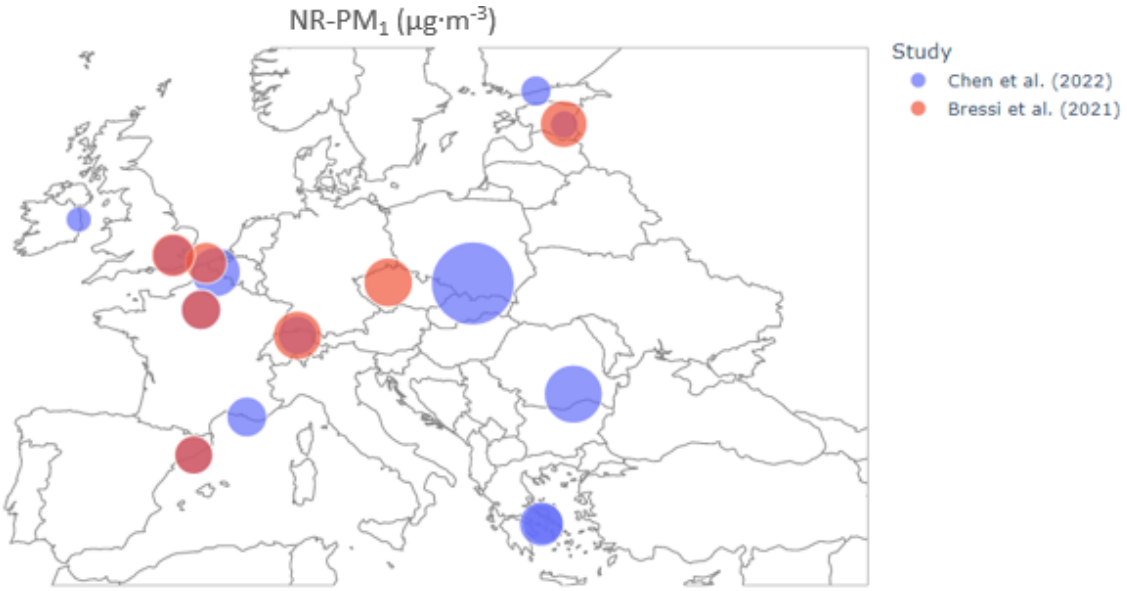

Figure 7. *European spatial distribution of the NR-PM_1 concentrations at urban sites compiled from the studies in Bressi et al. (2021) and Chen et al. (2022). The size of the circles corresponds to mass concentration. Note that some locations contain overlapped circles due to their participation in both studies.*

The OA concentrations vary season-wise depending on the availability of OA precursors, OA emissions and reactive species of the site. Contrarily, the seasonal behaviour of the Secondary Inorganic Aerosol (SIA) is quite spatially homogeneous across Europe. The high volatility of NO_3^- shows the largest seasonal variations with a minimum in summer and at midday hours which can be explained by a greater volatilization rate of NH_4NO_3 during warmer months and hours of the day, respectively. Similarly, many studies found that Cl^-, even being always very close or even below the detection limits is also affected by this volatility in warm periods (Tobler et al., 2020). Moreover, the likely emission of Cl^- in coal combustion episodes increases its concentrations in the coldest months (Tobler et al., 2021). The SO_4^{2-} concentrations increase during warmer months due to higher photochemistry. to a higher marine DMS production which in turn enhances SO_4^{2-} formation, amongst other causes. Oppositely, NH_4^+ concentrations are generally stable throughout the seasons.

In order to further investigate the spatio-temporal variability of OA, the identification of its components into sources is helpful. Source apportionment studies of the OA have been extensively carried out in Europe for more than a decade, and are usually conducted through the Positive Matrix Factorisation (PMF) receptor model. Two of the most complete studies showing the source apportionment of multiple sites in Europe are Crippa et al. (2014), joining AMS data from days-to-months periods without intraseasonal variability of chemical profiles ("seasonal PMF"), and Chen et al. (2022), which, in the framework of the RI-URBANS project, took advantage of the longer deployability of the ACSM and joined measurements lasting around a whole year, and allowing an intraseasonal variability of chemical profile ("rolling PMF"). These comprehensive studies and others are those used in Figures 8, 9, 10, and are described in Table 6 and a proper comparison of both "seasonal PMF" and "rolling PMF" methodologies in Via et al., (2022).

Figure 8 shows the OA source apportionment results of 20 datasets compiled at urban areas. The sources identified in these sites are: hydrocarbon-like OA (HOA), cooking OA (COA), biomass burning OA (BBOA), oxigenated OA (OOA), sometimes differentiated in less-oxidised OA (LO-OOA) and more-oxidised OOA (MO-OOA), cigarrete-smoke OA (CSOA), and shipping + industry OA (ShINDOA). This plot shows that in almost every site HOA, stemming from traffic activities, and biomass burning, both from agricultural emissions and residential heating, are present. This is

RI-URBANS (www.RIURBANS.eu) is supported by the European Commission under the Horizon 2020 – Research and Innovation Framework Programme, H2020-GD-2020, Grant Agreement number: 101036245

not the case for COA, which only appears at certain sites and periods (Zurich, Barcelona, Athens NOA, London, Athens DEM, and Marseille).

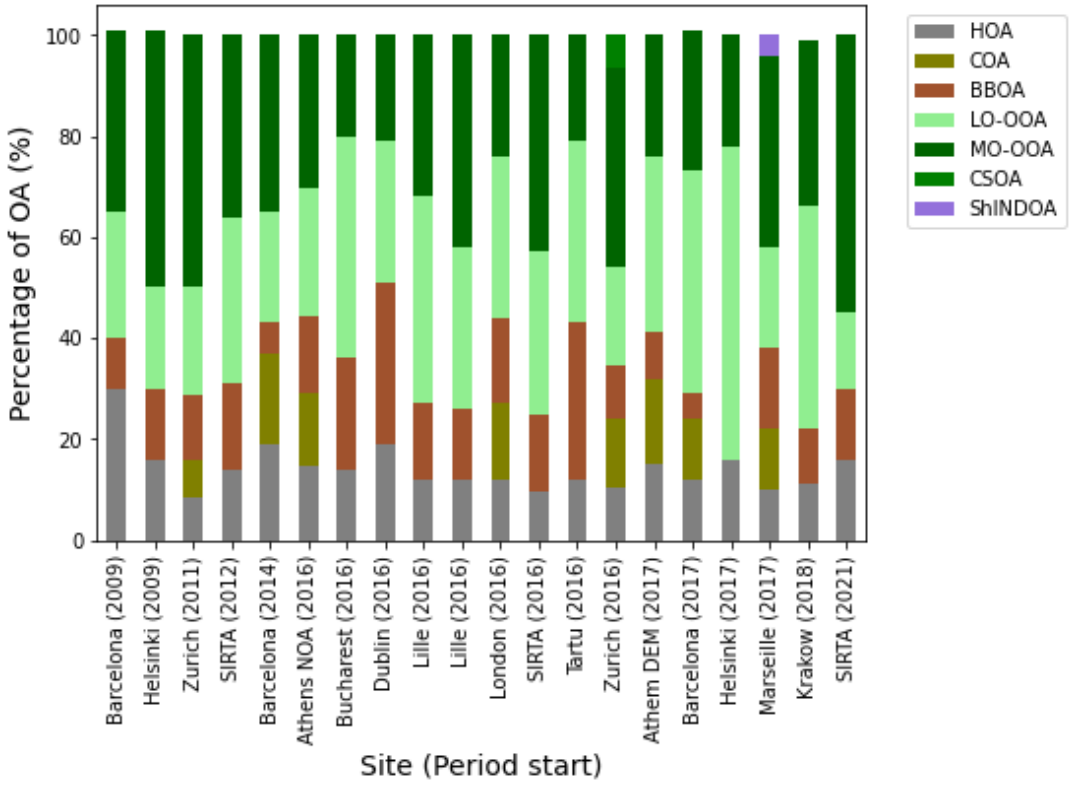

Figure 8. *Source apportionment overview of urban sites in Europe listed in Table 6. Site order is set on the starting year of the period of measurement.*

SOA is in all the cases the main constituent of OA. The differentiation of SOA into LO-OOA and MO-OOA is achieved in all the 20 presented datasets independently and the mean ratio LO-OOA-to-MO-OOA is 1.1 ± 0.6 (adim.). This ratio shows how even both states of SOA are balanced in mean, the variability is high (>60% of relative error), probably related to seasonal changes. Many studies point out that the LO-OOA might increase during summer related to the photochemical chemistry enhancement due to higher insolation, and MO-OOA, the more aged aerosol, is higher in winter.

Figure 8 does not depict any temporal trends from 2009 to 2021, neither concerning the primary nor the secondary OA. There is a lack of time and spatial coverage of source apportionment studies, hence long term trends in sources' contribution changes cannot be discarded. Some modelling studies already point out the likely decrease of OA emissions from the last 40 years (Yang et al., 2020) due to applied policies aiming to mitigate industrial, traffic and agricultural emissions. It is the aim of current research to study long-term aerosol trends of the OA and its sources and components.

Figure 9 shows the variability amongst the 20 European datasets of all factors in contributions (Fig. 9a) and in mass concentration (Fig. 9b). The highest contributions are those from the SOA factors, which in sum represents a 67% in median, being MO-OOA (34% median) slightly above the LO-OOA (32% median). Primary factors contribute in median a 13% for HOA, a 12% for COA, a 14% of BBOA, a 7% of CSOA (only identified in Zurich in 2016), and a 4% of ShINDOA (only identified in Marseille). Maximum proportions of POA do not exceed a 25% and SOA proportions are always a 45%, this is, its concentrations are often more than the half of the OA.

RI-URBANS (www.RIURBANS.eu) is supported by the European Commission under the Horizon 2020 – Research and Innovation Framework Programme, H2020-GD-2020, Grant Agreement number: 101036245

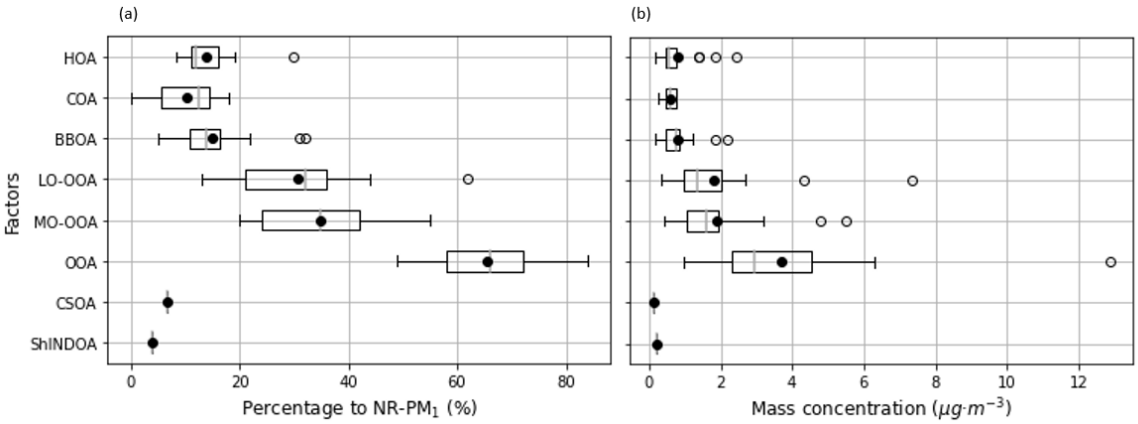

Figure 9. *Boxplots of the factors amongst the 25 urban datasets (a) in proportion and (b) in mass concentration. Boxes enclose the quartiles Q_1 and Q_1, the inside line represents the median and the whiskers 1.5·IQR range (IQR = Q_3-Q_1). Round solid dots represent the mean of all datasets and round transparent plots represent outliers.*

In terms, of absolute mass concentrations (Fig. 9b), POA concentrations are between 0 and 2 μg·m^{-3}. The HOA and BBOA concentrations present medians and means close to the upper ranges, meaning they include high concentrations at some sites. This observation implies that some sites can be referred as urban hotspots. SOA concentrations are in between 1 and 7 μg·m^{3} (excluding outliers) in total as mean of the whole periods, including the site with the lowest concentrations at least 1 μg·m^{-3}.

Using the same urban sites, an exploration of the effects of latitude showed a correlation of BBOA (Fig. 10a). This finding is supported in studies showing mid-latitudes present the highest concentrations of BBOA decreasing towards the equatorial latitudinal areas (Hu et al., 2013). In Europe, this must be related to higher emissions of biomass burning due to residential heating in the colder, higher latitude northern Europe compared to Mediterranean sites. Figure 10b shows a bad correlation of the ratio LO-OOA-to-MO-OOA, an indicator of how fresh is SOA, with latitude. This implies that is not only the quantity of insolation which regulates SOA formation in Europe, which is higher in lower latitudes, but also the precursor types and amounts' availability.

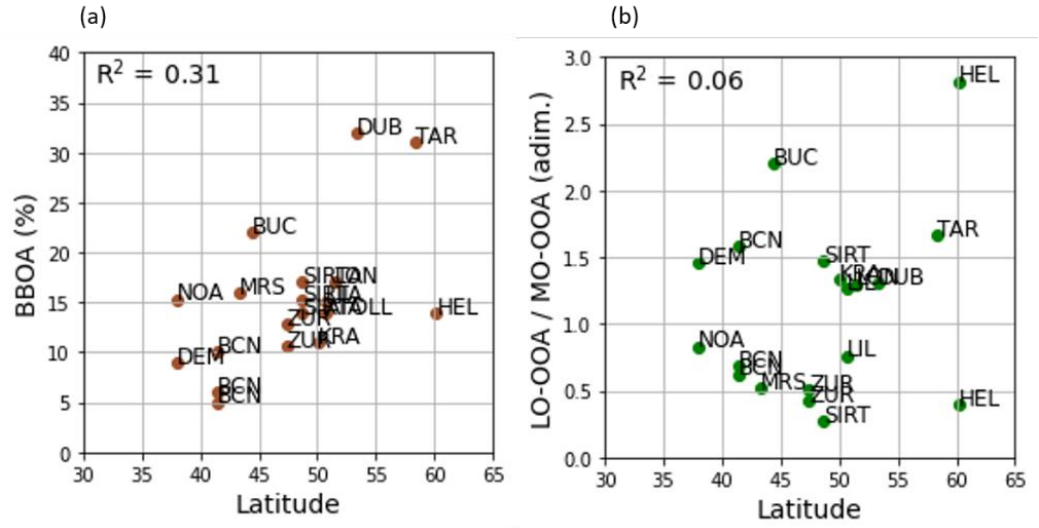

Figure 10. *Scatterplots of the urban European sites relation with latitude of (a) BBOA proportion and (b) LO-OOA-to-MO-OOA ratio. Labels refer to the acronyms of the sites.*

RI-URBANS (www.RIURBANS.eu) is supported by the European Commission under the Horizon 2020 – Research and Innovation Framework Programme, H2020-GD-2020, Grant Agreement number: 101036245

The accuracy and exactness of the determined sources cannot be determined beyond testing the receptor modelling error assessment. However, the verification of the accuracy of these sources' determination is usually conducted through the monitoring of these sources with their markers: HOA with BC_{lf} (black carbon emitted by combustion of liquid fuel, mainly related to traffic) and road dust metals, COA with m/z55 and cholesterol, BBOA with BC_{sf} (BC emitted by combustion of solic fuel, mainly related to biomass burning) and levoglucosan, and LO-OOA, MO-OOA with NO_3^-, and SO_4^{2-}, respectively and OOA with NH_4^+. However, some of these pairs are not expected to correlate perfectly such there might be other origins of these markers, or these could present also measurement error.

Also, anchoring the factors when running PMF has also been shown to guide the model towards better solutions (Crespi et al., 2016). The protocol established by Chen et al., (2022) advises to apply constraints from the general database both in the profiles and the time series at convenience for better performance. However, this application requires a testing phase in order to adjust the freedom of the receptor model with respect to the anchor applied. With this method, the outcoming factors can resemble those whose information was fed to the model, which are usually factors retrieved near the emission sources or retrieved in chamber studies so they are as pure as possible.

***Table 5**. Submicron aerosol composition of 20 year-long datasets across Europe. Mean concentrations of the non-refractory part and its mean contributions are shown.*

Site	Acronym	Country	Start date	End date	NR-PM_1 ($\mu g \cdot m^{-3}$)	OA (%)	SO4 (%)	NO3 (%)	NH4 (%)	Study	PM_1
Barcelona	BCN	ES	19/05/2014	26/05/2015	7.9	52	23	12	13	Bressi 2021	-
Durnkirk	DNK	FR	15/07/2013	11/09/2014	9.1	37	29	21	13	Bressi 2021	-
London	LND	UK	11/01/2012	23/01/2013	9.9	49	19	19	13	Bressi 2021	-
Prague	PRA	CZ	20/06/2012	15/05/2013	12.8	45	21	21	13	Bressi 2021	-
SIRTA	SIR	FR	01/06/2011	01/06/2014	8.3	57	12	19	12	Bressi 2021	-
Tartu	TTU	EE	05/02/2014	01/05/2015	11.8	64	14	9	13	Bressi 2021	-
Zurich	ZUR	CH	04/02/2011	23/02/2012	12.6	55	18	16	11	Bressi 2021	-
Athem DEM	DEM	EL	01/07/2017	01/08/2018	8.7	47	31	4	9	Chen 2022	9.6
Athens	NOA	EL	01/07/2016	01/07/2017	10.5	47	31	4	9	Chen 2022	11.5
Barcelona	BCN	ES	01/09/2017	01/10/2018	7.8	43	17	15	11	Chen 2022	9
Bucharest	BUC	RO	01/07/2016	01/08/2017	18.1	50	19	15	9	Chen 2022	19.7
Dublin	DUB	IR	01/08/2018	01/08/2018	3.6	46	11	13	12	Chen 2022	4.4
Helsinki	HEL	FI	01/04/2017	01/05/2018	5	53	13	11	5	Chen 2022	6.1
Krakow	KRA	PO	01/01/2018	01/04/2019	36.8	41	15	11	1	Chen 2022	40.4
Lille	LIL	FR	01/10/2016	01/11/2017	13	35	10	33	14	Chen 2022	14
London	LON	UK	01/10/2016	01/02/2018	8.6	43	9	28	12	Chen 2022	9.5
Marseille	MRS	FR	01/01/2017	01/10/2018	8.6	50	14	10	9	Chen 2022	10.2
SIRTA	SIRTA	FR	01/01/2016	01/05/2017	8.8	43	11	24	10	Chen 2022	9.7
Tartu	TAR	EE	01/08/2016	01/07/2017	4.2	42	15	8	5	Chen 2022	6

RI-URBANS (www.RIURBANS.eu) is supported by the European Commission under the Horizon 2020 – Research and Innovation Framework Programme, H2020-GD-2020, Grant Agreement number: 101036245

Table 6. *Overview of the OA source apportionment results for 25 urban datasets from ACSM or AMS measurements.*

Site	Acronym	Period start	Period (days)	Lat	Lon	Reference study
Barcelona	BCN	02/2009	35	41.386	2.118	Crippa et al. (2014)
Helsinki	HEL	02/2009	19	60.192	24.946	Crippa et al. (2014)
Zurich	ZUR	02/2011	365	47.4	8.5	Canonaco et al. (2013)
SIRTA	SIRTA	01/2012	60	48.7	2.2	Petit et al. (2014)
SIRTA	SIRTA	11/2012	1946	48.7	2.2	Zhang et al. (2019)
North Kensington	NK	03/2013	245	51.5215	-0.2129	Reyes-Villegas et al. (2016)
Atlanta	JST	03/2014	337	33.6867	-84.42	Rattanavaraha et al. (2014)
Barcelona	BCN	05/2014	365	41.386	2.118	Via et al. (2021)
SIRTA	SIRTA	01/2016	486	48.7	2.2	Petit et al. (2021), Zhang et al. (2019)
Athens NOA	NOA	07/2016	365	37.973	23.718	Stavroulas et al. (2019)
Bucharest	BUC	07/2016	396	44.44	26.096	Mărmureanu et al. (2020)
Zurich	ZUR	08/2016	334	47.4	8.5	Chen et al. (2022)
Tartu	TAR	08/2016	334	58.4	26.7	Chen et al. (2022)
Dublin	DUB	08/2016	730	53.35	-6.266	Lin et al. (2019)
London	LON	10/2016	488	51.5	0.2	Chen et al. (2022)
Lille	LIL	10/2016	396	50.629	3.057	Chen et al. (2022)
Lille	ATOLL	10/2016	1522	50.629	3.057	Chebaicheb et al. (2023)
Demokritos	DEM	01/2017	31	37.995	23.816	Zografou
Marseille	MRS	01/2017	638	43.296	5.37	Chazeau et al. (2021, 2022)
Helsinki	HEL	04/2017	395	60.192	24.946	Barreira et al. (2021)
Athem DEM	DEM	07/2017	457	37.995	23.816	Chen et al. (2022)
Barcelona	BCN	09/2017	395	41.386	2.118	Via et al. (2021)
Krakow	KRA	01/2018	455	50.05	19.945	Tobler et al. (2021)
SIRTA	SIRTA	03/2021	15	48.7	2.2	Srivastava et al. (2019)

3.1 Recommendations

NR-PM_1 compounds near-real-time measurements are usually captured from ACSM or AMS. These instruments use a mass spectrometer to measure the spectral composition of the incoming air after vaporisation and ionisation. Posteriorly, the ions are deconvolved to NR-PM_1 compounds by means of a fragmentation table and electronic signals to mass through calculations needing routine calibrations. After these steps, the software provides the non-refractory time series of OA, SO_4^{2-}, NO_3^-, NH_4^+, and Cl^-. The OA information can also be exported as a matrix of all the spectral species and time series. An error matrix is also provided, calculated as in Ulbrich et al. (2009).

These organic matrices are those which are introduced to receptor models, amongst which the most widely used and further developed is the Positive Matrix Factorisation (PMF), for OA source apportionment purposes. This model provides OA sources which explain the introduced matrices as a linear combination and an error matrix, which is minimised iteratively. These sources comprise a time series, showing the temporal evolution of the source and a profile, the proportions of the ions which contribute to that source. The profiles are considered static by the algorithm throughout the whole period of analysis, an assumption which has been refuted since the sources' fingerprints are expected to vary along the seasons (Canonaco et al., 2015), especially for the longer ACSM sampling deployments.

RI-URBANS (www.RIURBANS.eu) is supported by the European Commission under the Horizon 2020 – Research and Innovation Framework Programme, H2020-GD-2020, Grant Agreement number: 101036245

For this reason, methodologies to bridge this drawback were developed. The seasonal PMF consisted in splitting by seasons the initial matrices, apply PMF independently to all of them and after that, concatenate the resulting time series and show the seasonal profiles. Rolling PMF was developed so that a rolling PMF window of 7-28 days (user preference) sweeps the whole period and hence it adapts better profile-wise. This method was shown to enhance the PMF performance (Via et al., 2022), although some prior testing with seasonal PMF is advised before applying rolling PMF.

Another common practice when applying PMF to OA data is its coupling with other measurements. Combination of OA matrices and the rest of NR-PM_1 species was conducted and showed improved source identification with respect to the conventional OA source apportionment (Zografou et al., 2022). Also, there are studies combining ACSM instrumentation with other instruments: Aethalometer (Forello et al., 2019), X-ACT (Belis et al., 2019), offline filters (Srivastava et al., 2019) etc. For this purpose, it is advisable to employ the multi-time-resolution PMF, which through a modification of the PMF equation, it enables assimilating datasets of different time resolutions without averaging one of them, a practice which worsens the quality of the solution (Belis et al., 2019; Via et al., 2023). The coupling of ACSM OA datasets with other instrumentation datasets was always reported beneficial in terms of environmental feasibility of the sources studied.

Moreover, the acquisition of parallel measurements is also advised for monitoring purposes of co-variating species with sources. If clearly correlated, these ancillary measurements can even be used as an anchor for PMF time series anchoring. Besides for that purpose, the most advised co-located measurements are black carbon, if possible speciated upon their origin into liquid and solid fuel, used both for PM_1 mass closure and for verifying the correlation with traffic and biomass burning sources. Other useful ancillary measurements are NO, NO_2, SO_2, CO and O_3 gases concentrations and metals at high-time resolution from X-ACT.

4. Online and offline datasets combination in a single PMF: Multi-time-resolution PMF

It is important to highlight that Via et al. (2023), in the framework of RI-URBANS, has developed an online and offline datasets combination in a single PMF that allows combining for example 24 h resolution data on metals with the online ACSM speciation and this improves teh resolution of the source apportionment of the offline and online source apportionments.

There one year of co-located measurements in Barcelona, Spain, of non-refractory submicronic particulate matter (NR-PM1), black carbon (BC) and metals were obtained by a Q-ACSM (Aerodyne Research Inc.), an aethalometer (Aerosol d.o.o.) and fine offline quartz-fibre filters, respectively. These data were combined in a MTR PMF analysis preserving the high time resolution (30 min for the NR-PM1 and BC, and 24 h every 4^{th} day for the offline samples). The MTR-PMF outcomes were assessed varying the time resolution of the high-resolution data subset and exploring the error weightings of both subsets. The time resolution assessment revealed that averaging the high-resolution data was disadvantageous in terms of model residuals and environmental interpretability. The MTR-PMF resolved eight PM1 sources: ammonium sulphate + heavy oil combustion (25%), ammonium nitrate + ammonium chloride (17%), aged secondary organic aerosol (SOA) (16%), traffic (14%), biomass burning (9%), fresh SOA (8%), cooking-like organic aerosol (5%), and industry (4%). The MTR-PMF technique identified two more sources relative to the 24 h base case data subset using the same species and four more with respect to the pseudo-conventional approach mimicking offline PMF, indicating that the combination of both high and low TR data is significantly beneficial for SA. Besides the higher number of sources, the MTR-PMF technique has enabled some sources disentanglement compared to the pseudo-conventional and base case PMF as well as the characterisation of their intra-day patterns.

The species used in this SA consisted on the organic mass spectra, SO_4^{2-}, NO_3^-, NH_4^+, and Cl^- from Q-ACSM at a 30 min time resolution (TR); black carbon (BC) speciated into BC liquid fuel (BC_{lf}) and BC solid fuel (BC_{sf}) from aethalometer at 30 min TR; and metal species (Ca, Al, K, Mg, Na, Ti, V, Cr, Mn, Co, Ni, Cu, Zn, As, Sn, Sb, Pb) from

RI-URBANS (www.RIURBANS.eu) is supported by the European Commission under the Horizon 2020 – Research and Innovation Framework Programme, H2020-GD-2020, Grant Agreement number: 101036245

offline samples at a TR of 24 h every 4th day. The use of the Positive Matrix Factorisation (PMF) model for the ensemble of the so-called high-resolution data subset (HR, 30-minutes TR) and the low-resolution data subset (LR, 24 h every 4th day TR) taken together implied the use of the multi-time resolution (MTR) PMF.

The reader directed to Via et al. (2023) to see the details of the methodology.

4.1 Recommendations

The extended practice of averaging the high time resolution (TR) data subsets to reduce the TR difference with the lower TR data subsets or even to match it has been proven disadvantageous for model performance and error minimisation as also reported by Kuo et al., 2014, Liao et al., 2013. High TRs do not represent noise to PMF since stable, robust sources are retrieved profiting the 30 min TR for disentangling sources. For instance, the COA, which was only resolved by using high TR data since its diel cycle is vital for its differentiation.

The use of a greater number of species has enabled the characterisation of specific sources traced by key species not present in all datasets. This is the case, for instance, of the inclusion of industrial markers, which have enabled the characterisation of the industry source, whose description with only OA, SIA and BC species would have been less conclusive.

The MTR-PMF provided an environmentally reasonable PM1 SA with more speciated and detailed sources with respect to the other approaches and previous studies in the area using simpler SA methodologies, even if they contain longer time series or if they contain a greater number of species.

Coherent matches of OA fingerprints and SIA, BC, and metal species were found in the MTR-PMF solution. e.g. BBOA with BCsb, K; HOA with BClf, Sb; LO-OOA with AN; industry metal markers with Cl, m/z58, m/z86, etc.

The Foverlap method for weighting uncertainties proposed by Tong et al. (2022) does not necessarily lead to the most environmentally reasonable solution. The investigation of other runs whose Foverlap is similar to F*overlap is advisable to obtain the best SA.

This is the first study that applies MTR-PMF aiming to provide an exhaustive PM1 SA assessing both the uncertainty weighting and TR SA impacts. Further research should aim to standardise these assessments to be able to include all kinds of instrument measurements to retrieve more powerful SA results aimed for both modelling and health research and mitigation policy enforcements.

5. Equivalent Black Carbon (eBC)

Black carbon (BC) is a pollutant of growing interest originated by incomplete combustion. BC is usually estimated from the light abosrotion measuremrent at different waveleghts (see also Deliverable D1.1 at https://riurbans.eu/wp-content/uploads/2022/10/RI-URBANS_D1_D1_1.pdf). BC determined form absorption measurements by using Mass Absorption (or attenuation) cross section (MAC) is usually named as eBC equivalent black carbon (eBC).

To evaluate the relative contributors of eBC_T (emitted by traffic) and eBC_{RC} (emitted by residential and commercial combustion) at the RI-URBANS sites, an aethalometer model was employed; this uses the multi-wavelength absorption data obtained from the AE33 following a procedure initially developed by (Sandradewi et al., 2008). Briefly, the model uses a bilinear method to estimate both eBC sub-fractions. This model has been widely applied and used by numerous investigators, discriminating between mostly traffic (eBC_T,notably including diesel, gasoline and natural gas combustion) and residential and commercial (eBC_{RC}, biomass or coal combustion) eBC components (Becerril-Valle et al., 2017; Favez et al., 2010; Grange et al., 2020; Harrison et al., 2013; Helin et al., 2018; Tobler et al., 2021; Virkkula, 2021). The AE model was applied using 23 AE33 datasets taken from the RI-URBANS database (LINK a database). The source apportionment analysis used time series data between 2017–2019. The aethalometer

RI-URBANS (www.RIURBANS.eu) is supported by the European Commission under the Horizon 2020 – Research and Innovation Framework Programme, H2020-GD-2020, Grant Agreement number: 101036245

model uses pre-defined source-specific absorption Ångström exponents (AAEs) as recommended by Sandradewi et al. (2008) and Zotter et al. (2017).

The AAE is an optical parameter that describes the spectral dependence of light absorption by aerosols. It has been intensively employed for eBC source apportionment and aerosol characterization (e.g., BC, Brown Carbon "BrC", and dust) (Garg et al., 2016; Li et al., 2016; Liu et al., 2018; Wang et al., 2021; Zhang et al., 2019). An AAE of around 1 indicates that the absorption is dominated by BC; a progressive increase in AAE is associated with an increasing contribution from non-BC absorbing components such as BrC or mineral dust (Zhang et al., 2020a, 2020b). The application of the aethalometer model requires a priori knowledge of the AAE of the main sources of BC. Values of around 1 and 2 for the two wavelengths of 470 and 950 nm are commonly used for traffic and residential, commercial sources (e.g., biomass burning and coal combustion), respectively (Sandradewi et al., 2008). More recent estimates based on ^{14}C analysis have suggested values of 0.90 and 1.68 (Zotter et al., 2017). However, both AAE values may vary significantly depending on the type of fuels being burnt, burning conditions, and the microphysical properties of the BC particles (the size of the BC particle and internal mixing with non-absorbing or less absorbing material): a single value cannot be representative of the whole measurement period considered (Helin et al., 2021; Li et al., 2016; Liu et al., 2018). For this reason, the aethalometer source apportionment model is associated with uncertainties related to fixed specific AAEs for traffic-related and for residential and commercial emission sources [AAE_T and AAE_{RC}, respectively] (Harrison et al., 2013; Helin et al., 2021; Zotter et al., 2017).

Thus, the selection of robust AAE values is a critical component of the aethalometer model and has been validated in previous studies using ^{14}C observations as well as other auxiliary measurements such as Elemental Carbon, Organic Carbon (EC/OC) (Sandradewi et al., 2008; Zotter et al., 2017). This study follows the conventional approach of using fixed AAE values for the source apportionment of AE33 observations due to the lack of ancillary measurements (such as ^{14}C measurement data) that could be used to determine site-dependent AAEs. Thus, AAE values of 1 and 0.90 were used for eBC_T, while AAE values of 2 and 1.68 were used for eBC_{RC} for the wavelengths of 470 nm and 950 nm, respectively. The results obtained were compared to evaluate the variations across different regions due to the limitation of constant AAE values (Savadkoohi et al., 2023).

Figure 11 shows the results of the aethalometer source apportionment model in Europe for $AAE_T = 1$ and $AAE_{RC} = 2$ (Sandradewi et al., 2008). It shows the regional variations in the relative contributions of eBC_T and eBC_{RC} with an increasing trend in the relative contribution of eBC_T from Northern to Central, Western, and South-Western Europe. The outcomes of the source apportionment analysis are summarized in Figure 12, which provides a comparison of the relative contributions of eBC_T and eBC_{RC} between the TR and the UB/SUB sites using stacked histograms; the error bars indicate the respective variances of the two sources. It shows that eBC_T had consistently higher relative contributions compared to eBC_{RC}. The highest relative contribution of eBC_T was obtained in PAR_TR (88%), STH-TR (87%), and MLN_TR (82%) sites. However, there were some regions and sites at which eBC_{RC} contributions were also relatively high (Savadkoohi et al., 2023).

Previous research has shown that eBC mass concentrations are predominantly influenced by residential and commercial combustion sources—particularly wood burning—during heating seasons (Crilley et al., 2015; Herich et al., 2011; Zhang et al., 2020). The greatest relative eBC_{RC} contribution was observed at BUC_SUB (39%), the HEL_SUB sites (30–34%), GRA_UB (30%), BER_UB (27%), and MLN_UB (26%). The lowest eBC_T contributions were observed in Eastern Europe, while the highest contributions were recorded in Central and Western Europe (88%, 82%, and 74% at PAR_TR, MLN_TR2, and MLN_UB, respectively). It is worth noting that the relative contribution of eBC_T in the Northern TR sites was much lower compared to TR sites in Western Europe, such as PAR_TR, with the exception of the UB and TR sites of MLN in Central Europe. In contrast, in South-Eastern Europe, both ATH_UB and ATH_SUB exhibited higher relative contributions of eBC_T despite being recognized as hot spots for residential wood burning, especially during winter (Kaskaoutis et al., 2021; Liakakou et al., 2020). There was a clear decreasing trend

RI-URBANS (www.RIURBANS.eu) is supported by the European Commission under the Horizon 2020 – Research and Innovation Framework Programme, H2020-GD-2020, Grant Agreement number: 101036245

in eBC_{RC} contributions from Northern to Central and Southern Europe. In Central, Eastern, and Northern Europe, the relative contribution of eBC_{RC} to eBC was found to be higher compared to other regions (39% in BUC_SUB, 30–34% in HEL_SUB sites, and 26% in MLN_UB). This pattern may be due to the increased emissions of solid fuel from residential areas during the cold season in these particular regions (Savadkoohi et al., 2023).

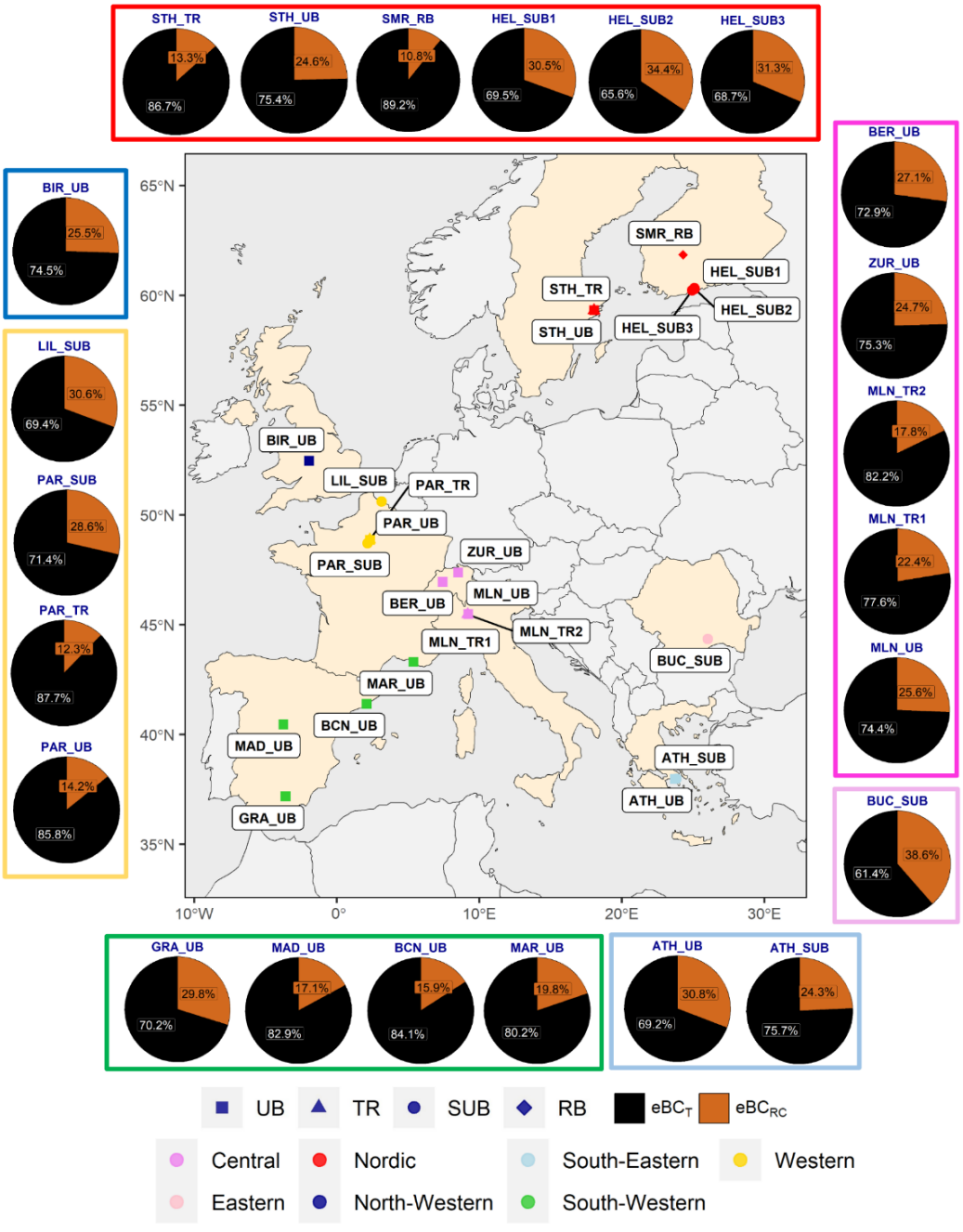

Figure 11. *The results of the source apportionment analysis of eBC mass concentrations for 23 European sites used over the study period (2017–2019). The aethalometer model was applied using (AAE_T =1) for traffic emission sources and (AAE_{RC} = 2) for residential and commercial emission sources. The colors highlight the geographic locations of the sites that supplied AE33 eBC data. Figure from* Savadkoohi et al., 2023

RI-URBANS (www.RIURBANS.eu) is supported by the European Commission under the Horizon 2020 – Research and Innovation Framework Programme, H2020-GD-2020, Grant Agreement number: 101036245

The higher relative eBC_{RC} contributions in South-Eastern Europe (ATH sites) during winter are likely attributed to the burning of wood for heating purposes (ATH_UB 31%, ATH_SUB 24%). Consequently, the ratio of biomass to fossil-fuel combustion emissions in this region was higher in winter, particularly on weekends (Kaskaoutis et al., 2021; Merabet et al., 2019). The SMR_RB station is mainly affected by regionally sourced and long-range transported pollutants in Northern Europe (Hyvärinen et al., 2011). In addition, the SMR_RB station may be affected by the surrounding station buildings as well as the city of Tampere itself (Yttri et al., 2011). In the Helsinki region, stations HEL_SUB1 to HEL_SUB3 are located in detached housing areas that are affected by the utilization of fireplaces for wood burning in winter (32% relative contribution to eBC_{RC}) in addition to road traffic emissions (Helin et al., 2018; Fung et al., 2022). STH_TR, located in the city center, is heavily influenced by traffic emissions (75% eBC_T) (Krecl et al., 2011, 2017).

Of the South-Western UB sites, high contributions of eBC_T and eBC_{RC} were observed in BCN_UB (84%) and GRA_UB (30%), respectively. Similarly, MAD_UB (83%) and MAR_UB (80%) also exhibited high relative contributions of eBC_T, consistent with findings reported by Baldasano (2020). MAR_UB site is located in the most important Mediterranean seaport and is consequently influenced by a substantial amount of industrial urban emissions (Chazeau et al., 2022; El Haddad et al., 2013; Salameh et al., 2018). In Western sites, high eBC_T and eBC_{RC} contributions were observed in sites that are influenced by heavy traffic and biomass burning, such as PAR_TR (88%) and LIL_SUB (31%), respectively. In particular, LIL_SUB is highly influenced by biomass-burning emissions during spring, autumn, and winter as previously reported by Cordell et al. (2016). A recent study conducted at the LIL_SUB site revealed that, during the winter season, a significant portion of the organic aerosols consisted of less oxidized fractions (LO-OOA), which was identified as originating from aged biomass burning. The study suggests that approximately half of the organic aerosols generated during winter can be attributed to wood combustion (Chebaicheb et al., 2023). In North-Western Europe, BIR_UB exhibited a dominant contribution of eBC_T (74%) due to its higher traffic emissions compared to domestic heating; this was consistent with a previous study on the variations and level of the eBC_T contribution at BIR_UB by Singh et al. (2018). In general, the relative contribution of eBC_T and eBC_{RC} is influenced by the geographical location and the prevailing type of combustion source at each station.

Moreover, we performed a comparison of the relative contributions of eBC_{RC} and eBC_T using two sets of AAE values: 1 and 2, and the AAE values proposed by Zotter et al. (2017). In general, the relative contribution of residential and commercial sources to eBC increased by 25–45% when using the Zotter values. It should be noted that the AAE values proposed by Zotter et al. (2017), were determined at Swiss sites that were strongly influenced by biomass-burning emissions. However, based on the available data, we cannot definitively conclude which AAE pair (1, 2 vs. 0.90, 1.68) was more appropriate for the sites considered in our study. It is reasonable to apply the Zotter AAE values at sites with similar characteristics to those used in Zotter et al. (2017). However, there are some concerns regarding the extensive use of Zotter values. For instance, in Barcelona, the Zotter values result in an excessively high contribution of eBC_{RC} to eBC (41% in winter), which contradicts recent studies demonstrating the very low contribution of biomass-burning to OA in the city (4–6% in winter; Via et al. 2021).

It thus cannot be assumed that the AAE values remain constant across all sites. To minimize these uncertainties, the use of site-specific AAE values is recommended; alternatively, a range of robust and consistent AAE values that accounts for the variability observed in the specific study area should be used. There are studies that have recommended the use of AAE frequency distributions as an alternative method to estimate site-specific AAE values (Tobler et al., 2021). Alternatively, the incorporation of time-dependent AAEs into the aethalometer model can be proposed, with the aim of evaluating its performance.

RI-URBANS (www.RIURBANS.eu) is supported by the European Commission under the Horizon 2020 – Research and Innovation Framework Programme, H2020-GD-2020, Grant Agreement number: 101036245

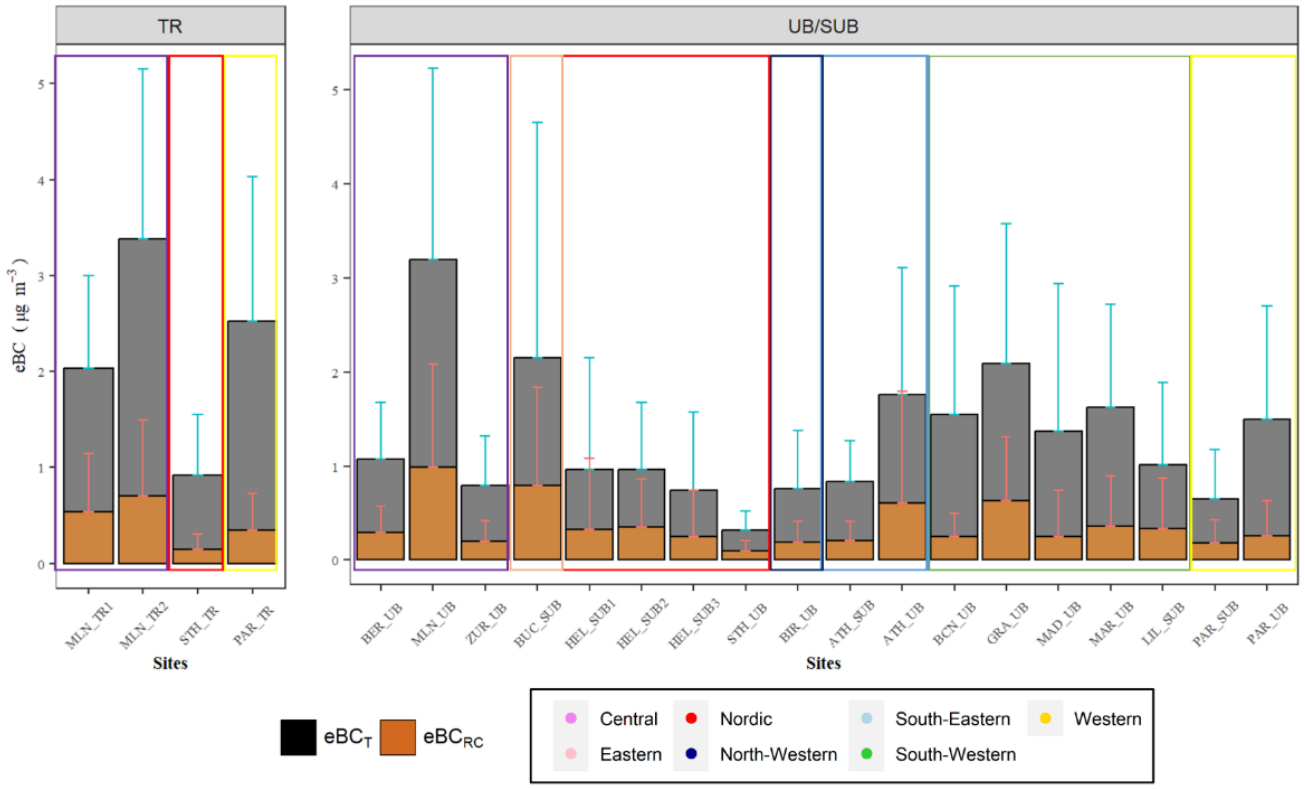

Figure 12. *The source apportionment analysis results of TR (traffic) vs UB/SUB (urban/suburban) sites. Stacked histograms with error bars were used to present the variance associated with the two sources based on geographic regions. Figure from Savadkoohi et al., (2023)*

5.1 Recommendations

5.1.1 eBC concentrations as provided by Aethalometers

eBC concentrations are calculated by AE software through two steps. In the first step (Step 1) the measured ATN is converted into absorption coefficient (ABS). For this, two artifacts related to the presence of the filter tape are considered. One artifact consists in an increase of the measured ATN due to the scattering of light by the filter tape (C_0). The other artifact consists in the progressive loss of sensitivity due to the progressive accumulation of particles on the filter tape (factor loading effect; FL). In the second step (Step 2) the ABS is converted into eBC concentrations assuming a specific and constant Mass absorption (or attenuation) cross section (MAC) of BC particles.

Step 1:

All AE instruments convert ATN to ABS using predefined and constant C_0 that depends on the filter tape used. For the older filter tapes (M8020 and M8050) C_0 is equal to 1.57. For the new filter tape (M8060) C_0 is 1.39. The filter tape M8060 is the recommended one (available since October 2017). The C_0 values are set in the instrument software and must be changed manually if the filter tape is replaced with a different one. The older AE models (AE31, AE22) do no correct online for FL and offline correction is needed. Thus, the users have to correct eBC concentrations for FL. Different schemes are available to correct AE data for this artefact (Savadkoohi et al., 2023). This document does not recommend a specific scheme. Conversely, the new AE33 model corrects online for FL.

RI-URBANS (www.RIURBANS.eu) is supported by the European Commission under the Horizon 2020 – Research and Innovation Framework Programme, H2020-GD-2020, Grant Agreement number: 101036245

Step 2:

Old AE models calculate eBC from ATN at 880 nm using a MAC of 16.6 m^2g^{-1} at 880 nm and C_0=1.57.

$$\mathrm{eBC}\ [\mu g\ m^{-3}] = \frac{\mathrm{ATN}^{880\ nm}\ [Mm^{-1}]}{16.6\ [m^2g^{-1}]\cdot 1.57}$$

eBC concentrations from AE31 and AE22 models have to be corrected for FL by the users.

The new AE33 model calculates eBC from ATN at 880 nm using a MAC of 7.77 m^2g^{-1} at 880 nm and C_0=1.57 or 1.39 depending on the filter tape used.

$$\mathrm{eBC}\ [\mu g\ m^{-3}] = \frac{\mathrm{ATN}^{880\ nm}\ [Mm^{-1}]}{7.77\ [m^2g^{-1}]\cdot C_0}$$

5.1.2 Harmonization of absorption measurements

eBC source apportionment is commonly performed using the Aethalometer model (Sandradewi et al., 2008). This model uses the 7-□ absorption measurements provided by AE instruments. ACTRIS provides the harmonization factors necessary to convert the ATN measured with AE instruments into ABS. These harmonization factors are needed because the C_0 is different from the one used in the AE software. Below the equations are reported:

For AE31 and AE21:

$$\mathrm{ABS}_\lambda\ [\mu g\ m^{-3}] = \frac{\mathrm{eBC}_\lambda [\mu g\ m^{-3}]\cdot \mathrm{MAC}_\lambda\ [m^2g^{-1}]}{3.5}$$

Where:

Wavelength [nm]	370	470	520	590	660	880	950
MAC [m^2g^{-1}]	39.5	31.1	28.1	24.8	22.2	16.6	15.4

For AE31 and AE22, the eBC data have to be corrected for FL before calculating the ABS.

For AE33:

$$\mathrm{ABS}_\lambda\ [\mu g\ m^{-3}] = \frac{\mathrm{eBC}_\lambda [\mu g\ m^{-3}]\cdot \mathrm{MAC}_\lambda\ [m^2g^{-1}]}{H^*}$$

Where:

Wavelength [nm]	370	470	520	590	660	880	950
MAC [m^2g^{-1}]	18.47	14.54	13.14	11.58	10.35	7.77	7.19

And

Filter	H*	C_0
M8020/ M8050	2.21	1.57
M8060	1.76	1.39

5.1.3 Selection of AAE_T and AAE_{RC} for eBC source apportionment

For the application of the Aethalometer model the Absorption Angstrom Exponent (AAE) of liquid fuel combustion (mainly related to traffic; AAE_T) and solid fuel combustion (mainly from residential and commercial wood and coal burning; AAE_{RC}) have to be selected. The Aethalometer model is based on the fact that solid fuel sources emit eBC

RI-URBANS (www.RIURBANS.eu) is supported by the European Commission under the Horizon 2020 – Research and Innovation Framework Programme, H2020-GD-2020, Grant Agreement number: 101036245

together with specific organic aerosols (OA) that can absorb in the UV-VIS spectral range (the so-called Brown Carbon, BrC) thus causing an increase of AAE. Conversely, it is commonly assumed that BrC is not emitted, or it is emitted in very low amounts, from liquid fuel combustion sources as traffic and that the AAE is close to one. Usually, two pairs of values are used: 1 and 2 for AAE_T and AAE_{RC}, respectively (Sandradewi et al., 2008), and 0.90 and 1.68, respectively (Zotter et al., 2017). The values from Zotter were calibrated using ^{14}C measurements and are considered as the values that should be used where traffic and biomass burning (BB) are the only sources of eBC. However, other solid sources than BB (e.g., coal combustion), or liquid fuel sources as shipping, can emit BrC but the AAE_{RC} associated to these sources has been poorly characterized.

In summary:

- The model performance was investigated resulting from using site-dependent AAE_{lf} and AAE_{sf} determined from measurements in ambient air.
- Values of around 1 (AAE_{lf}; liquid) and 2 (AAE_{sf}; solid) were commonly used for liquid fuel and solid fuel burning aerosols, respectively Sandradewi et al (2008), Zotter et al (2017).
- Recent studies on comparison of the relative contributions of eBC_{sf} and eBC_{lf} using two sets of AAE values: 1 and 2, and the AAE values proposed by Zotter et al. (2017) revealed that, the relative contribution of solid fuel sources to eBC increased by 25–45% when using the Zotter values (Savadkoohi et al. 2023).
- AAE values proposed by Zotter et al. (2017), were determined at Swiss sites that were strongly influenced by biomass-burning emissions.
- We cannot definitively conclude which AAE pair (1, 2 vs. 0.90, 1.68) was more appropriate for the different European sites.
- It is reasonable to apply the Zotter AAE values at sites with similar characteristics to those used in Zotter et al. (2017). However, there are some concerns regarding the extensive use of Zotter values. For instance, in Barcelona, the Zotter values resulted in an excessively high contribution of eBC_{sf} to eBC (41% in winter; Savadkoohi et al. 2023), which contradicts recent studies demonstrating the very low contribution of biomass-burning to OA in the city of Barcelona (4–6% in winter; Via et al. 2021).
- If, on one side, the determination of the proper AAE_{RC} can be challenge, the determination of AAE_T from experimental data is possible.
- AAE_T can be set as the first percentile of the AAE frequency distribution. Only AAE values obtained from fit with R^2>0.99 should be used.
- The AAE can be calculated as the linear fit in a log-log space between the seven harmonized absorptions from AE instruments and the corresponding wavelengths.
- Preliminary results indicated that whilst the 1st percentile provides a robust AAE_{lf} for the Aethalometer model, the use of the 99th percentile to estimate the AAE_{sf} is limited to those measurement sites with a strong impact from solid sources.
- Performing a sensitivity study using simultaneous measurements of 3 sites in BCN and 1 site in a small town (Manlleu) performing a winter campaign affected by traffic and high biomass burning emission provided distinct AAE values (e.g., Manlleu: Percentile 99^{th}=1.7 approximately; see Figure 13).
- At BCN, shipping emissions contribute predominantly to Brown Carbon (BrC). Despite ships burning fossil fuels, the emissions classified as fossil-based eBC actually fall into the category of solid fuel. The use of 14C as a tracer can only be effective when distinguishing between fossil sources exclusively characterized as LIQUID and non-fossil sources exclusively characterized as SOLID.
- Considering this, shipping emissions represent a significant source of light-absorbing organic aerosols, particularly in port areas. As a result, precisely defining liquid and solid sources of BC to accurately attribute emissions from different sources is important.

RI-URBANS (www.RIURBANS.eu) is supported by the European Commission under the Horizon 2020 – Research and Innovation Framework Programme, H2020-GD-2020, Grant Agreement number: 101036245

- In fact, the percentile 99th calculated for example at traffic sites with low impact from solid sources can often be too low (e.g., < 1.4-1.5), thus resulting in an overestimation of solid fuel contribution to BC from the AE model (Figure 14).

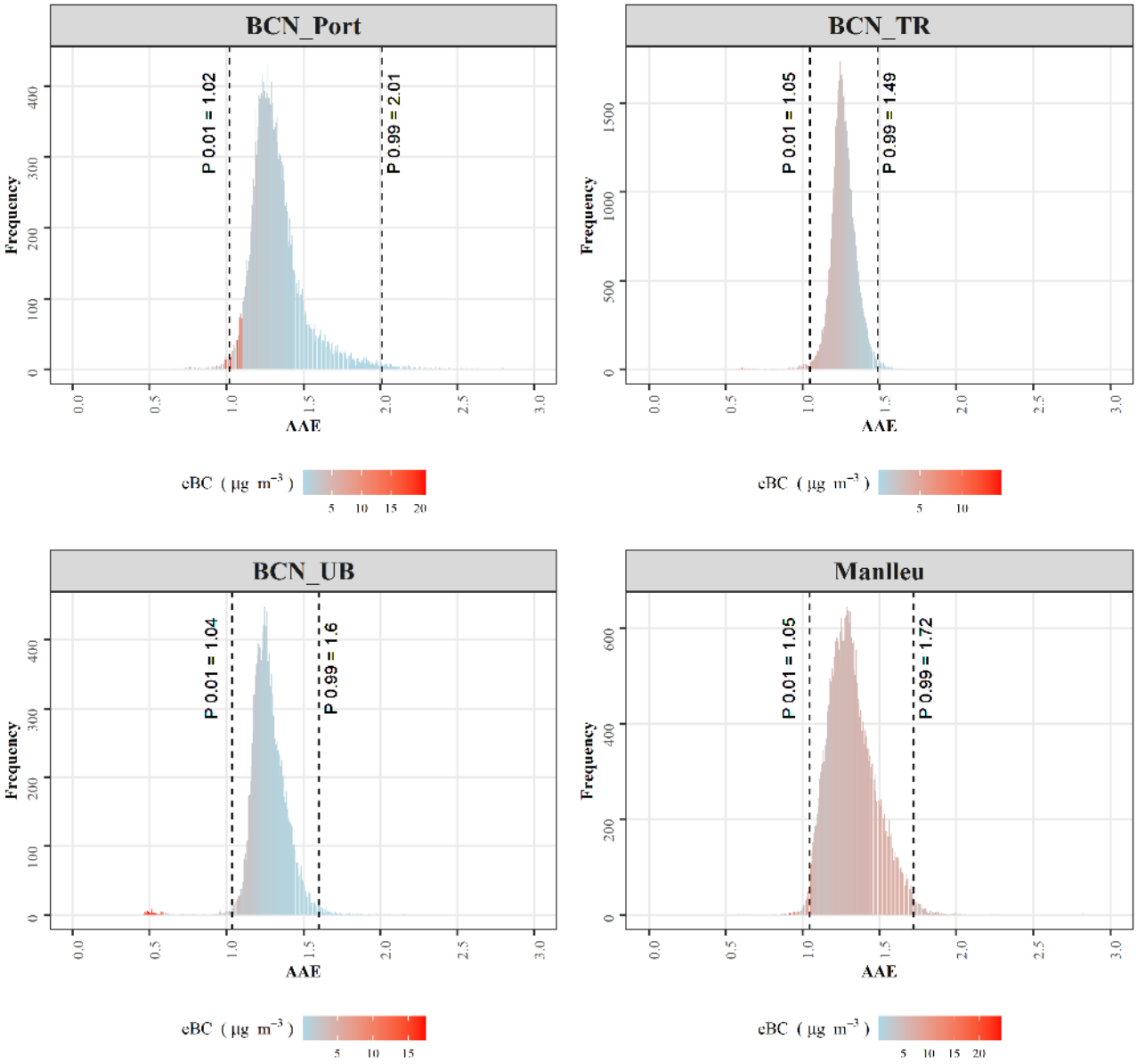

***Figure 13**. Simultaneous measurement of BC-AETH data Barcelona, use Percentile 1 and 99 of AAE frequency distribution.*

RI-URBANS (www.RIURBANS.eu) is supported by the European Commission under the Horizon 2020 – Research and Innovation Framework Programme, H2020-GD-2020, Grant Agreement number: 101036245

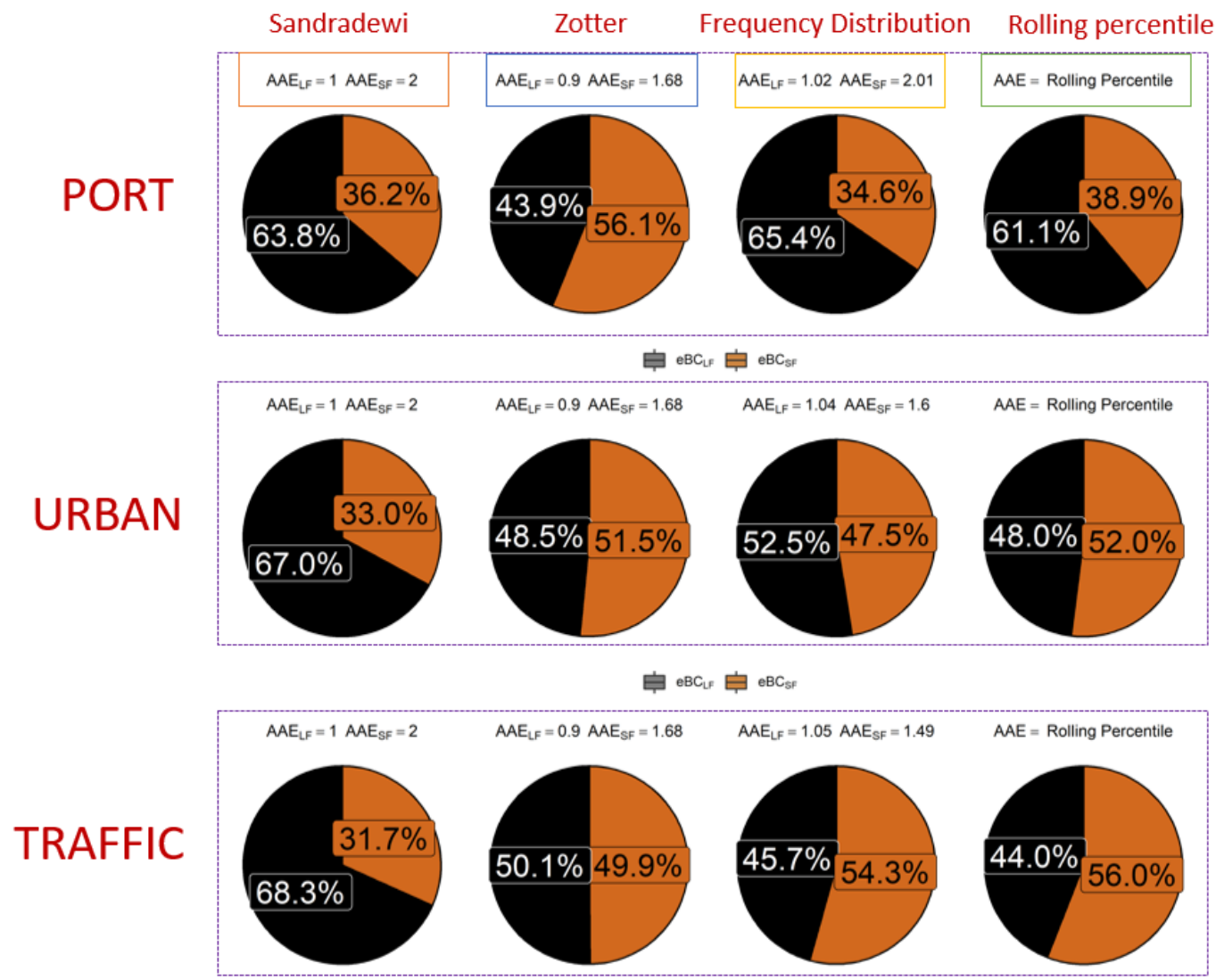

Figure 14. *Simultaneous measurement of BC-AETH data, at the UB and TR sites of BCN, Zotter AAE values provide too high solid contribution (mathematical consequence of using low AAE_sf in the Sandradewi Model.*

- A sensitivity study on 18 urban and non-urban European sites were performed to analyze the correlation of eBCsf with mass to charge ratio (M/Z60) from ACSM measurements by filtering data by R2 using percentiles and frequency distribution.
- The findings revealed a diverse range of values when fixing the lower percentiles and examining the impact of different upper percentiles on the coefficient of determination (R2). In some sites, filtering the data led to an improvement in R2, whereas in others, this improvement was not observed. Notably, the application of the 1st percentile appeared to be suitable by filtering approach based on the R2 results. However, uncertainties persist concerning the use of upper percentiles, and it is possible that these uncertainties could be addressed by exclusively utilizing data from winter nights for AAE estimation.

Our observations at the BCN_UB site (Figure 15) demonstrated that the R2 did not exhibit significant improvement when applying filtering to the AAE values using a fixed percentile 1 in combination with various upper percentiles

RI-URBANS (www.RIURBANS.eu) is supported by the European Commission under the Horizon 2020 – Research and Innovation Framework Programme, H2020-GD-2020, Grant Agreement number: 101036245

(95th, 96th, 97th, 98th, and 99th). Conversely, Figure 16 revealed that at the ATOLL_SUB site, a noticeable improvement in the correlation was achieved when filtering AAE values with R2 greater than 0.99.

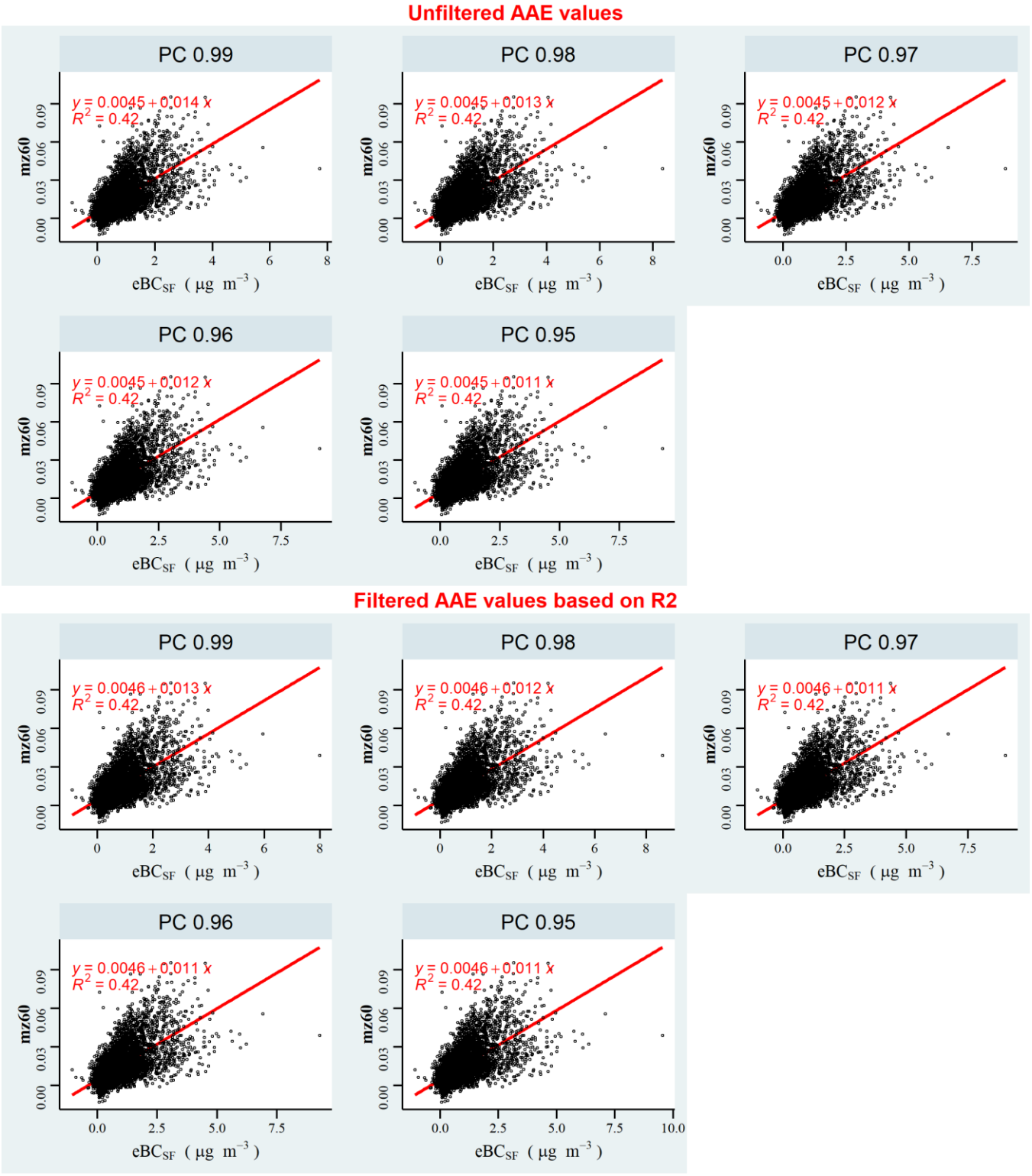

***Figure 15**. Data from BCN_UB site, eBC_{sf} vs M/Z60 correlation, AAE frequency distribution using percentiles, Filtered and unfiltered by R2.*

RI-URBANS (www.RIURBANS.eu) is supported by the European Commission under the Horizon 2020 – Research and Innovation Framework Programme, H2020-GD-2020, Grant Agreement number: 101036245

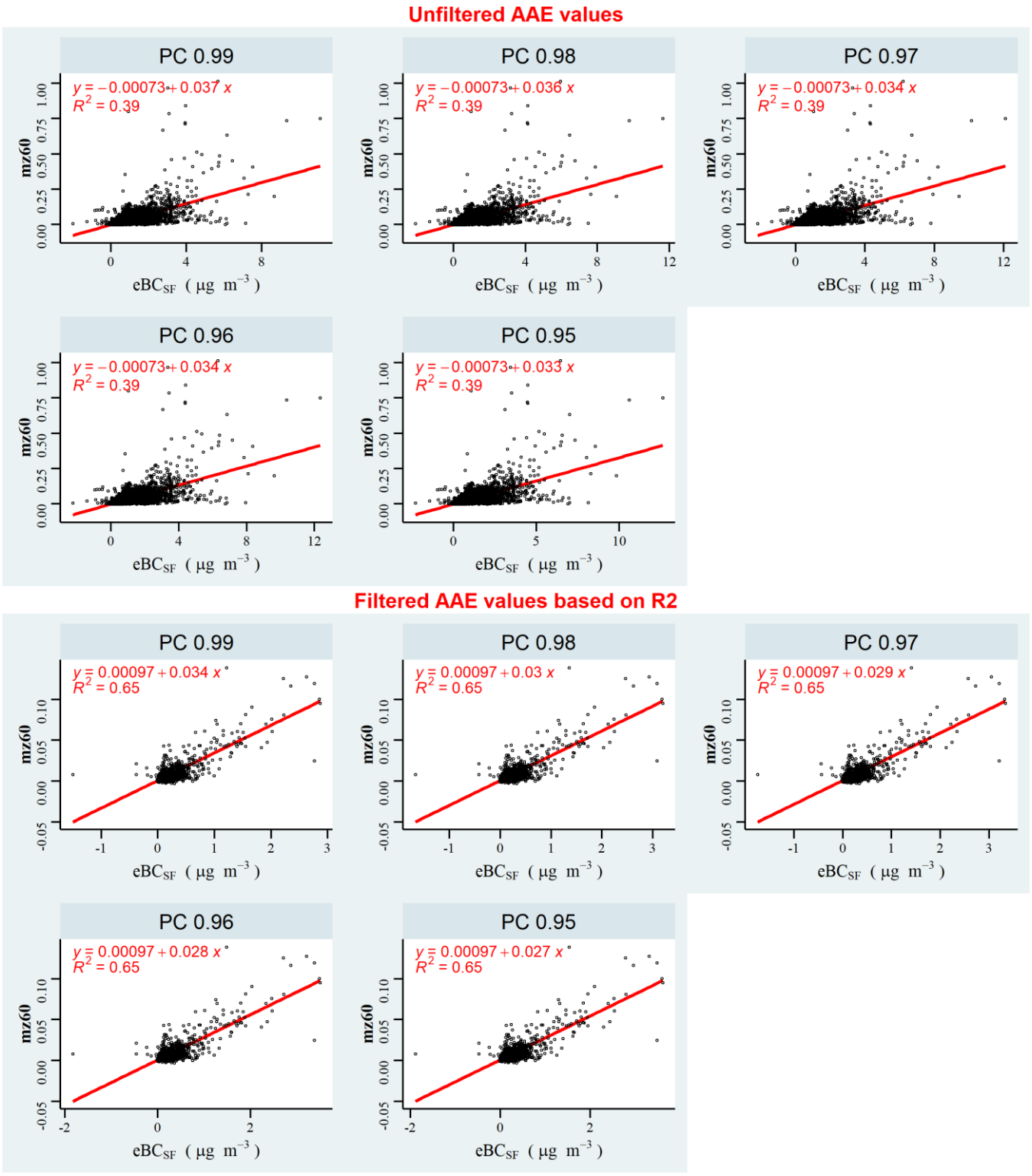

Figure 16. *Data from ATOLL_SUB site, eBCsf vs M/Z60 correlation, AAE frequency distribution using percentiles, Filtered and unfiltered by R2.*

- In practice, recommending the use of harmonized and fixed AAE values for BC source apportionment is challenging due to the mathematical limitations of the aethalometer model. The aethalometer model primarily

RI-URBANS (www.RIURBANS.eu) is supported by the European Commission under the Horizon 2020 – Research and Innovation Framework Programme, H2020-GD-2020, Grant Agreement number: 101036245

provides qualitative rather than quantitative results, making it difficult to achieve robust and precise outcomes. Moreover, the aethalometer model's qualitative nature limits its ability to quantitatively estimate source contributions accurately. As a result, using fixed and standardized AAE values across different locations or scenarios may not yield reliable and consistent results. The selection of AAE values is reliant on the site operators and can be analyzed through the utilization of collocated BC measurements with other auxiliary measurements, such as M/Z60 or 14C. This approach allows for the derivation of robust AAE values adapted to the specific site characteristics. However still a certain degree of subjectivity will remain. Nevertheless, despite the robustness of this approach, a certain degree of subjectivity may remain in the process.

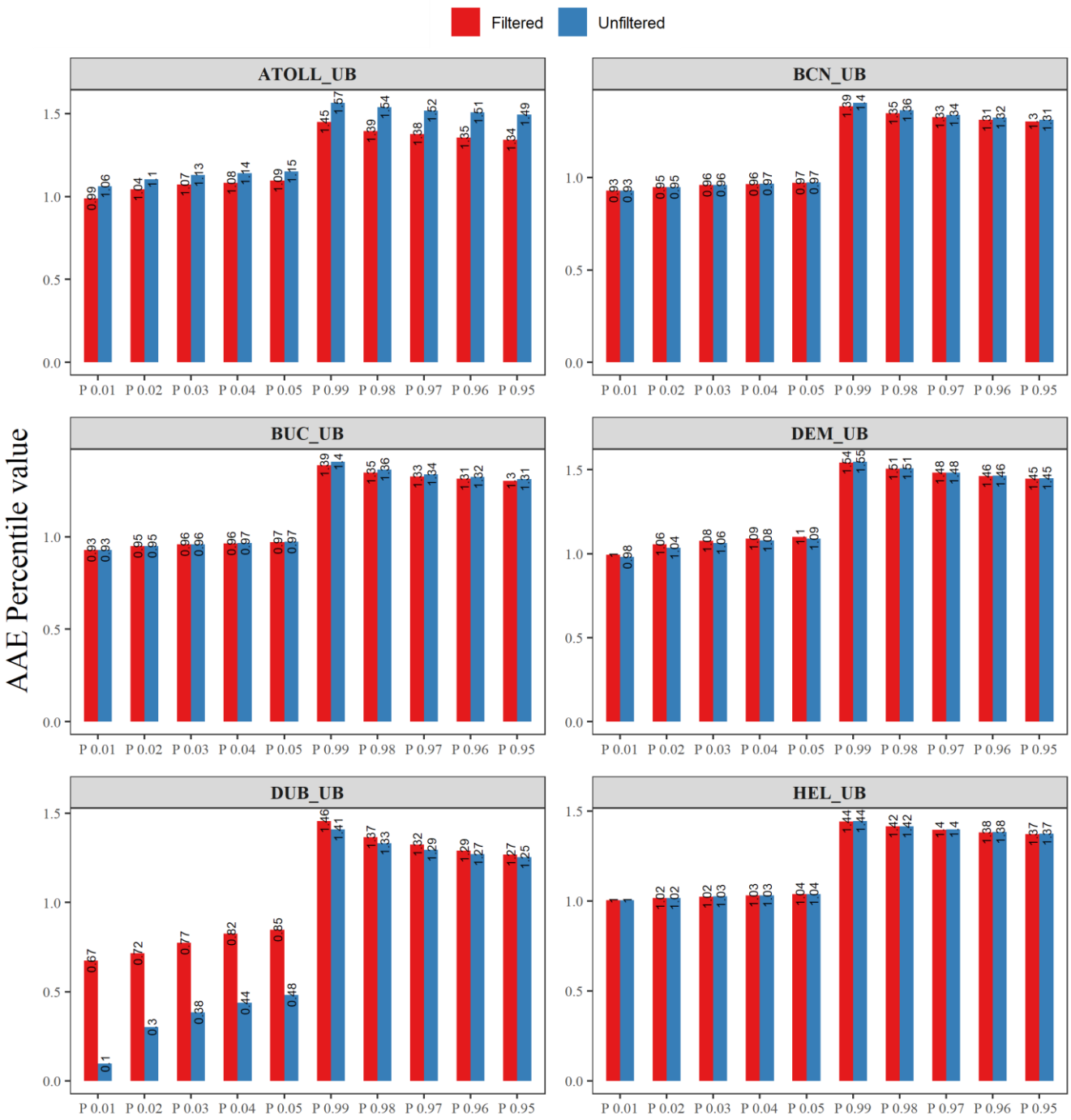

Figure 17. *Frequency distribution of AAE using percentiles by filtering and unfaltering by R2 estimated for European urban sites.*

RI-URBANS (www.RIURBANS.eu) is supported by the European Commission under the Horizon 2020 – Research and Innovation Framework Programme, H2020-GD-2020, Grant Agreement number: 101036245

- In general, the process of testing various lower and upper percentiles to determine the optimal AAE value presents complexities and should be performed based on the user's selection, in accordance with site-specific attributes. For instance, in the case of BCN, alterations in the percentage contributions of BClf and BCsf exhibit only marginal shifts with the inclusion or exclusion of filtering based on R2 criteria. Nonetheless, the absence of data filtering caused an enhanced correlation between BCsf and M/Z60, leading to an improvement in R2, as demonstrated in Figure 18.
- Furthermore, sensitivity analyses and uncertainty assessments (Figure 17, 19, and 20) are crucial to assess the robustness of the findings and communicate the potential limitations associated with this method. This approach could be tested for BC source apportionment in near-real time, improving our understanding of AAE uncertainties and providing a more accurate way to differentiate between BC sources.

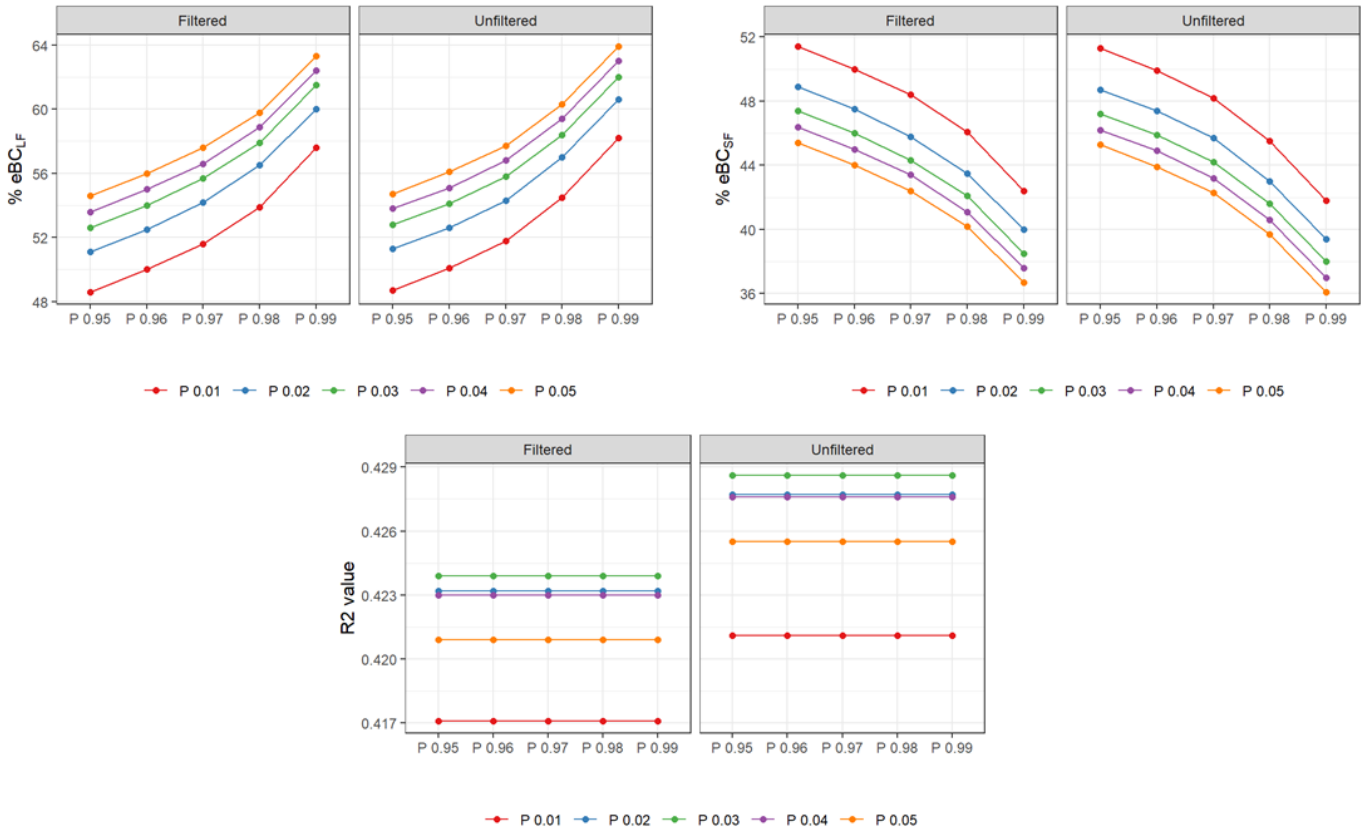

Figure 18. *eBC_{lf} and eBC_{sf} relative contribution based on percentiles and the correlation of eBCsf with MZ/60.*

Here are some applicable and general recommendations to consider while implementing the site-specific method using aethalometer model:

- Site Characterization: Ensure a comprehensive site characterization, including detailed information about local emission sources, meteorological conditions, traffic patterns, and other relevant factors. A thorough understanding of the site-specific context will improve the accuracy of BC source apportionment results.
- High-Quality Data: Use high-quality and continuous measurements of BC concentrations to study the AAE variation. Consistent and reliable data are crucial for robust source apportionment.
- Reference Measurements: Incorporate reference measurements as 14C from nearby locations to validate source apportionment accuracy and reliability of the results.

RI-URBANS (www.RIURBANS.eu) is supported by the European Commission under the Horizon 2020 – Research and Innovation Framework Programme, H2020-GD-2020, Grant Agreement number: 101036245

- Statistical Methods: Utilize appropriate statistical techniques, as well as the post-processing of aethalometer data, considering measurement noises to perform the source apportionment analysis.
- Sensitivity Analysis: Conduct sensitivity analyses to evaluate the impact of different assumptions and uncertainties in the input data on the source apportionment results.
- Temporal Variability: Consider the temporal variability of black carbon sources, as source contributions may vary throughout the day, week, or season.
- Transparent Reporting: Provide detailed documentation of the methodology, assumptions, and uncertainties involved in the BC source apportionment process to ensure the transparency and reproducibility of the findings.

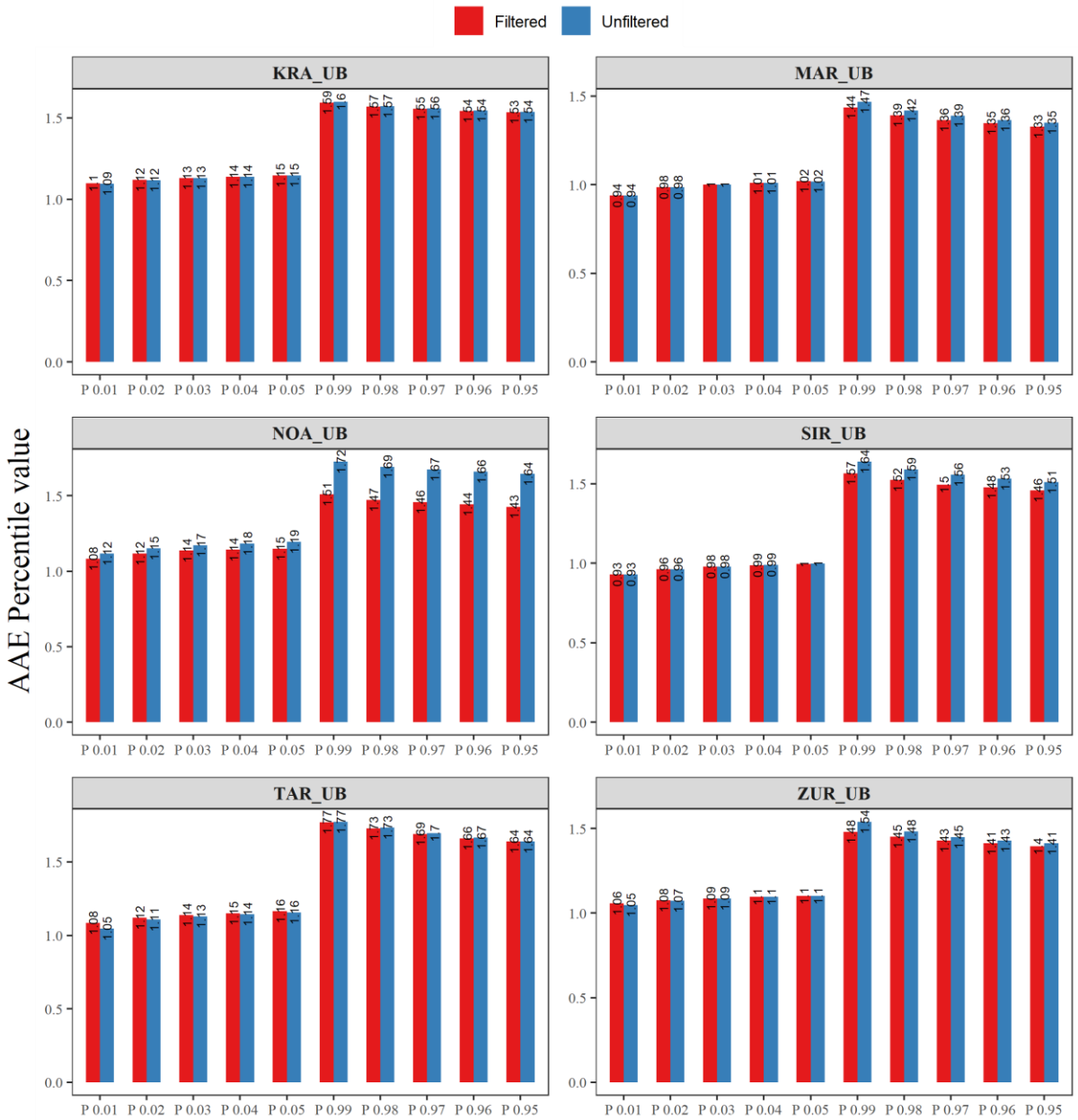

Figure 19. *Frequency distribution of AAE using percentiles by filtering and unfaltering by R2 estimated for European urban sites.*

RI-URBANS (www.RIURBANS.eu) is supported by the European Commission under the Horizon 2020 – Research and Innovation Framework Programme, H2020-GD-2020, Grant Agreement number: 101036245

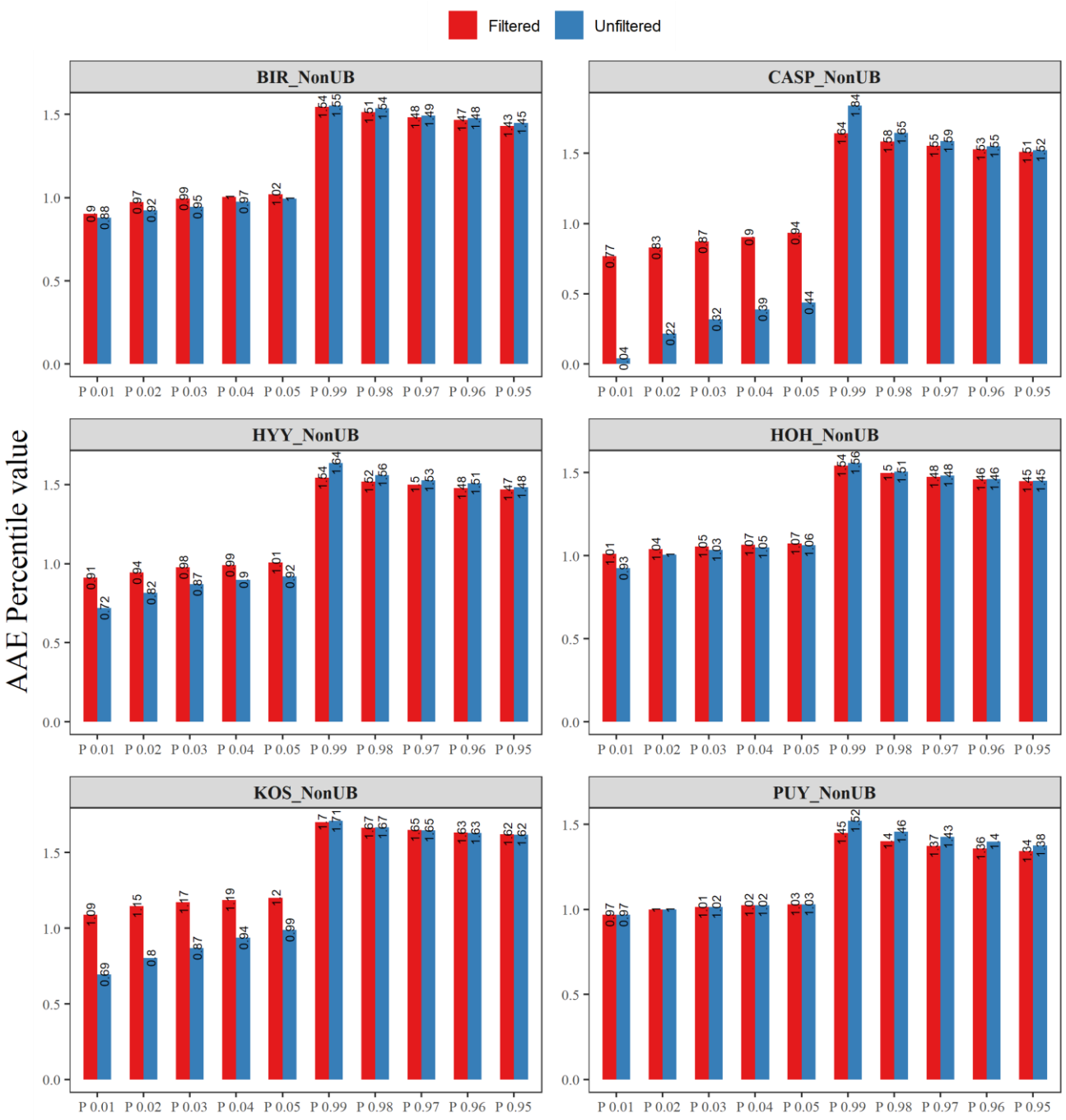

Figure 20. *Frequency distribution of AAE using percentiles by filtering and unfaltering by R2 estimated for European non-urban sites.*

RI-URBANS (www.RIURBANS.eu) is supported by the European Commission under the Horizon 2020 – Research and Innovation Framework Programme, H2020-GD-2020, Grant Agreement number: 101036245

6. Particle Number Size Distribution (PNSD)

Source apportionment for the urban sites studied by Trechera et al. (2023) is being analyzed with an extended period from 2009 to 2019. The analysis will be performed in 24 sites distributed in 18 cities in Europe and 1 in USA. These are 14 urban background sites (Athens, Barcelona, Budapest, Dresden, Granada, Helsinki, Langen, Lecce, Leipzig, London, Madrid, Mulheim, Zurich and Rochester NY), 5 traffic (Dresden, Helsinki, Leipzig, London and Stockholm), 4 suburban background (Athens, Lille, Paris and Prague) and 1 regional background site (Ispra).

In this report will be presented the results of source apportionment of 4 urban background sites from European cities in regions with different meteorological conditions:

- Barcelona, located in the western Mediterranean Basin, in the south of Europe, with one of the highest car densities in Europe and one of the main harbours in the Mediterranean basin. The measurements were carried out at the Palau Reial UB monitoring site, influenced by vehicular emissions from one of the main traffic avenues of the city. PNSD measurements were performed from 10 nm.
- Budapest, located in the central-north of Hungary, in the middle of eastern Europe. The UB site is located in the city center on the bank of the Danube River. PNSD measurements were performed from 10 nm. London, the largest city in the United Kingdom, located in southeastern England, with a very high car density and a high proportion of diesel cars and buses. The North Kensington UB monitoring site is located in a mainly residential area. PNSD measurements were performed from 17 nm.
- Mulheim, located in western Germany, in central Europe. The UB site is located in Styrum district within a residential area next to a sports field. It is surrounded by a motorway about 250 m north running in an east-west direction and a road about 400 m west running from north to south. Industrial estates and the Mannesmann tube works are located to the east and southeast, respectively, at a distance of about 1 km. PNSD measurements were performed from 10 nm.

In Barcelona, Budapest and Mulheim we obtained 6 factors from the PMF, but split one of them into two, thus 7 source- related factors were identified at each site. In London, 4 sources were identified from the PMF. To split one factor into two sources we followed the methodology applied by Rivas et al. (2019), inspired by that proposed by Rodríguez and Cuevas (2007). In Budapest and Mulheim, the Nucleation factor was split into Photonucleation and Traffic – Nucleation, and in Barcelona Traffic – Gasoline was split into Traffic – Gasoline and Regional Photonucleation. To this end, we used NOx as a proxy for traffic emissions and considering that at the morning peak most of the particles would be from traffic, we multiplied the NO_x concentration by a scaling factor. This scaling factor (the ratio between the factor concentration and NO_x) was calculated for each day. Also, at some sites we attributed all the particles from Photonucleation to a traffic source during the night hours, as no photonucleation would be expected since these particles are formed due to solar radiation. An example of the splitting is shown in Figure 21, from the site of Budapest, where Nucleation has been split into "Traffic Nucleation" and "Photonucleation" with NO_x. The diurnal cycles before the splitting, the splitting into two factors, and the result of all the sources after the splitting are shown.

Figure 22 shows the profiles obtained from PMF at each station before applying the splitting methodology. This shows the fraction of total particle number concentration (PNC) and the error bars represent the minimum and maximum fractional displacement (DISP) values. Figure 23 shows the relative contribution of the sources at each station after the splitting of the factors.

Sources in Barcelona: Six factors (split into seven sources) were identified for the Barcelona site. Traffic – Gasoline is the factor identified with the largest relative contribution and was split into two sources, Traffic – Gasoline (17.5% of PNC) and Regional Photonucleation (7.7%). This size mode peaks at 25-28 nm coinciding with typical traffic modes in urban background PNSD measurements associated with gasoline vehicle emissions (Liu et al., 2014). Some studies

RI-URBANS (www.RIURBANS.eu) is supported by the European Commission under the Horizon 2020 – Research and Innovation Framework Programme, H2020-GD-2020, Grant Agreement number: 101036245

also suggest that this mode represents freshly emitted traffic particles on the nearby roads (Gu et al., 2011), or that can be associated to nucleation of particles generated during dilution of diesel exhaust emissions (Harrison et al., 2011, 2018). In the diurnal cycle, two peaks at rush hours in the morning and evening are observed associated with Traffic – Gasoline, but a delayed midday peak associated with Regional Photonucleation is also observed, thus the splitting was performed in order to separate the two sources. The origin of Traffic – Gasoline is also supported by the lowest PNCs registered in August (when most population take holidays in the city) and in weekends, their moderate contributions to the variance of CO, NO_2, BC and NO, and a major local origin as deduced from the polar plot. Regional Photonucleation is associated with high winds from the South, where the harbour is located. Mixed traffic is the second source identified with a greater contribution (24.6%), associated with traffic with a mixed origin (Dall'Osto et al., 2012) and a size mode peaking at 41-46 nm. It has rush hour peaks, minimum values in August and weekends, high contributions of NO_2, CO, BC and PM_{10}, and a local origin. Local Photonucleation contributes to 23.8% of the average annual PNC and peaks at 12-14 nm coinciding with typical photonucleation modes (Brines et al., 2015). This has a prominent peak at midday associated with high solar radiation and higher values in summer. The origin of this source is supported by high contributions to the variance of O_3 and SO_2 and it is associated with light breezes and moderate wind speeds blowing from the South. Probably it is influenced by nucleated particles in the high SO_2 plumes emitted from the harbour, located about 10 km from the site in this direction. Traffic – Diesel contributes 18.2% and peaks at 82-91 nm coinciding with typical traffic modes associated with diesel vehicle emissions (Ogulei et al., 2007b), although some studies also suggest that this larger mode of traffic is due to the coagulation of the particle moving from the sources, i.e., an aged traffic emission (Zhu et al., 2002a; Gu et al., 2011). It peaks at rush hours, has low PNCs in August and weekends, very high contributions to the variance of BC and NO_2 and a local origin. Regional background contributes to 5.8% and has a bimodal distribution, with a main peak at 146-157 nm coinciding with typical regional background modes (Rivas et al., 2019) and a lower peak at 29-33 nm, also observed in other locations in previous studies (e.g. Kasumba et al., 2009; Liu et al., 2014). Higher PNCs are observed in summer and have high contributions of $PM_{2.5}$ and PM_{10}, SO_2, CO and O_3. Its regional origin from the E is mostly associated to the winds blowing from the Mediterranean Sea, and the large number of cruises in summer may explain the seasonal pattern. The source with the lowest contribution is Long distance transport (2.2%), that has a multimodal distribution, with a main peak at 280-310 nm and two lower peaks at 64-71 nm and 16-18 nm, and high contributions of $PM_{2.5}$ and PM_{10}. It is mainly associated with particles from the Sahara Desert in Africa, due to the high contributions observed with winds from SW with the highest wind speeds. But lower contributions with a local origin are also observed, related to road dust emitted from traffic. Influence by sea sulfates and forest fires is also observed.

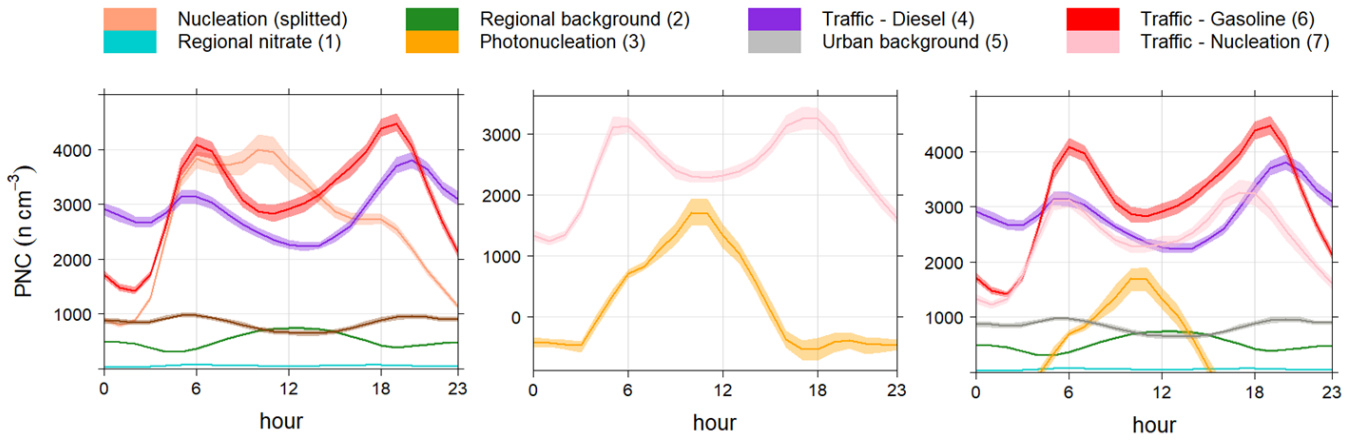

Figure 21. *Intra-daily variation of PNC from 7 sources in Budapest urban background. Left: before splitting the Nucleation factor; Middle: factors splitted from the Nucleation factor into Photonucleation and Traffic - Nucleation; Right: final after splitting the Nucleation factor.*

RI-URBANS (www.RIURBANS.eu) is supported by the European Commission under the Horizon 2020 – Research and Innovation Framework Programme, H2020-GD-2020, Grant Agreement number: 101036245

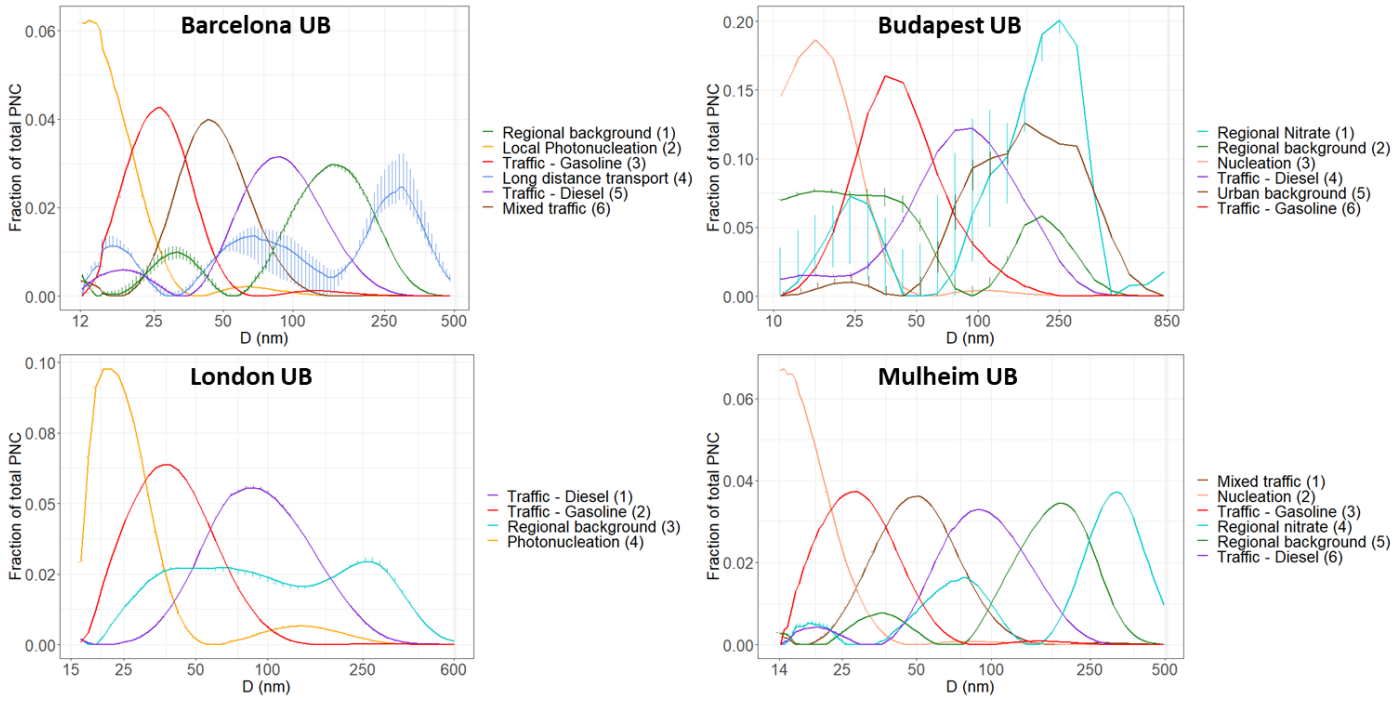

Figure 22. *Source profiles of normalized particle number size distribution for four urban background sites in Europe.*

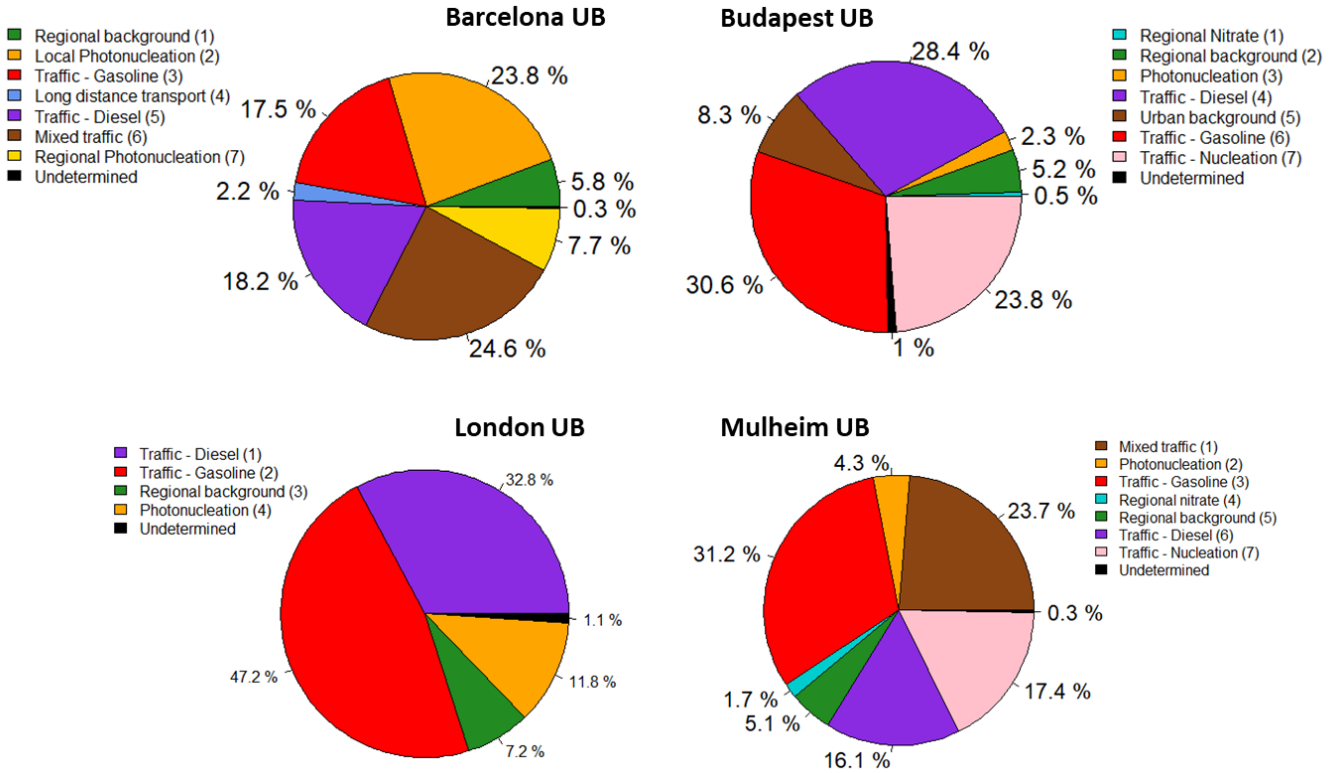

Figure 23. *Relative contribution of the final sources at the different sites after the splitting of factors by applying the methodology proposed by Rivas et al., 2019.*

RI-URBANS (www.RIURBANS.eu) is supported by the European Commission under the Horizon 2020 – Research and Innovation Framework Programme, H2020-GD-2020, Grant Agreement number: 101036245

Sources in Budapest: Six factors (split into seven sources) were identified for the Budapest site. Traffic – Gasoline is the source identified with most of the relative contribution (30.6%) and peaks at 35 nm. It has low weekend PNCs, low values in July (when most population take holidays in the city) and high contributions of NO_2, CO and NO. It has a local origin since it is predominant at low wind speeds, and also high contributions are observed with winds from SW and NE, where are located high traffic intensity roads. Traffic – Diesel contributes 28.4% of the average annual PNC and peaks at 94 nm. Diurnal cycle very similar to the previous source are observed, a similar origin with much lower wind speeds. The Nucleation factor obtained from PMF was split into two sources, Traffic – Nucleation (23.8% of PNC) and Photonucleation (2.3%), due to the peaks observed at rush hours and at midday, the first related to traffic and the latter related to the nucleation of the particles associated with photochemical processes. High contributions of Photonucleation are observed with winds from SW and NE blowing at moderate wind speeds, while Traffic – Nucleation is more associated with stagnation. Urban background contributes 8.3% and peaks at 169 nm, coinciding with typical urban background modes (Beddows et al., 2015). This has peaks at rush hours since it is influenced by traffic and the lowest values are found in summer and weekends as expected. It has high contributions to the variances of PM_{10}, CO, SO_2, NO and NO_2, and has a local origin. Regional background contributes 5.2% and has a bimodal distribution with peaks at 16 and 206 nm. The origin of this source is supported by high PNCs in summer and high contributions to the variances of O_3, SO_2 and PM_{10}. The regional origin from the NE is associated with the presence of coal-fired power plants, probably the SO_2 source that contributes to new particle formation episodes (Bousiotis et al., 2019). The source with the lowest contribution is Regional nitrate (0.5%), with a main peak at 250 nm and a lower peak at 24 nm. Highest values are found in winter as expected for nitrates, since ammonium nitrate evaporates in summer due to the high temperatures and lower humidity (Pakkanen et al., 2001) but it is also influenced by traffic, with a high contribution of NO and a local origin. High contributions from SW and NE are also observed due to its regional origin.

Sources in London: Four sources were identified for the London site. Traffic – Gasoline has the highest relative contribution (47.2%) and this size mode peaks at 37 nm. It has two peaks at traffic rush hours, lowest values in weekends and high contributions to the variance of NO_2, CO and BC. This suggests a contribution from diesel, but the two cannot be separated. It has a local origin and high contributions from the NE, the direction of the city center and important roads of London. Traffic – Diesel contributes 32.8 % of the average annual PNC and peaks at 87 nm. Very similar diurnal cycle to the previous source are observed, with very high contributions of BC, CO, $PM_{2.5}$ and NO_2, and a local origin. Photonucleation contributes 11.8% and peaks at 22 nm. It has to be noted that at this site the measurements start from 17 nm, and hence a high fraction of nucleating (<17nm) particles are not measured. It has a very wide peak at midday due to the photochemistry but the peaks at traffic rush hours are not appreciable, thus the splitting of nucleation in London has not been applied. It has the highest values in summer and a very high contribution of O_3. High contributions from SWW are observed, and also from E and N, with a minor local origin. The last source identified in this site is Regional background, contributing 7.2% of the average annual PNC. It has a bimodal distribution with a main peak at 255 nm and a lower peak at 65 nm. Very high contributions of $PM_{2.5}$ are found as expected. This source is influenced by regional nitrates consistent with lower values of PNCs at midday and in summer (when there is more solar radiation). It has high contributions from the E.

Sources in Mulheim: Six factors (split into seven sources) were identified for the Mulheim site. Traffic – Gasoline is the source identified with the highest relative contribution (31.2%) and peaks at 29 nm. It has peaks at rush hours, low values at weekends and a seasonally flat evolution. Contributions from NW, SW and NE are observed, where are located important roads in the city. Mixed traffic contributes 23.7% to the average annual PNC and peaks at 50 nm. It has a high contribution of NO_2, peaks at rush hours and maximum values are found in summer, probably because it is influenced by other sources. Similar to the previous source, it is influenced by particles emitted from the roads to the NW and NE. The Nucleation factor obtained from PMF, that peaks at 15 nm, was split into two sources, Traffic – Nucleation (17.4% of PNC), showing two peaks at traffic rush hours, and Photonucleation (4.3%), with a peak at midday associated with solar radiation. Traffic - Nucleation is seasonally flat, has lower values at

RI-URBANS (www.RIURBANS.eu) is supported by the European Commission under the Horizon 2020 – Research and Innovation Framework Programme, H2020-GD-2020, Grant Agreement number: 101036245

weekends and has a more local origin or with contributions from nearby roads. Photonucleation has much higher values in summer and very high contributions from NW at high wind speeds are observed, probably winds coming the Atlantic Ocean. Traffic – Diesel contributes 16.1% and peaks at 88 nm. The diel cycles and the seasonal evolution are similar to those of Traffic – Gasoline, but with a higher contribution of NO_2 and also PM_{10} and a major local origin. Regional background contributes 5.1% to the average annual PNC and has a bimodal distribution with a main peak at 188 nm and a lower peak at 36 nm. Diurnal cycles are flat and high contributions are observed from N, NE and E, where industries and farming are located. Regional nitrate has the lowest relative contribution (1.7%) and has a main peak at 322 nm and two lower peaks at 78 nm and 19 nm. It has high contributions of PM_{10} and NO_2, the latter due to a traffic influence. Trends are similar to Regional background but with a more noticeable decrease of the particles in summer due to the evaporation of ammonium nitrate. It has a local origin due to the traffic influence and high contributions are observed from NE and E.

6.1 Recommendations

As already recommended in D1, the first recommendation is to measure PNSD following a standard measurement, measuring from 10 nm or lower sizes if possible. Measuring from upper sizes may limit the number of sources. Positive Matrix Factorization (PMF) is the most recently used data analysis method to identify and apportion the sources of Particle number size distribution (PNSD). The current implementation of EPA-PMF, a graphic user interface coupled to the underlying solver, the multilinear engine 2 (ME-2), does not handle datasets of more than approximately 500,000 data points. Thus, Hopke et al. (2023) has developed a tool that would permit the PMF analysis of large data sets using ME-2.

To start the process, a comma separated values (.csv) file has to be prepared, in which data/time values are provided in the first column and the pairs of data values and related uncertainties are provided for each variable until all of the variables have been included. The first variable would be Particle number concentration (PNC), then all the size bins, and then particulate matter (PM_{10}, $PM_{2.5}$), gaseous pollutants (NO_2, NO, SO_2, O_3, CO) and black carbon (BC) if available. These variables should be included in order to help the interpretation of the results, since they can be related to important sources.

PMF requires individual uncertainty estimates for each data value. The uncertainty of PNC must be three times the concentration, since it is the total variable. To calculate the uncertainties of the size bins, a methodology established by Ogulei et al. (2007) is followed:

$$s_{ij} = \alpha_{ij} + C_3 \cdot n_{ij},$$

where $\alpha_{ij} = 0.01(n_{ij} + \bar{n}_j)$ and C_3 is a constant determined by trial-and-error testing values between 0.01 and 0.1

Uncertainties for the other variables are calculated following the methodology established by Polissar et al. (1998).

The program reads a control file that is modified for the specific data set and the stage of the analysis. A step-by-step set of instructions are provided in the supplemental material files of Hopke et al. (2023). The initial step is to choose the number of factors (sources) to obtain and to execute the base run in which the number of random starts is specified by the number of tasks. Each solution provides an objective value Q, and the lowest value is typically explored to determine the utility of this solution. The residuals (difference between the measured and modeled values for a given measured variable) need to be plotted to examine if the given number of factors has provided an adequate fit to the data. Then, factor profiles and contributions that are obtained should be plotted to explore their physical interpretability. If the results are not consistent, PMF should be run again with a different number of factors.

RI-URBANS (www.RIURBANS.eu) is supported by the European Commission under the Horizon 2020 – Research and Innovation Framework Programme, H2020-GD-2020, Grant Agreement number: 101036245

Once the number of factors has been determined and the related base case solution has been selected, the displacement (DISP) analysis should be run. This calculation assesses the amount of rotational displacement that exists in each preselected element of each profile for a very small change in the Q value. This will give the minimum and maximum DISP results, and these values can then be plotted along with the base case results.

After running the PMF, the plots have to be analyzed and sources have to be identified using existing literature.

For some sites, nucleation-related factors identified from PMF should be splitted into two sources: photonucleation (new particle formation through photochemistry processes, with a peak at maximum solar activity hours) and nucleation particles emitted from road traffic (with peaks at rush hours). To split one factor into two sources, a methodology developed by Rivas et al. (2019) can be applied, inspired by the one proposed by Rodríguez and Cuevas (2007), using traffic tracers. To this end, NO_x and BC can be used as proxys for traffic emissions. Since most of the nucleation particles at morning rush hour would be from traffic, the traffic proxy is multiplied by a scaling factor (the ratio between the factor concentration and the proxy) so it matches nucleation concentrations. This scaling factor should be calculated for each day to account for possible variations in the ratio. Also, during night hours all the particles may be attributed to the traffic source since no photonucleation would be expected when there is not solar radiation.

It is also important to mention that there might be a large benefit of simultaneous close-by observations and doing the PMF together. This would help in identifying regional photo nucleation and long-range transport factors affecting at simyultaneous measurments from different sites.

Furtermore, it is found that differentiation between diesel and gasoline engine emissions purely based on size distribution in urban environment would have to be supported also by high resolution mass spectrometry, and even then very challenging.

RI-URBANS (www.RIURBANS.eu) is supported by the European Commission under the Horizon 2020 – Research and Innovation Framework Programme, H2020-GD-2020, Grant Agreement number: 101036245

7. Recommendations on on-line elements

Recent advancements in technology have made it possible to create instruments with integrated analytical capabilities for real-time analysis of PM samples. These instruments have the potential to measure the levels of various elements in the atmosphere with hourly or sub-hourly resolution (Hasheminassab et al. 2020). One commercially available instrument that offers these features is the Xact 625i Ambient Metals Monitor developed by Cooper Environmental. The Xact allows for automated in situ measurements of elemental concentrations in ambient PM10, PM2.5, or PM1, and users can define a specific set of 24 or more elements to monitor with a sampling time resolution ranging from 15 to 240 minutes (Furger et al. 2017; Tremper et al. 2018). By analyzing high-resolution elemental data, it becomes possible to identify sources contributing to episodic or unusual air pollution events.

In recent research, (Furger et al. 2020) developed an automated system that alternates the collection of PM2.5 and PM10 samples using a single Xact instrument. This innovation allows for more efficient and convenient sampling of different particulate matter sizes.

Furthermore, elemental analysis methods typically rely on sample collection, often for 24 hours or more, resulting in low time resolution of the obtained results. As a result, important information about diurnal cycles or short-term pollution events can be lost or difficult to identify (Manousakas et al. 2021; Viana et al. 2008). In multivariate analysis, the quality of the results can be compromised if source emissions exhibit high covariance, as the models rely on the variation between source emissions for source separation. When the time resolution of the elemental composition data is low, it becomes challenging to incorporate enough variation into the dataset, with seasonal variation being the primary source of variability.

In contrast, higher time resolutions (such as 1 hour or less) capture the diurnal variation in source emissions, making it possible to account for short-term events and changes in local meteorology, thereby increasing the overall variation in the dataset. Additionally, by utilizing the switching inlet if is also possible to include variables with different size ranges in the dataset, which introduce extra variation and improve the accuracy of estimating emission processes and source fingerprinting. Size-differentiated composition data enables a more precise characterization of sources.

Various studies have utilized the Xact data (Hasheminassab et al. 2020; Liu et al. 2019; Rai et al. 2021; 2020; 2019; H. Wang et al. 2021; Q. Wang et al. 2018; Yu et al. 2019). However, just a handful of studies (seven in total) have taken place in Europe (Figure 24). A synopsis of the studies that took place in Europe is provided in Milestone 1.4.

Xact is a relatively new instrument and even though it more and more used in sites around Europe, the published data are still scarce. There is increasing scientific interest in high time resolution XRF instrumentation for atmospheric aerosol measurements. Imperial College London and Paul Scherrer Institute, who were amongst the first users of such instrumentation, established (also within the frameworks of RI Urbans) a new Working Group for users which will focus on use, calibration, data treatment, and best practices. The group is being supported by Cooper Environmental, US, as the manufacturer of the Xact. The purpose of this group is to draft operational (SOP and data treatment QA/QC and reporting data/uncertainties) and source apportionment recommendations and guidance documents. Currently there are over 60 participants in the group, covering 12 countries around Europe. The group is since June 2023, part of the ACTRIS network.

Until now, the availability of long series of element concentrations with high temporal resolution is scarce. Some measurements are being performed on RI-URBANS pilots simultaneously with other online measurements (ACSM and AE33) and offline measurements (chemical characterization of filters. PMF will be applied to these data sets during the Project.

RI-URBANS (www.RIURBANS.eu) is supported by the European Commission under the Horizon 2020 – Research and Innovation Framework Programme, H2020-GD-2020, Grant Agreement number: 101036245

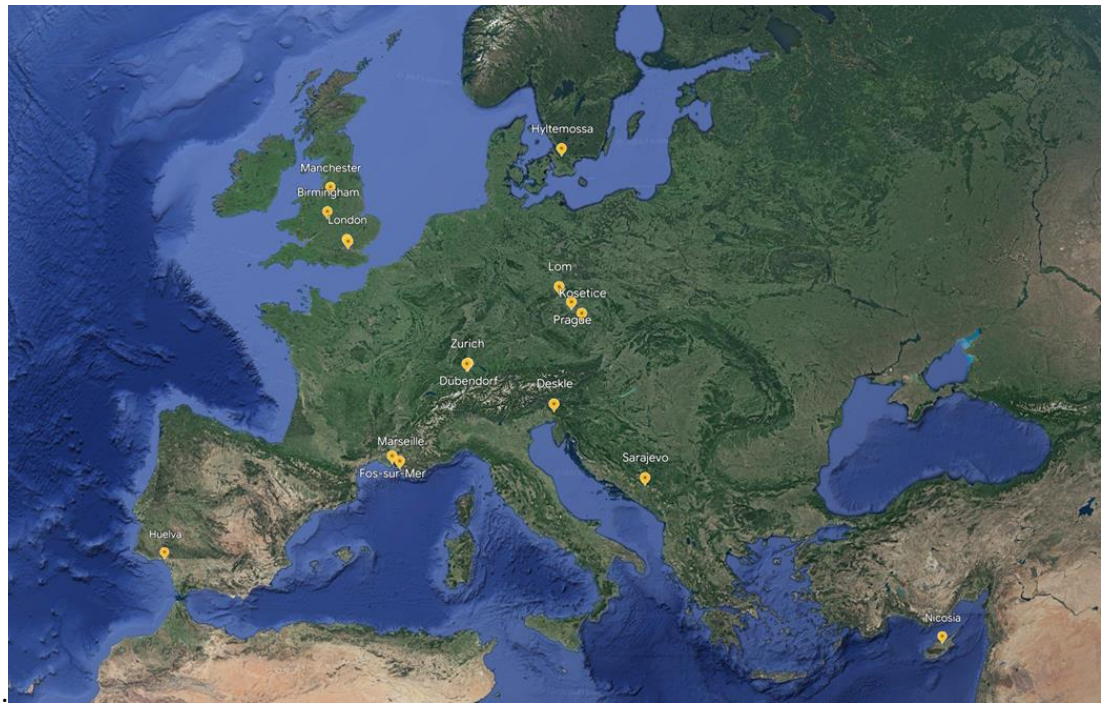

***Figure 24**. The sites that are participating in the online XRF WG around Europe.*

8. Volatile organic compounds

A total of 21 VOC datasets have been collected. These datasets cover a wide variety of sites (urban, suburban, traffic-related, background, industrial) and are from both online and off-line VOC measurements. Online VOC measurements are mainly from Gas Chromatography (GC) measurements and off-line VOC measurements are mainly by adsorbent tubes analyzed by GC.

Two source apportionment studies performed after data collection (PMF Off-line) have been performed at two urban/urban background sites with different VOC datasets in Marseille - France and Zurich – Switzerland. The Marseille database covers one year and a half of hourly measurements of C2 – C16 non-methane hydrocarbons (NMHCs) while the Zurich database covers two-years of hourly measurements of C2 – C7 NMHCs, monoterpenes, C2 – C5 oxygenated VOCs (OVOCs), and acetonitrile. Both datasets have been obtained by using online Thermal-Desorption Gas-Chromatography Flame-Ionization-Dectector (TD-GC-FID) on an hourly basis (Marseille) and each 90 minutes (Zurich).

The 5.0 version of the positive matrix factorization (PMF) tool from the Environmental Protection Agency (EPA) has been used, on a seasonal basis for both datasets. Therefore, the source apportionment studies have been performed for 6 seasons from Spring 2019 to Summer 2020 in Marseille, and for 7 seasons from Winter 2016 to Fall 2017 in Zurich. The PMF has not been applied to Spring 2017 data in Zurich due to the too high proportion of missing data.

The PMF inputs are the measured concentrations and their associated uncertainties. At both sites, the uncertainties estimation followed the ACTRIS guideline (https://www.actris.eu/sites/default/files/inline-files/WP3_D3.17_M42_0.pdf).

RI-URBANS (www.RIURBANS.eu) is supported by the European Commission under the Horizon 2020 – Research and Innovation Framework Programme, H2020-GD-2020, Grant Agreement number: 101036245

For both datasets, some data were missing or below the Limit of Detection (LoD) which should be replaced since missing values are not accepted by the PMF. Concerning concentrations below the LoD, the concentrations were replaced by the LoD divided by 2 and uncertainties were calculated following the Eq. (1):

$$U = \frac{5}{6} \times LoD \qquad (1)$$

Where U is the uncertainty (in $\mu g.m^{-3}$).

The missing values are replaced with the hourly median of the same month where there are missing values. In this case, the associated uncertainty is the hourly median multiplied by 4. These replaced values have a low impact on the PMF results as the weight given by the PMF, to a measurement depends on the uncertainty.

For each season of both datasets, twenty runs were performed with a number of factors varying from 3 to 12. Several parameters have been plotted versus the number of factors to determine the best solution following the method from Lee et al., 1999 and Hopke, 2000.

The selected solutions are between six and seven factors in Marseille depending on the season, and four factors were selected in Zurich. All quality indicators are summarized in Tables 7 and 8. The "bootstrap" test results showed determination coefficients above 0.6 for all seasons indicating the robustness and stability of PMF results for both databases.

Concerning the Zurich database, the concentration of ethanol was highly affecting the PMF analysis due to the high measured values in comparison to the other VOCs. The average concentration of the ethanol during the two-years measurement is equal to the third of the mean of the sum of all measured VOCs. Then, this compound has not been considered in the PMF database but used as an auxiliary data, after PMF analysis. Nevertheless, ethanol and other VOCs (propane, limonene) show some particular events with very high concentrations corresponding to periods with parties/events at some specific dates close to the station. Further work will be done on the PMF to try to identify a source related to party events.

Table 7. *Mathematical diagnostic for the PMF results on the Marseille database.*

	Spring 2019	Summer 2019	Fall 2019	Winter 2020	Spring 2020	Summer 2020
n (sample)	1034	1528	2183	1706	2208	1201
m (species)	62	59	57	56	42	54
k (factors)	6	7	7	7	6	6
$NMHC_{modeled}$ vs $NMHC_{measured}$ (r^2)	0.874	0.924	0.905	0.896	0.909	0.937
F Peak	-0.5	-1.5	-2.5	-4	-2.5	-2
Mean ratio (modeled vs measured)	0.93	0.96	0.92	0.92	0.90	0.84
Number of species with $r^2 > 0.75$ for modeled vs measured	15	19	15	20	16	7
"Bootstrap" minimum (in %)	80	99	94	96	93	79

Table 8. *Mathematical diagnostic for the PMF results on the Zurich database.*

	Winter 2016	Spring 2016	Summer 2016	Fall 2016	Winter 2017	Summer 2017	Fall 2017
n (sample)	1438	2204	2160	2105	2142	2216	2196
m (species)	29	29	29	29	26	26	29
k (factors)	4	4	4	4	4	4	4

RI-URBANS (www.RIURBANS.eu) is supported by the European Commission under the Horizon 2020 – Research and Innovation Framework Programme, H2020-GD-2020, Grant Agreement number: 101036245

$VOC_{modeled}$ vs $VOC_{measured}$ (r^2)	0.989	0.960	0.865	0.951	0.986	0.960	0.953
Mean ratio (modeled vs measured)	1.01	0.98	0.90	0.91	1.00	0.96	0.96
Number of species with $r^2 > 0.75$ for modeled vs measured	23	20	18	18	20	15	18
"Bootstrap" minimum (in %)	98	98	73	97	92	73	99

The comparison of the concentrations of the NMHCs in common between Marseille and Zurich shows higher concentrations in Marseille than in Zurich and also a less pronounced seasonal variation in Marseille than in Zurich.

In Marseille, highest VOC concentrations were observed during winter. It is explained by the lower height of the planetary boundary layer (PBL) than in summer, the contribution of an additional source (residential heating), and a longer lifetime of NMHC in winter than in summer due to a less effective photochemical depletion. In Zurich, the opposite is observed with highest VOCs concentrations observed in summer. As mentioned earlier, the measured VOCs in Zurich cover NMHC and OVOC, whereas in Marseille only NMHC were measured. These two VOCs families have opposite behavior in Zurich (Fig 25). In summer, the photochemistry has an impact on both depletion of NMHCs and formation of OVOCs explaining the differences observed on VOCs concentrations between Marseille and Zurich.

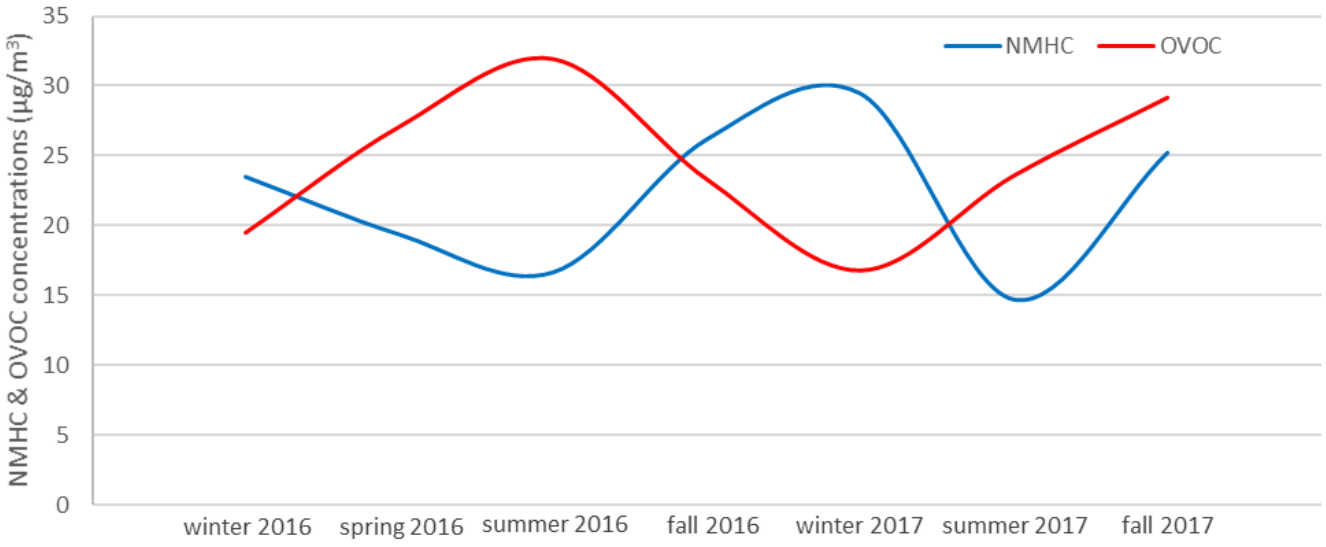

***Figure 25**. Concentrations of NMHCs and OVOCs measured in Zurich along the seasons in 2016 and 2017.*

In Marseille, 8 factors have been identified whereas 4 factors have been identified in Zurich. The "traffic exhaust" and the "heating/wood" burning were two common sources in Marseille and Zurich. Nevertheless, the "heating" factor is found only during wintertime in Marseille, and during all the seasons in Zurich. A possible reason is the presence of BBQs and fires at 300m around the Zurich station. The "urban background" factor is also identified at both sites. In Zurich, this factor is combined with natural gas contribution since important proportion of light alkanes (2 to 4 carbon atoms) are found in this factor. Furthermore, during wintertime, a significant part of light

RI-URBANS (www.RIURBANS.eu) is supported by the European Commission under the Horizon 2020 – Research and Innovation Framework Programme, H2020-GD-2020, Grant Agreement number: 101036245

alkenes contributes to this factor which means that the natural gas source could be related to the residential heating. The last factor identified in Zurich is the "local emissions and fuel evaporation" factor which is a combination of all factors that are impacted by the temperature and then, has its highest estimated contribution to VOCs concentration in summer. This "local emissions and fuel evaporation" factor is explaining:

- a part of the fuel evaporation source since a part of the MTBE concentration is explained by this factor
- the biogenic emissions with an important part of isoprene explained by this factor in summer and also some OVOCs with possible biogenic origin, like methanol
- an important part of many OVOCs that could be from secondary origin.

In comparison, in Marseille the fuel evaporation and the biogenic factors are clearly identified and separated. The factor related to the "secondary formation" is not detected as OVOCs are not measured in Marseille.

The factors observed in Marseille and not in Zurich are two industrial factors and a factor linked to IVOCs (Intermediate volatility organic compounds). The industrial sources are very specific and depend on the location of the measurement site and its surrounding sources. The other factor is linked specifically to IVOCs which were not measured in Zurich.

In Marseille the road transportation (traffic exhaust & fuel evaporation) is explaining the majority of the measured NMHCs with a contribution around 40 % for each season (fig 2). The residential heating is also an important contributor during wintertime with a contribution of 20 % to NMHCs measured concentrations (fig 2).

In Zurich, the local emissions and fuel evaporation factor is estimated to be by far the most important contributor to VOCs concentration with a contribution varying from 20% to 49%, with the lowest contribution occurring in winter (Fig. 26). In the opposite, the urban background and natural gas factor is explaining between 32 % and 38 % of measured VOCs concentration in winter against 13 – 14 % during summer (Fig. 26). The road transport has a contribution between 24 % and 32 % during all seasons with the exception of fall season where the contribution of this factor is 38 – 40 % which is close to the contribution found in Marseille (Fig. 26).

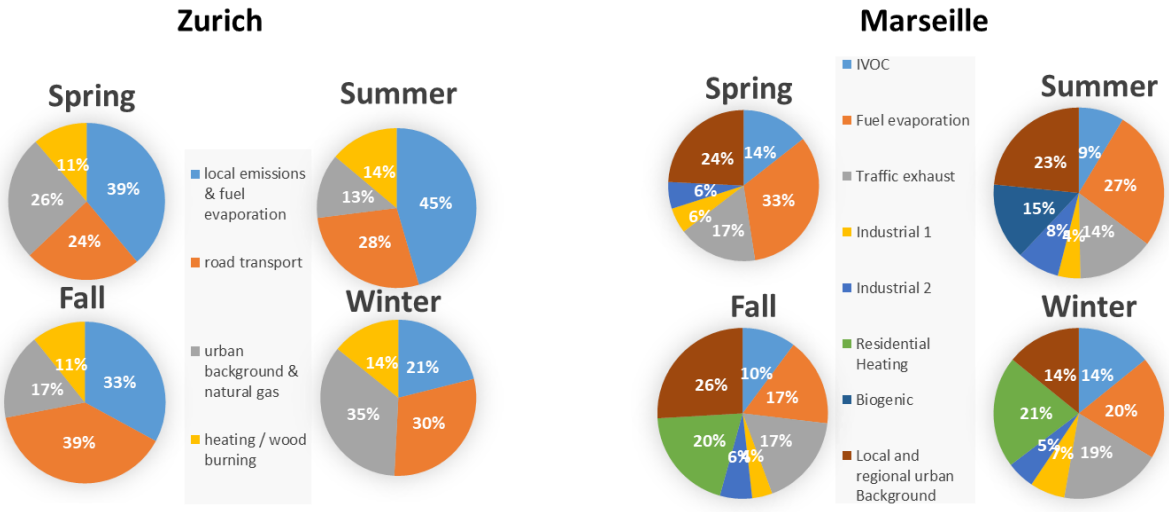

***Figure 26**. Factor contribution to VOC concentration in Zurich (left) and Marseille (right)*

To summarize, the latest two PMF studies at two European urban background sites show some common sources between Marseille and Zurich like road transport and residential heating. Additional sources were identified in

RI-URBANS (www.RIURBANS.eu) is supported by the European Commission under the Horizon 2020 – Research and Innovation Framework Programme, H2020-GD-2020, Grant Agreement number: 101036245

Marseille related to industrial sources surrounding the site. Since the two datasets were not covering the same VOCs, the importance to have a wide range of volatility of VOCs (IVOC) and of primary (NMHC) and secondary origins (OVOC) can help in identifying new sources and their importance. In Zurich dataset, we didn't include ethanol in the PMF application but more investigation will be conducted in order to identify its related source and eventually a solvent use source. Additionally, the measurement of OVOCs is important as it is an indicator of the impact of photochemistry and cover some markers of solvent use emission source.

8.1 Recommendations

- Before applying the PMF on a dataset, the possible outliers have to be checked by applying the lognormal law. If a value is detected as a possible outlier, this does not mean that the value is invalid (QA/QC measures should apply), but uncommon concentrations considered as outliers disrupt the performance of the PMF analysis and have to be ignored from the database used for PMF.
- If a specific compound has very high concentration values, much higher than the other VOCs, it should be treated differently (subtraction of the background or other statistical analysis) and should not be considered in the VOC database used for PMF, but as ancillary data.
- We recommend that the uncertainties calculated for the PMF analysis should follow the ACTRIS guideline since they have an impact on the weight attributed by the PMF gives to a measurement. Then, a harmonization of the uncertainties calculation method is useful to compare the source apportionment studies from different measurement sites.
- QA/QC measures based on ACTRIS guideline, should apply before running PMF to be sure about the good quality of the measurement. Afterwards, during PMF analysis, each compound will be considered "strong", "weak", "bad" depending on its measurement quality and S/N ratio (Signal/Noise).
- When determining the optimal number of factors, many parameters have to be taken into consideration. IM and IS which are respectively the highest residual mean value of all compounds and the highest residual standard deviation value have to be minimized. The r^2 between model and measurement should also be checked. For each n+1 factor, it is important to verify how the fingerprint of the previous factors has changed to generate a new factor, and how independent the factors are between them. The determination of the optimal solution is finding the right balance between these parameters.
- When the optimal number of factors has been decided it is important to check the r^2 between all factors. If there is a correlation between some factors the determination of an optimal FPeak value can help on establishing independency and stability of the factors.
- For annual or multi-annual data series, the PMF is usually applied on a seasonal basis. If a season has a high proportion of missing data (higher than 50%), it is recommended to ignore the PMF analysis of this season because this could lead to a misinterpretation of the results and bad representativeness of the season.
- Where possible, it is very useful when conducting a source apportionment study to have a large variety of VOCs covering primary anthropogenic and biogenic NMHCs but also secondary compounds (OVOCs) which contain markers helping to identify and confirm new sources.
- The use of meteorological data (temperature, solar radiation, wind speed, and wind direction) can give the possibility to create a conditional probability function (CPF) plots based on wind speed and direction, which could help in identifying the sources of various factors, such as specific industries, given their specific location. Temperature and solar radiation correlation help in the identification of secondary and biogenic sources
- Correlations with NO_x (NO_2 + NO), O_3, CO, and SO_2 could further aid in the identification of various sources. For instance, NO_x and CO are clear indicators of anthropogenic activities.

It must be mentioned that most of the VOC source apportionment studies are in regards to the observed VOC concentrations and not the initial VOC concentrations. Many VOCs, especially alkenes and aromatics, have a

RI-URBANS (www.RIURBANS.eu) is supported by the European Commission under the Horizon 2020 – Research and Innovation Framework Programme, H2020-GD-2020, Grant Agreement number: 101036245

substantial decrease from photochemical loss, and therefore their contribution might be underestimated. Although, this did not hinder the source identification, it is important to assess the impact of photochemistry on the dataset before.

9. References

Albinet, A., Leoz-Garziandia, E., Budzinski, H., Villenave, E., 2006. Simultaneous analysis of oxygenated and nitrated polycyclic aromatic hydrocarbons on standard reference material 1649a (urban dust) and on natural ambient air samples by gas chromatography–mass spectrometry with negative ion chemical ionisation. J. Chromatogr. A 1121, 106–113

Albinet, A., Nalin, F., Tomaz, S., Beaumont, J., Lestremau, F., 2014. A simple QuEChERS-like extraction approach for molecular chemical characterization of organic aerosols: application to nitrated and oxygenated PAH derivatives (NPAH and OPAH) quantified by GC–NICIMS. Anal. Bioanal. Chem. 406, 3131–3148.

Albinet, A., Tomaz, S., Lestremau, F., 2013. A really quick easy cheap effective rugged and safe (QuEChERS) extraction procedure for the analysis of particle-bound PAHs in ambient air and emission samples. Sci. Total Environ. 450-451, 31–38.

Alier, M., Van Drooge, B.L., Dall'Osto, M., Querol, X., Grimalt, J.O., Tauler, R. Source apportionment of submicron organic aerosol at an urban background and a road site in Barcelona (Spain) during SAPUSS (2013) Atmospheric Chemistry and Physics, 13 (20), pp. 10353-10371.

Amato, F., Alastuey, A., Karanasiou, A., Lucarelli, F., Nava, S., Calzolai, G., Severi, M., Becagli, S., Gianelle, V.L., Colombi, C., Alves, C., Custódio, D., Nunes, T., Cerqueira, M., Pio, C., Eleftheriadis, K., Diapouli, E., Reche, C., Minguillón, M.C., Manousakas, M.-I., Maggos, T., Vratolis, S., Harrison, R.M., Querol, X. AIRUSE-LIFE+: A harmonized PM speciation and source apportionment in five southern European cities (2016) Atmospheric Chemistry and Physics, 16 (5), pp. 3289-3309.

Amato, F., Pandolfi, M., Escrig, A., Querol, X., Alastuey, A., Pey, J., Perez, N., Hopke, P.K. Quantifying road dust resuspension in urban environment by Multilinear Engine: A comparison with PMF2 (2009) Atmospheric Environment, 43 (17), pp. 2770-2780.

Backman, J., Schmeisser, L., Virkkula, A., Ogren, J.A., Asmi, E., Starkweather, S., Sharma, S., Eleftheriadis, K., Uttal, T., Jefferson, A., Bergin, M., Makshtas, A., Tunved, P., Fiebig, M., 2017. On Aethalometer measurement uncertainties and an instrument correction factor for the Arctic. Atmos. Meas. Tech. 10, 5039–5062. https://doi.org/10.5194/amt-10-5039-2017

Baduel, C., Voisin, D., Jaffrezo, J.L., 2010. Seasonal variations of concentrations and optical properties of water soluble HULIS collected in urban environments. Atmos. Chem. Phys. 10, 4085–4095.

Baldasano, J.M., 2020. COVID-19 lockdown effects on air quality by NO2 in the cities of Barcelona and Madrid (Spain). Sci. Total Environ. 741. https://doi.org/10.1016/j.scitotenv.2020.140353

Becerril-Valle, M., Coz, E., Prévôt, A.S.H., Močnik, G., Pandis, S.N., Sánchez de la Campa, A.M., Alastuey, A., Díaz, E., Pérez, R.M., Artíñano, B., 2017. Characterization of atmospheric black carbon and co-pollutants in urban and rural areas of Spain. Atmos. Environ. 169, 36–53. https://doi.org/10.1016/j.atmosenv.2017.09.014

RI-URBANS (www.RIURBANS.eu) is supported by the European Commission under the Horizon 2020 – Research and Innovation Framework Programme, H2020-GD-2020, Grant Agreement number: 101036245

Belis, C. A., M. Pikridas, F. Lucarelli, E. Petralia, F. Cavalli, G. Calzolai, M. Berico, and J. Sciare. 2019. "Source Apportionment of Fine PM by Combining High Time Resolution Organic and Inorganic Chemical Composition Datasets." Atmospheric Environment: X 3 (August): 100046. https://doi.org/10.1016/j.aeaoa.2019.100046.

Belis, C., Favez, O., Mircea, M., Diapouli, E., Manousakas, M., Vratolis, S., Gilardoni, S., Paglione, M., Decesari, S., Mocnik, G., Mooibroek, D., Salvador, P., Takahama, S., Vecchi, R. and Paatero, P., European guide on air pollution source apportionment with receptor models, EUR 29816 EN, Publications Office of the European Union, Luxembourg, 2019, ISBN 978-92-76-09001-4, https://doi:10.2760/439106, JRC117306

Belis, C.A., Karagulian, F., Larsen, B.R., Hopke, P.K., 2013. Critical review and meta-analysis of ambient particulate matter source apportionment using receptor models in Europe. Atmos. Environ. 69, 94–108. https://doi.org/10.1016/j.atmosenv.2012.11.009

Bibi, Z., Coe, H., Brooks, J., Williams, P.I., Reyes-Villegas, E., Priestley, M., Percival, C.J., Allan, J.D., 2021. Technical note: A new approach to discriminate different black carbon sources by utilising fullerene and metals in positive matrix factorisation analysis of high-resolution soot particle aerosol mass spectrometer data. Atmos. Chem. Phys. 21, 10763–10777. https://doi.org/10.5194/acp-21-10763-2021

Blanco-Donado, E.P., Schneider, I.L., Artaxo, P., Lozano-Osorio, J., Portz, L., Oliveira, M.L.S., 2022. Source identification and global implications of black carbon. Geosci. Front. 13, 101149. https://doi.org/10.1016/j.gsf.2021.101149

Bressi, M., Cavalli, F., Putaud, J. P., Fröhlich, R., Petit, J. E., Aas, W., Äijälä, M., Alastuey, A., Allan, J. D., Aurela, M., Berico, M., Bougiatioti, A., Bukowiecki, N., Canonaco, F., Crenn, V., Dusanter, S., Ehn, M., Elsasser, M., Flentje, H., Graf, P., Green, D. C., Heikkinen, L., Hermann, H., Holzinger, R., Hueglin, C., Keernik, H., Kiendler-Scharr, A., Kubelová, L., Lunder, C., Maasikmets, M., Makeš, O., Malaguti, A., Mihalopoulos, N., Nicolas, J. B., O'Dowd, C., Ovadnevaite, J., Petralia, E., Poulain, L., Priestman, M., Riffault, V., Ripoll, A., Schlag, P., Schwarz, J., Sciare, J., Slowik, J., Sosedova, Y., Stavroulas, I., Teinemaa, E., Via, M., Vodička, P., Williams, P. I., Wiedensohler, A., Young, D. E., Zhang, S., Favez, O., Minguillón, M. C. and Prevot, A. S. H.: A European aerosol phenomenology - 7: High-time resolution chemical characteristics of submicron particulate matter across Europe, Atmos. Environ. X, 10(March), doi:10.1016/j.aeaoa.2021.100108, 2021

Briggs, N.L., Long, C.M., 2016. Critical review of black carbon and elemental carbon source apportionment in Europe and the United States. Atmos. Environ. 144, 409–427. https://doi.org/10.1016/j.atmosenv.2016.09.002

Brown, S.G., Eberly, S., Paatero, P., Norris, G.A. Methods for estimating uncertainty in PMF solutions: Examples with ambient air and water quality data and guidance on reporting PMF results (2015) Science of the Total Environment, 518-519, pp. 626-635.

Camman, J., Chazeau, B., Marchand, N., Durand, A., Gille, G., Lanzi, L., Jaffrezo, J.-L., Wortham, H., and Uzu, G.: Oxidative potential apportionment of atmospheric PM1: A new approach combining high-sensitive online analysers for chemical composition and offline OP measurement technique, Atmos. Chem. Phys., Submitted.

Canonaco, F., Slowik, J. G., Baltensperger, U. and Prévôt, A. S. H.: Seasonal differences in oxygenated organic aerosol composition: Implications for emissions sources and factor analysis, Atmos. Chem. Phys., 15(12), 6993–7002, doi:10.5194/acp-15-6993-2015, 2015

Cavalli, F., Viana, M., Yttri, K., Genberg, J., Putaud, J.-P., 2010. Toward a standardised thermal-optical protocol for measuring atmospheric organic and elemental carbon: the EUSAAR protocol. Atmos. Meas. Tech. 3, 79–89.

RI-URBANS (www.RIURBANS.eu) is supported by the European Commission under the Horizon 2020 – Research and Innovation Framework Programme, H2020-GD-2020, Grant Agreement number: 101036245

Cesari, D., Amato, F., Pandolfi, M., Alastuey, A., Querol, X., Contini, D. An inter-comparison of PM10 source apportionment using PCA and PMF receptor models in three European sites (2016) Environmental Science and Pollution Research, 23 (15), pp. 15133-15148.

Chazeau, B., El Haddad, I., Canonaco, F., Temime-Roussel, B., D'Anna, B., Gille, G., Mesbah, B., Prévôt, A.S.H., Wortham, H., Marchand, N., 2022. Organic aerosol source apportionment by using rolling positive matrix factorization: Application to a Mediterranean coastal city. Atmos. Environ. X 14. https://doi.org/10.1016/j.aeaoa.2022.100176

Chebaicheb, H., Brito, J.F. De, Chen, G., Tison, E., Favez, O., Marchand, C., Pr, S.H., 2023. Investigation of four-year chemical composition and organic aerosol sources of submicron particles at the ATOLL site in northern France ☆ 330. https://doi.org/10.1016/j.envpol.2023.121805

Chen, G., Canonaco, F., Tobler, A., Aas, W., Alastuey, A., Allan, J., Atabakhsh, S., Aurela, M., Baltensperger, U., Bougiatioti, A., De Brito, J. F., Ceburnis, D., Chazeau, B., Chebaicheb, H., Daellenbach, K. R., Ehn, M., El Haddad, I., Eleftheriadis, K., Favez, O., Flentje, H., Font, A., Fossum, K., Freney, E., Gini, M., Green, D. C., Heikkinen, L., Herrmann, H., Kalogridis, A.-C., Keernik, H., Lhotka, R., Lin, C., Lunder, C., Maasikmets, M., Manousakas, M. I., Marchand, N., Marin, C., Marmureanu, L., Mihalopoulos, N., Močnik, G., Nęcki, J., O'Dowd, C., Ovadnevaite, J., Peter, T., Petit, J.-E., Pikridas, M., Matthew Platt, S., Pokorná, P., Poulain, L., Priestman, M., Riffault, V., Rinaldi, M., Różański, K., Schwarz, J., Sciare, J., Simon, L., Skiba, A., Slowik, J. G., Sosedova, Y., Stavroulas, I., Styszko, K., Teinemaa, E., Timonen, H., Tremper, A., Vasilescu, J., Via, M., Vodička, P., Wiedensohler, A., Zografou, O., Cruz Minguillón, M. and Prévôt, A. S. H.: European aerosol phenomenology − 8: Harmonised source apportionment of organic aerosol using 22 Year-long ACSM/AMS datasets, Environ. Int., 166(May), 107325, doi:10.1016/j.envint.2022.107325, 2022.

Cordell, R.L., Mazet, M., Dechoux, C., Hama, S.M.L., Staelens, J., Hofman, J., Stroobants, C., Roekens, E., Kos, G.P.A., Weijers, E.P., Frumau, K.F.A., Panteliadis, P., Delaunay, T., Wyche, K.P., Monks, P.S., 2016. Evaluation of biomass burning across North West Europe and its impact on air quality. Atmos. Environ. 141, 276–286. https://doi.org/10.1016/j.atmosenv.2016.06.065

Crespi, A., Bernardoni, V., Calzolai, G., Lucarelli, F., Nava, S., Valli, G. and Vecchi, R.: Implementing constrained multi-time approach with bootstrap analysis in ME-2: An application to PM2.5 data from Florence (Italy), Sci. Total Environ., 541, 502–511, doi:10.1016/j.scitotenv.2015.08.159, 2016

Crilley, L.R., Bloss, W.J., Yin, J., Beddows, D.C.S., Harrison, R.M., Allan, J.D., Young, D.E., Flynn, M., Williams, P., Zotter, P., Prevot, A.S.H., Heal, M.R., Barlow, J.F., Halios, C.H., Lee, J.D., Szidat, S., Mohr, C., 2015. Sources and contributions of wood smoke during winter in London: Assessing local and regional influences. Atmos. Chem. Phys. 15, 3149–3171. https://doi.org/10.5194/acp-15-3149-2015

Crippa, M., Canonaco, F., Lanz, V. A., Äijälä, M., Allan, J. D., Carbone, S., Capes, G., Ceburnis, D., Dall'Osto, M., Day, D. A., DeCarlo, P. F., Ehn, M., Eriksson, A., Freney, E., Ruiz, L. H., Hillamo, R., Jimenez, J. L., Junninen, H., Kiendler-Scharr, A., Kortelainen, A. M., Kulmala, M., Laaksonen, A., Mensah, A. A., Mohr, C., Nemitz, E., O'Dowd, C., Ovadnevaite, J., Pandis, S. N., Petäjä, T., Poulain, L., Saarikoski, S., Sellegri, K., Swietlicki, E., Tiitta, P., Worsnop, D. R., Baltensperger, U. and Prévôt, A. S. H.: Organic aerosol components derived from 25 AMS data sets across Europe using a consistent ME-2 based source apportionment approach, Atmos. Chem. Phys., 14(12), 6159–6176, doi:10.5194/acp-14-6159-2014, 2014

El Haddad, I., D'Anna, B., Temime-Roussel, B., Nicolas, M., Boreave, A., Favez, O., Voisin, D., Sciare, J., George, C., Jaffrezo, J.L., Wortham, H., Marchand, N., 2013. Towards a better understanding of the origins, chemical

RI-URBANS (www.RIURBANS.eu) is supported by the European Commission under the Horizon 2020 – Research and Innovation Framework Programme, H2020-GD-2020, Grant Agreement number: 101036245

composition and aging of oxygenated organic aerosols: Case study of a Mediterranean industrialized environment, Marseille. Atmos. Chem. Phys. 13, 7875–7894. https://doi.org/10.5194/acp-13-7875-2013

Favez, O., Cachier, H., Sciare, J., Sarda-Estève, R., Martinon, L., 2009. Evidence for a significant contribution of wood burning aerosols to PM2.5 during the winter season in Paris, France. Atmos. Environ. 43, 3640–3644. https://doi.org/10.1016/j.atmosenv.2009.04.035

Favez, O., El Haddad, I., Piot, C., Boréave, A., Abidi, E., Marchand, N., Jaffrezo, J.L., Besombes, J.L., Personnaz, M.B., Sciare, J., Wortham, H., George, C., D'Anna, B., 2010. Inter-comparison of source apportionment models for the estimation of wood burning aerosols during wintertime in an Alpine city (Grenoble, France). Atmos. Chem. Phys. 10, 5295–5314. https://doi.org/10.5194/acp-10-5295-2010

Favez, O., El Haddad, I., Piot, C., Boréave, A., Abidi, E., Marchand, N., Jaffrezo, J.L., Besombes, J.L., Personnaz, M.B., Sciare, J., Wortham, H., George, C., D'Anna, B., 2010. Inter-comparison of source apportionment models for the estimation of wood burning aerosols during wintertime in an alpine city (Grenoble, France). Atmos. Chem. Phys. 10, 5295–5314.

Ferrero, L., Bernardoni, V., Santagostini, L., Cogliati, S., Soldan, F., Valentini, S., Massabò, D., Močnik, G., Gregorič, A., Rigler, M., Prati, P., Bigogno, A., Losi, N., Valli, G., Vecchi, R., Bolzacchini, E., 2021. Consistent determination of the heating rate of light-absorbing aerosol using wavelength- and time-dependent Aethalometer multiple-scattering correction. Sci. Total Environ. 791. https://doi.org/10.1016/j.scitotenv.2021.148277

Font, Anna, Anja H. Tremper, Max Priestman, Frank J. Kelly, Francesco Canonaco, André S.H. Prévôt, and David C. Green. 2022. "Source Attribution and Quantification of Atmospheric Nickel Concentrations in an Industrial Area in the United Kingdom (UK)." Environmental Pollution 293 (November 2021). https://doi.org/10.1016/j.envpol.2021.118432

Fontal, M., van Drooge, B.L., López, J.F., Fernández, P., Grimalt, J.O. Broad spectrum analysis of polar and apolar organic compounds in submicron atmospheric particles (2015) Journal of Chromatography A, 1404, pp. 28-38.

Forello, A. C., Bernardoni, V., Calzolai, G., Lucarelli, F., Massabò, D., Nava, S., Pileci, R. E., Prati, P., Valentini, S., Valli, G. and Vecchi, R.: Exploiting multi-wavelength aerosol absorption coefficients in a multi-time source apportionment study to retrieve source-dependent absorption parameters, Atmos. Chem. Phys. Discuss., 1–26, doi:10.5194/acp-2019-123, 2019

Fourtziou, L., Liakakou, E., Stavroulas, I., Theodosi, C., Zarmpas, P., Psiloglou, B., Sciare, J., Maggos, T., Bairachtari, K., Bougiatioti, A., Gerasopoulos, E., Sarda-Estève, R., Bonnaire, N., Mihalopoulos, N., 2017. Multi-tracer approach to characterize domestic wood burning in Athens (Greece) during wintertime. Atmos. Environ. 148, 89–101. https://doi.org/10.1016/j.atmosenv.2016.10.011

Fung, P.L., Sillanpää, S., Niemi, J. V., Kousa, A., Timonen, H., Zaidan, M.A., Saukko, E., Kulmala, M., Petäjä, T., Hussein, T., 2022. Improving the current air quality index with new particulate indicators using a robust statistical approach. Sci. Total Environ. 844. https://doi.org/10.1016/j.scitotenv.2022.157099

Furger, Markus, María Cruz Minguillón, Varun Yadav, Jay G. Slowik, Christoph Hüglin, Roman Fröhlich, Krag Petterson, Urs Baltensperger, and André S.H. Prévôt. 2017. "Elemental Composition of Ambient Aerosols Measured with High Temporal Resolution Using an Online XRF Spectrometer." Atmospheric Measurement Techniques 10 (6): 2061–76. https://doi.org/10.5194/amt-10-2061-2017

Furger, Markus, Pragati Rai, Jay G. Slowik, Junji Cao, Suzanne Visser, Urs Baltensperger, and André S.H. Prévôt. 2020. "Automated Alternating Sampling of PM10 and PM2.5 with an Online XRF Spectrometer." Atmospheric Environment: X 5. https://doi.org/10.1016/j.aeaoa.2020.100065

RI-URBANS (www.RIURBANS.eu) is supported by the European Commission under the Horizon 2020 – Research and Innovation Framework Programme, H2020-GD-2020, Grant Agreement number: 101036245

Garg, S., Chandra, B.P., Sinha, V., Sarda-Esteve, R., Gros, V., Sinha, B., 2016. Limitation of the Use of the Absorption Angstrom Exponent for Source Apportionment of Equivalent Black Carbon: A Case Study from the North West Indo-Gangetic Plain. Environ. Sci. Technol. 50, 814–824. https://doi.org/10.1021/acs.est.5b03868

Gregorič, A., Drinovec, L., JeÅ3/4ek, I., Vaupotič, J., Grauf, D., Wang, L., Stanič, S., 2020. The determination of highly time-resolved and source-separated black carbon emission rates using radon as a tracer of atmospheric dynamics. Atmos. Chem. Phys. 20, 14139–14162. https://doi.org/10.5194/acp-20-14139-2020

Hamilton, S.D., Harley, R.A., 2021. High-Resolution Modeling and Apportionment of Diesel-Related Contributions to Black Carbon Concentrations. Environ. Sci. Technol. 55, 12250–12260. https://doi.org/10.1021/acs.est.1c03913

Harrison, R.M., Beddows, D.C.S., Jones, A.M., Calvo, A., Alves, C., Pio, C., 2013. An evaluation of some issues regarding the use of aethalometers to measure woodsmoke concentrations. Atmos. Environ. 80, 540–548. https://doi.org/10.1016/j.atmosenv.2013.08.026

Hasheminassab, Sina, Mohammad H. Sowlat, Payam Pakbin, Aaron Katzenstein, Jason Low, and Andrea Polidori. 2020. “High Time-Resolution and Time-Integrated Measurements of Particulate Metals and Elements in an Environmental Justice Community within the Los Angeles Basin: Spatio-Temporal Trends and Source Apportionment.” Atmospheric Environment: X 7 (July): 100089. https://doi.org/10.1016/j.aeaoa.2020.100089

Helin, A., Niemi, J. V., Virkkula, A., Pirjola, L., Teinilä, K., Backman, J., Aurela, M., Saarikoski, S., Rönkkö, T., Asmi, E., Timonen, H., 2018. Characteristics and source apportionment of black carbon in the Helsinki metropolitan area, Finland. Atmos. Environ. 190, 87–98. https://doi.org/10.1016/j.atmosenv.2018.07.022

Helin, A., Virkkula, A., Backman, J., Pirjola, L., Sippula, O., Aakko-Saksa, P., Väätäinen, S., Mylläri, F., Järvinen, A., Bloss, M., Aurela, M., Jakobi, G., Karjalainen, P., Zimmermann, R., Jokiniemi, J., Saarikoski, S., Tissari, J., Rönkkö, T., Niemi, J. V., Timonen, H., 2021. Variation of Absorption Ångström Exponent in Aerosols From Different Emission Sources. J. Geophys. Res. Atmos. 126, 1–21. https://doi.org/10.1029/2020JD034094

Herich, H., Hueglin, C., Buchmann, B., 2011. A 2.5 year’s source apportionment study of black carbon from wood burning and fossil fuel combustion at urban and rural sites in Switzerland. Atmos. Meas. Tech. 4, 1409–1420. https://doi.org/10.5194/amt-4-1409-2011

Hopke, P. K.: A GUIDE TO POSITIVE MATRIX FACTORIZATION, 16, 2000.

Hopke, P.K., 2016. Review of receptor modeling methods for source apportionment. J. Air Waste Manag. Assoc. 66, 237–259. https://doi.org/10.1080/10962247.2016.1140693

Hopke, P.K., Chen, Y., Rich, D.Q., Mooibroek, D., Sofowote, U.M., 2023. Chemometrics and Intelligent Laboratory Systems The application of positive matrix factorization with diagnostics to BIG DATA. Chemom. Intell. Lab. Syst. 240, 104885. https://doi.org/10.1016/j.chemolab.2023.104885

Hu, Q. H., Xie, Z. Q., Wang, X. M., Kang, H. and Zhang, P.: Levoglucosan indicates high levels of biomass burning aerosols over oceans from the Arctic to Antarctic, Sci. Rep., 3, 1–7, doi:10.1038/srep03119, 2013

Hyvärinen, A.P., Kolmonen, P., Kerminen, V.M., Virkkula, A., Leskinen, A., Komppula, M., Hatakka, J., Burkhart, J., Stohl, A., Aalto, P., Kulmala, M., Lehtinen, K.E.J., Viisanen, Y., Lihavainen, H., 2011. Aerosol black carbon at five background measurement sites over Finland, a gateway to the Arctic. Atmos. Environ. 45, 4042–4050. https://doi.org/10.1016/j.atmosenv.2011.04.026

Jafar, H.A., Harrison, R.M., 2021. Spatial and temporal trends in carbonaceous aerosols in the United Kingdom. Atmos. Pollut. Res. 12, 295–305. https://doi.org/10.1016/j.apr.2020.09.009

RI-URBANS (www.RIURBANS.eu) is supported by the European Commission under the Horizon 2020 – Research and Innovation Framework Programme, H2020-GD-2020, Grant Agreement number: 101036245

Jaffrezo, J.L., Aymoz, G., Delaval, C., Cozic, J., 2005. Seasonal variations of the water soluble organic carbon mass fraction of aerosol in two valleys of the French Alps. Atmos. Chem. Phys. 5, 2809–2821.

K Grange, S., Lötscher, H., Fischer, A., Emmenegger, L., Hueglin, C., 2020. Evaluation of equivalent black carbon source apportionment using observations from Switzerland between 2008 and 2018. Atmos. Meas. Tech. 13, 1867–1885. https://doi.org/10.5194/amt-13-1867-2020

Kaskaoutis, D.G., Grivas, G., Stavroulas, I., Bougiatioti, A., Liakakou, E., Dumka, U.C., Gerasopoulos, E., Mihalopoulos, N., 2021. Apportionment of black and brown carbon spectral absorption sources in the urban environment of Athens, Greece, during winter. Sci. Total Environ. 801, 149739. https://doi.org/10.1016/j.scitotenv.2021.149739

Krecl, P., Johansson, C., Targino, A.C., Ström, J., Burman, L., 2017. Trends in black carbon and size-resolved particle number concentrations and vehicle emission factors under real-world conditions. Atmos. Environ. 165, 155–168. https://doi.org/10.1016/j.atmosenv.2017.06.036

Krecl, P., Targino, A.C., Johansson, C., 2011. Spatiotemporal distribution of light-absorbing carbon and its relationship to other atmospheric pollutants in Stockholm. Atmos. Chem. Phys. 11, 11553–11567. https://doi.org/10.5194/acp-11-11553-2011

Kumar, S., Wang, S., Lin, N., Chantara, S., Lee, C., Thepnuan, D., 2020. Black carbon over an urban atmosphere in northern peninsular Southeast Asia : Characteristics , source apportionment , and associated health risks *. Environ. Pollut. 259, 113871. https://doi.org/10.1016/j.envpol.2019.113871

Kuo, C.-P., Liao, H.-T., Chou, C.C.-K., Wu, C.-F. Source apportionment of particulate matter and selected volatile organic compounds with multiple time resolution data (2014) Science of the Total Environment, 472, pp. 880-887.

Kutzner, R.D., von Schneidemesser, E., Kuik, F., Quedenau, J., Weatherhead, E.C., Schmale, J., 2018. Long-term monitoring of black carbon across Germany. Atmos. Environ. 185, 41–52. https://doi.org/10.1016/j.atmosenv.2018.04.039

Laborde, M., Crippa, M., Tritscher, T., Jurányi, Z., Decarlo, P.F., Temime-Roussel, B., Marchand, N., Eckhardt, S., Stohl, A., Baltensperger, U., Prévôt, A.S.H., Weingartner, E., Gysel, M., 2013. Black carbon physical properties and mixing state in the European megacity Paris. Atmos. Chem. Phys. 13, 5831–5856. https://doi.org/10.5194/acp-13-5831-2013

Lee, E., Chan, C. K., and Paatero, P.: Application of positive matrix factorization in source apportionment of particulate pollutants in Hong Kong, Atmos. Environ., 33, 3201–3212, https://doi.org/10.1016/S1352-2310(99)00113-2, 1999

Li, J., Liu, C., Yin, Y., Kumar, K.R., 2016. Numerical investigation on the Ångström exponent of black carbon aerosol. J. Geophys. Res. Atmos. 121, 3506–3518. https://doi.org/10.1002/2015jd024718

Liakakou, E., Stavroulas, I., Kaskaoutis, D.G., Grivas, G., Paraskevopoulou, D., Dumka, U.C., Tsagkaraki, M., Bougiatioti, A., Oikonomou, K., Sciare, J., Gerasopoulos, E., Mihalopoulos, N., 2020. Long-term variability, source apportionment and spectral properties of black carbon at an urban background site in Athens, Greece. Atmos. Environ. 222, 117137. https://doi.org/10.1016/j.atmosenv.2019.117137

Liu, C., Chung, C.E., Yin, Y., Schnaiter, M., 2018. The absorption Ångström exponent of black carbon: From numerical aspects. Atmos. Chem. Phys. 18, 6259–6273. https://doi.org/10.5194/acp-18-6259-2018

RI-URBANS (www.RIURBANS.eu) is supported by the European Commission under the Horizon 2020 – Research and Innovation Framework Programme, H2020-GD-2020, Grant Agreement number: 101036245

Liu, X., Zheng, M., Liu, Y., Jin, Y., Liu, J., Zhang, B., Yang, X., Wu, Y., Zhang, T., Xiang, Y., Liu, B., Yan, C., 2022. Intercomparison of equivalent black carbon (eBC) and elemental carbon (EC) concentrations with three-year continuous measurement in Beijing, China. Environ. Res. 209, 112791. https://doi.org/10.1016/j.envres.2022.112791

Liu, Yue, Mei Zheng, Mingyuan Yu, Xuhui Cai, Huiyun Du, Jie Li, Tian Zhou, et al. 2019. "High-Time-Resolution Source Apportionment of PM2.5 in Beijing with Multiple Models." Atmospheric Chemistry and Physics 19 (9): 6595–6609. https://doi.org/10.5194/acp-19-6595-2019

Luo, J., Li, Z., Qiu, J., Zhang, Y., Fan, C., Li, L., Wu, H., Zhou, P., Li, K., Zhang, Q., 2023. The Simulated Source Apportionment of Light Absorbing Aerosols: Effects of Microphysical Properties of Partially-Coated Black Carbon. J. Geophys. Res. Atmos. 128. https://doi.org/10.1029/2022JD037291

Luoma, K., Niemi, J. V., Aurela, M., Lun Fung, P., Helin, A., Hussein, T., Kangas, L., Kousa, A., Rönkkö, T., Timonen, H., Virkkula, A., Petäjä, T., 2021. Spatiotemporal variation and trends in equivalent black carbon in the Helsinki metropolitan area in Finland. Atmos. Chem. Phys. 21, 1173–1189. https://doi.org/10.5194/acp-21-1173-2021

Lyamani, H., Olmo, F.J., Foyo, I., Alados-Arboledas, L., 2011. Black carbon aerosols over an urban area in south-eastern Spain: Changes detected after the 2008 economic crisis. Atmos. Environ. 45, 6423–6432. https://doi.org/10.1016/j.atmosenv.2011.07.063

Manousakas, M, E Diapouli, C A Belis, V Vasilatou, M Gini, F Lucarelli, X Querol, and K Eleftheriadis. 2021. "Quantitative Assessment of the Variability in Chemical Profiles from Source Apportionment Analysis of PM10 and PM2.5 at Different Sites within a Large Metropolitan Area." Environmental Research 192: 110257. https://doi.org/10.1016/j.envres.2020.110257

Manousakas, M, M Furger, K R Daellenbach, F Canonaco, G Chen, A Tobler, P Rai, et al. 2022. "Source Identification of the Elemental Fraction of Particulate Matter Using Size Segregated , Highly Time-Resolved Data and an Optimized Source Apportionment Approach." Atmospheric Environment: X 14 (100165). https://doi.org/10.1016/j.aeaoa.2022.100165

Masiol, M., Squizzato, S., Rich, D.Q., Hopke, P.K., 2019. Long-term trends (2005–2016) of source apportioned PM2.5 across New York State. Atmos. Environ. 201, 110–120. https://doi.org/10.1016/j.atmosenv.2018.12.038

Massabò, D., Prati, P., 2021. An overview of optical and thermal methods for the characterization of carbonaceous aerosol, Rivista del Nuovo Cimento. Springer Berlin Heidelberg. https://doi.org/10.1007/s40766-021-00017-8

Mbengue, S., Serfozo, N., Schwarz, J., Holoubek, I., Ziková, N., Šmejkalová, A.H., Holoubek, I., 2020. Characterization of Equivalent Black Carbon at a regional background site in Central Europe: Variability and source apportionment☆. Environ. Pollut. 260. https://doi.org/10.1016/j.envpol.2019.113771

Merabet, H., Kerbachi, R., Mihalopoulos, N., Stavroulas, I., Kanakidou, M., Yassaa, N., 2019. Measurement of atmospheric black carbon in some south mediterranean cities: Seasonal variations and source apportionment. Clean Air J. 29, 1–19. https://doi.org/10.17159/caj/2019/29/2.7500

Milinković, A., Gregorič, A., Grgičin, V.D., Vidič, S., Penezić, A., Kušan, A.C., Alempijević, S.B., Kasper-Giebl, A., Frka, S., 2021. Variability of black carbon aerosol concentrations and sources at a Mediterranean coastal region. Atmos. Pollut. Res. 12. https://doi.org/10.1016/j.apr.2021.101221

Minderytė, A., Pauraite, J., Dudoitis, V., Plauškaitė, K., Kilikevičius, A., Matijošius, J., Rimkus, A., Kilikevičienė, K., Vainorius, D., Byčenkienė, S., 2022. Carbonaceous aerosol source apportionment and assessment of transport-related pollution. Atmos. Environ. 279. https://doi.org/10.1016/j.atmosenv.2022.119043

RI-URBANS (www.RIURBANS.eu) is supported by the European Commission under the Horizon 2020 – Research and Innovation Framework Programme, H2020-GD-2020, Grant Agreement number: 101036245

Mousavi, A., Sowlat, M.H., Hasheminassab, S., Polidori, A., Sioutas, C., 2018. Spatio-temporal trends and source apportionment of fossil fuel and biomass burning black carbon (BC) in the Los Angeles Basin. Sci. Total Environ. 640–641, 1231–1240. https://doi.org/10.1016/j.scitotenv.2018.06.022

Mousavi, A., Sowlat, M.H., Lovett, C., Rauber, M., Szidat, S., Bo, R., Borgini, A., Marco, C. De, Ruprecht, A.A., Sioutas, C., Boffi, R., Borgini, A., De Marco, C., Ruprecht, A.A., Sioutas, C., Bo, R., Borgini, A., Marco, C. De, Ruprecht, A.A., Sioutas, C., 2019. Source apportionment of black carbon (BC) from fossil fuel and biomass burning in metropolitan Milan, Italy. Atmos. Environ. 203, 252–261. https://doi.org/10.1016/j.atmosenv.2019.02.009

Nozière, B., Kalberer, M., Claeys, M., Allan, J., D'Anna, B., Decesari, S., Finessi, E., Glasius, M., Grgić, I., Hamilton, J.F., Hoffmann, T., Iinuma, Y., Jaoui, M., Kahnt, A., Kampf, C.J., Kourtchev, I., Maenhaut, W., Marsden, N., Saarikoski, S., Schnelle-Kreis, J., Surratt, J.D., Szidat, S., Szmigielski, R., Wisthaler, A., 2015. The molecular identification of organic compounds in the atmosphere: state of the art and challenges. Chem. Rev. 115, 3919–3983.

Paatero, P., Hopke, P.K., 2003. Discarding or downweighting high-noise variables in factor analytic models. Anal. Chim. Acta 490, 277–289

Pandolfi, M., Ripoll, A., Querol, X., Alastuey, A., 2014. Climatology of aerosol optical properties and black carbon mass absorption cross section at a remote high-altitude site in the western Mediterranean Basin. Atmos. Chem. Phys. 14, 6443–6460. https://doi.org/10.5194/acp-14-6443-2014

Petit, J. E., Favez, O., Sciare, J., Canonaco, F., Croteau, P., Močnik, G., Jayne, J., Worsnop, D. and Leoz-Garziandia, E.: Submicron aerosol source apportionment of wintertime pollution in Paris, France by double positive matrix factorization (PMF2) using an aerosol chemical speciation monitor (ACSM) and a multi-wavelength Aethalometer, Atmos. Chem. Phys., 14(24), 13773–13787, doi:10.5194/acp-14-13773-2014, 2014

Querol X., Alastuey A., Rodriguez S., Plana F., Mantilla E., Ruiz C.R. Monitoring of PM10 and PM2.5 around primary particulate anthropogenic emission sources (2001) Atmospheric Environment, 35 (5), pp. 845 - 858

Rai, Pragati, Jay G Slowik, Markus Furger, Imad El Haddad, Suzanne Visser, Yandong Tong, Atinderpal Singh, et al. 2021. “Highly Time-Resolved Measurements of Element Concentrations in PM 10 and PM 2 . 5 : Comparison of Delhi , Beijing , London , and Krakow.” Atmospheric Chemistry and Physics 21: 717–30.

Rai, Pragati, Markus Furger, Imad El Haddad, Varun Kumar, Liwei Wang, Atinderpal Singh, Kuldeep Dixit, et al. 2020. “Real-Time Measurement and Source Apportionment of Elements in Delhi’s Atmosphere.” Science of the Total Environment 742: 140332. https://doi.org/10.1016/j.scitotenv.2020.140332

Rai, Pragati, Markus Furger, Jay Slowik, Francesco Canonaco, Roman Fröhlich, Christoph Hüglin, María Cruz Minguillón, Krag Petterson, Urs Baltensperger, and André S. H. Prévôt. 2019. “Source Apportionment of Highly Time Resolved Trace Elements during a Firework Episode from a Rural Freeway Site in Switzerland.” Atmospheric Chemistry and Physics Discussions, 1–25. https://doi.org/10.5194/acp-2018-1229

Reimann, S., Wegener, R., Claude, A., and Sauvage, S.: Milestone 3.10. Released Measurement Guideline for VOCs and NOx., 2, 2020.

Rivas, I., Beddows, D.C.S., Amato, F., Green, D.C., Järvi, L., Hueglin, C., Reche, C., Timonen, H., Fuller, G.W., Niemi, J. V., Pérez, N., Aurela, M., Hopke, P.K., Alastuey, A., Kulmala, M., Harrison, R.M., Querol, X., Kelly, F.J., 2020. Source apportionment of particle number size distribution in urban background and traffic stations in four European cities. Environ. Int. 135, 105345. https://doi.org/10.1016/j.envint.2019.105345

RI-URBANS (www.RIURBANS.eu) is supported by the European Commission under the Horizon 2020 – Research and Innovation Framework Programme, H2020-GD-2020, Grant Agreement number: 101036245

Salameh, D., Pey, J., Bozzetti, C., El Haddad, I., Detournay, A., Sylvestre, A., Canonaco, F., Armengaud, A., Piga, D., Robin, D., Prevot, A.S.H., Jaffrezo, J.L., Wortham, H., Marchand, N., 2018. Sources of PM2.5 at an urban-industrial Mediterranean city, Marseille (France): Application of the ME-2 solver to inorganic and organic markers. Atmos. Res. 214, 263–274. https://doi.org/10.1016/j.atmosres.2018.08.005

Sandradewi, J., Prévôt, A.S.H., Weingartner, E., Schmidhauser, R., Gysel, M., Baltensperger, U., 2008. A study of wood burning and traffic aerosols in an Alpine valley using a multi-wavelength Aethalometer. Atmos. Environ. 42, 101–112. https://doi.org/10.1016/j.atmosenv.2007.09.034

Sandradewi, Jisca, Prévôt, A.S.H., Szidat, S., Perron, N., Alfarra, M.R., Lanz, V.A., Weingartner, E., Baltensperger, U.R.S., 2008. Using aerosol light abosrption measurements for the quantitative determination of wood burning and traffic emission contribution to particulate matter. Environ. Sci. Technol. 42, 3316–3323. https://doi.org/10.1021/es702253m

Savadkoohi, M., Pandolfi, M., Reche, C., Niemi, J. V, Mooibroek, D., Titos, G., Green, D.C., Tremper, A.H., Hueglin, C., Coz, E., Liakakou, E., Mihalopoulos, N., Stavroulas, I., Alados-arboledas, L., Beddows, D., Brito, J.F. De, Bastian, S., Baudic, A., Colombi, C., Costabile, F., Estell, V., Matos, V., Gaag, E. Van Der, Norman, M., Silvergren, S., Petit, J., Putaud, J., Rattigan, O. V, Timonen, H., Tuch, T., Merkel, M., Weinhold, K., Vratolis, S., Vasilescu, J., Favez, O., Harrison, R.M., Laj, P., Wiedensohler, A., Hopke, P.K., Pet, T., Querol, X., 2023. The variability of mass concentrations and source apportionment analysis of equivalent black carbon across urban Europe 178. https://doi.org/10.1016/j.envint.2023.108081

Schaap, M., Denier van der Gon, H.A.C., 2007. On the variability of Black Smoke and carbonaceous aerosols in the Netherlands. Atmos. Environ. 41, 5908–5920. https://doi.org/10.1016/j.atmosenv.2007.03.042

Segersson, D., Eneroth, K., Gidhagen, L., Johansson, C., Omstedt, G., Nylén, A.E., Forsberg, B., 2017. Health impact of PM10, PM2.5 and black carbon exposure due to different source sectors in Stockholm, Gothenburg and Umea, Sweden. Int. J. Environ. Res. Public Health 14, 11–14. https://doi.org/10.3390/ijerph14070742

Shen, X., Vogel, H., Vogel, B., Huang, W., Mohr, C., Ramisetty, R., Leisner, T., Prévôt, A.S.H., Saathoff, H. Composition and origin of PM2.5 aerosol particles in the upper Rhine valley in summer (2019) Atmospheric Chemistry and Physics, 19 (20), pp. 13189-13208.

Singh, V., Ravindra, K., Sahu, L., Sokhi, R., 2018. Trends of atmospheric black carbon concentration over United Kingdom. Atmos. Environ. 178, 148–157. https://doi.org/10.1016/j.atmosenv.2018.01.030

Squizzato, S., Masiol, M., Rich, D.Q., Hopke, P.K., 2018. A long-term source apportionment of PM2.5 in New York State during 2005–2016. Atmos. Environ. 192, 35–47. https://doi.org/10.1016/j.atmosenv.2018.08.044

Srivastava, D., Favez, O., Petit, J. E., Zhang, Y., Sofowote, U. M., Hopke, P. K., Bonnaire, N., Perraudin, E., Gros, V., Villenave, E. and Albinet, A.: Speciation of organic fractions does matter for aerosol source apportionment. Part 3: Combining off-line and on-line measurements, Sci. Total Environ., 690, 944–955, doi:10.1016/j.scitotenv.2019.06.378, 2019

Srivastava, D., Tomaz, S., Favez, O., Lanzafame, G.M., Golly, B., esombes, J.-L., Alleman, L.Y., Jaffrezo, J.-L., Jacob, V., erraudin, E., Villenave, E., Albinet, A. Speciation of organic fraction does matter for source apportionment. Part 1: A one-year campaign in Grenoble (France) (2018) Science of the Total Environment, 624, pp. 1598-1611.

Thera, B.T.P., Dominutti, P., Öztürk, F., Salameh, T., Sauvage, S., Afif, C., Çetin, B., Gaimoz, C., Keleş, M., Evan, S., Borbon, A. Composition and variability of gaseous organic pollution in the port megacity of Istanbul: Source attribution, emission ratios, and inventory evaluation (2019) Atmospheric Chemistry and Physics, 19 (23), pp. 15131-15156.

RI-URBANS (www.RIURBANS.eu) is supported by the European Commission under the Horizon 2020 – Research and Innovation Framework Programme, H2020-GD-2020, Grant Agreement number: 101036245

Tian, Y., Zhang, Y., Liang, Y., Niu, Z., Xue, Q., Feng, Y. PM2.5 source apportionment during severe haze episodes in a Chinese megacity based on a 5-month period by using hourly species measurements: Explore how to better conduct PMF during haze episodes (2020) Atmospheric Environment, 224, art. no. 117364

Titos, G., del Águila, A., Cazorla, A., Lyamani, H., Casquero-Vera, J.A., Colombi, C., Cuccia, E., Gianelle, V., Močnik, G., Alastuey, A., Olmo, F.J., Alados-Arboledas, L., 2017. Spatial and temporal variability of carbonaceous aerosols: Assessing the impact of biomass burning in the urban environment. Sci. Total Environ. 578, 613–625. https://doi.org/10.1016/j.scitotenv.2016.11.007

Tobler, A. K., Canonaco, F., Skiba, A., Styszko, K., Nęcki, J., Slowik, J. G. and Baltensperger, U.: Characterization and source apportionment of PM 1 organic aerosol in Krakow , Poland, , (April), 8299, 2021.

Tobler, A., Skiba, A., Wang, D., Croteau, P., Styszko, K., Nęcki, J., Baltensperger, U., Slowik, J. and Prévôt, A.: Improved chloride quantification in quadrupole aerosol chemical speciation monitors (Q-ACSMs), Atmos. Meas. Tech. Discuss., 36(May), 1–17, doi:10.5194/amt-2020-117, 2020

Tobler, A.K., Skiba, A., Canonaco, F., Močnik, G., Rai, P., Chen, G., Bartyzel, J., Zimnoch, M., Styszko, K., Nęcki, J., Furger, M., Rózański, K., Baltensperger, U., Slowik, J.G., Prevot, A.S.H., 2021. Characterization of non-refractory (NR) PM1and source apportionment of organic aerosol in Kraków, Poland. Atmos. Chem. Phys. 21, 14893–14906. https://doi.org/10.5194/acp-21-14893-2021

Tomaz, S., Shahpoury, P., Jaffrezo, J.-L., Lammel, G., Perraudin, E., Villenave, E., Albinet, A., 2016. One-year study of polycyclic aromatic compounds at an urban site in Grenoble (France): seasonal variations, gas/particle partitioning and cancer risk estimation. Sci. Total Environ. 565, 1071–1083

Tremper, Anja H., Anna Font, Max Priestman, Samera H. Hamad, Tsai Chia Chung, Ari Pribadi, Richard J.C. Brown, et al. 2018. "Field and Laboratory Evaluation of a High Time Resolution X-Ray Fluorescence Instrument for Determining the Elemental Composition of Ambient Aerosols." Atmospheric Measurement Techniques 11 (6): 3541–57. https://doi.org/10.5194/amt-11-3541-2018.

Ulbrich, I. M., Canagaratna, M. R., Zhang, Q., Worsnop, D. R. and Jimenez, J. L.: Interpretation of organic components from Positive Matrix Factorization of aerosol mass spectrometric data, Atmos. Chem. Phys., 9(9), 2891–2918, doi:10.5194/acp-9-2891-2009, 2009

Vanderstraeten, P., Forton, M., Brasseur, O., Offer, Z.Y., 2011. Black Carbon Instead of Particle Mass Concentration as an Indicator for the Traffic Related Particles in the Brussels Capital Region. J. Environ. Prot. (Irvine,. Calif). 02, 525–532. https://doi.org/10.4236/jep.2011.25060

Veld M.I., Alastuey A., Pandolfi M., Amato F., Pérez N., Reche C., Via M., Minguillón M.C., Escudero M., Querol X. Compositional changes of PM2.5 in NE Spain during 2009–2018: A trend analysis of the chemical composition and source apportionment (2021) Science of the Total Environment, 795, art. no. 148728

Via, M., Chen, G., Canonaco, F., Daellenbach, K. R., Chazeau, B., Chebaicheb, H., Jiang, J., Keernik, H., Lin, C., Marchand, N., Marin, C., O'Dowd, C., Ovadnevaite, J., Petit, J.-E., Pikridas, M., Riffault, V., Sciare, J., Slowik, J. G., Simon, L., Vasilescu, J., Zhang, Y., Favez, O., Prévôt, A. S. H., Alastuey, A. and Minguillón, M. C.: Rolling vs. Seasonal PMF: Real-world multi-site and synthetic dataset comparison, EGUsphere, 2022, 1–29 [online] Available from: https://egusphere.copernicus.org/preprints/egusphere-2022-269/, 2022

Via, M., Minguillón, M.C., Reche, C., Querol, X., Alastuey, A., 2021. Increase in secondary organic aerosol in an urban environment. Atmos. Chem. Phys. 21, 8323–8339. https://doi.org/10.5194/acp-21-8323-2021

RI-URBANS (www.RIURBANS.eu) is supported by the European Commission under the Horizon 2020 – Research and Innovation Framework Programme, H2020-GD-2020, Grant Agreement number: 101036245

Via, M., Yus-díez, J., Canonaco, F., Petit, J., Hopke, P., Reche, C., Pandolfi, M., Ivan, M., Rigler, M., Prev, S. H., Querol, X. and Cruz, M.: Towards a better understanding of fine PM sources : Online and offline datasets combination in a single PMF, , 177(February), doi:10.1016/j.envint.2023.108006, 2023

Viana, M., Kuhlbusch, T.A.J., Querol, X., Alastuey, A., Harrison, R.M., Hopke, P.K., Winiwarter, W., Vallius, M., Szidat, S., Prévôt, A.S.H., Hueglin, C., Bloemen, H., Wåhlin, P., Vecchi, R., Miranda, A.I., Kasper-Giebl, A., Maenhaut, W., Hitzenberger, R., 2008. Source apportionment of particulate matter in Europe: A review of methods and results. J. Aerosol Sci. 39, 827–849. https://doi.org/10.1016/j.jaerosci.2008.05.007

Viana, M., M. Pandolfi, M.C. Minguillón, X. Querol, A. Alastuey, E. Monfort, and I. Celades. 2008. "Inter-Comparison of Receptor Models for PM Source Apportionment: Case Study in an Industrial Area." Atmospheric Environment 42 (16): 3820–32. https://doi.org/10.1016/j.atmosenv.2007.12.056 .

Virkkula, A., 2021. Modeled source apportionment of black carbon particles coated with a light-scattering shell. Atmos. Meas. Tech. 14, 3707–3719. https://doi.org/10.5194/amt-14-3707-2021

Wang, Honglei, Qing Miao, Lijuan Shen, Qian Yang, Yezheng Wu, and Heng Wei. 2021. "Air Pollutant Variations in Suzhou during the 2019 Novel Coronavirus (COVID-19) Lockdown of 2020: High Time-Resolution Measurements of Aerosol Chemical Compositions and Source Apportionment." Environmental Pollution 271: 116298. https://doi.org/10.1016/j.envpol.2020.116298.

Wang, Q., Liu, H., Ye, J., Tian, J., Zhang, T., Zhang, Y., Liu, S., Cao, J., 2021. Estimating Absorption Ångström Exponent of Black Carbon Aerosol by Coupling Multiwavelength Absorption with Chemical Composition. Environ. Sci. Technol. Lett. 8, 121–127. https://doi.org/10.1021/acs.estlett.0c00829

Wang, Qiongqiong, Liping Qiao, Min Zhou, Shuhui Zhu, Stephen Griffith, Li Li, and Jian Zhen Yu. 2018. "Source Apportionment of PM2.5 Using Hourly Measurements of Elemental Tracers and Major Constituents in an Urban Environment: Investigation of Time-Resolution Influence." Journal of Geophysical Research: Atmospheres 123 (10): 5284–5300. https://doi.org/10.1029/2017JD027877.

Yang, Y., Lou, S., Wang, H., Wang, P. and Liao, H.: Trends and source apportionment of aerosols in Europe during 1980-2018, Atmos. Chem. Phys., 20(4), 2579–2590, doi:10.5194/acp-20-2579-2020, 2020

Yttri, K.E., Simpson, D., Nojgaard, J.K., Kristensen, K., Genberg, J., Stenström, K., Swietlicki, E., Hillamo, R., Aurela, M., Bauer, H., Offenberg, J.H., Jaoui, M., Dye, C., Eckhardt, S., Burkhart, J.F., Stohl, A., Glasius, M., 2011. Source apportionment of the summer time carbonaceous aerosol at Nordic rural background sites. Atmos. Chem. Phys. 11, 13339–13357. https://doi.org/10.5194/acp-11-13339-2011

Yu, Yiyong, Shuyan He, X. Wu, Chi Zhang, Ying Yao, Hong Liao, Qin'geng Wang, and Mingjie Xie. 2019. "PM2.5 Elements at an Urban Site in Yangtze River Delta, China: High Time-Resolved Measurement and the Application in Source Apportionment." Environmental Pollution 253: 1089–99. https://doi.org/10.1016/j.envpol.2019.07.096

Zhang, G., Peng, L., Lian, X., Lin, Q., Bi, X., Chen, D., Li, M., Li, L., Wang, X., Sheng, G., 2019. An improved absorption Ångström exponent (AAE)-based method for evaluating the contribution of light absorption from brown carbon with a high-time resolution. Aerosol Air Qual. Res. 19, 15–24. https://doi.org/10.4209/aaqr.2017.12.0566

Zhang, X., Mao, M., Chen, H., Tang, S., 2020a. The Angstrom exponents of black carbon aerosols with non-absorptive coating: A numerical investigation. J. Quant. Spectrosc. Radiat. Transf. 257, 107362. https://doi.org/10.1016/j.jqsrt.2020.107362

RI-URBANS (www.RIURBANS.eu) is supported by the European Commission under the Horizon 2020 – Research and Innovation Framework Programme, H2020-GD-2020, Grant Agreement number: 101036245

Zhang, X., Mao, M., Yin, Y., Tang, S., 2020b. The absorption Ångstrom exponent of black carbon with brown coatings: Effects of aerosol microphysics and parameterization. Atmos. Chem. Phys. 20, 9701–9711. https://doi.org/10.5194/acp-20-9701-2020

Zhang, Y., Albinet, A., Petit, J.E., Jacob, V., Chevrier, F., Gille, G., Pontet, S., Chrétien, E., Dominik-Sègue, M., Levigoureux, G., Močnik, G., Gros, V., Jaffrezo, J.L., Favez, O., 2020. Substantial brown carbon emissions from wintertime residential wood burning over France. Sci. Total Environ. 743. https://doi.org/10.1016/j.scitotenv.2020.140752

Zheng, H., Kong, S., Chen, N., Fan, Z., Zhang, Y., Yao, L., Cheng, Y., Zheng, S., Yan, Y., Liu, D., Zhao, D., Liu, C., Zhao, T., Guo, J., Qi, S., 2021. A method to dynamically constrain black carbon aerosol sources with online monitored potassium. npj Clim. Atmos. Sci. 4. https://doi.org/10.1038/s41612-021-00200-y

Zografou, O., Gini, M., Manousakas, M. I., Chen, G., Kalogridis, A. C., Diapouli, E., Pappa, A. and Eleftheriadis, K.: Combined organic and inorganic source apportionment on yearlong ToF-ACSM dataset at a suburban station in Athens, Atmos. Meas. Tech., 15(16), 4675–4692, doi:10.5194/amt-15-4675-2022, 2022

Zotter, P., Herich, H., Gysel, M., El-Haddad, I., Zhang, Y., Mocnik, G., Hüglin, C., Baltensperger, U., Szidat, S., Prévôt, A.S.H., 2017. Evaluation of the absorption Ångström exponents for traffic and wood burning in the Aethalometer-based source apportionment using radiocarbon measurements of ambient aerosol. Atmos. Chem. Phys. 17, 4229–4249. https://doi.org/10.5194/acp-17-4229-2017

RI-URBANS (www.RIURBANS.eu) is supported by the European Commission under the Horizon 2020 – Research and Innovation Framework Programme, H2020-GD-2020, Grant Agreement number: 101036245